The Effects of Beta-Adrenergic Receptor Signalling on Ventricular Conduction System Cell Development

By

Kajanan Sivapalan

Submitted in partial fulfilment of the requirements
for the degree of Master of Science

at

Dalhousie University
Halifax, Nova Scotia
August 2021

Dedicated to my parents, Vanaja and Sivapalan, my sisters Shiyama and Jyothiesha, and my brother Shrishan for their unwavering support and affection, without which I would not be here today

Table of Contents

LIST OF TABLES ..... *vi*

LIST OF FIGURES ..... *vii*

ABSTRACT ..... *viii*

LIST OF ABBREVIATIONS AND SYMBOLS USED ..... *ix*

ACKOWLEDGMENTS ..... *xiii*

Chapter 1: Introduction *1*

1.1 Thesis Overview **1**

1.2 Cardiac Injury and Healing **4**

1.2.1 Myocardial wound healing 4

1.2.2 Scar formation 5

1.2.3 Post-MI Treatment 6

1.3 Potential Cardiac Cell-based Therapy **8**

1.3.1 Skeletal Myoblasts 9

1.3.2 Bone Marrow-Derived Stem Cells 10

1.3.3 Embryonic Stem Cells 10

1.3.4 Cardiac-Derived Stem Cells/ Cardiac Progenitor cells 11

1.4 Cardiac Development **14**

1.4.1 Working Cardiomyocytes and Cardiac Contractions 15

1.4.2 Conductive Cardiomyocytes and CCS development 18

1.5 The Cardiac Conduction System **20**

1.5.1 Conduction system protein Cx40 21

1.5.2 Conduction system protein HCN4 22

1.5.3 Conduction system protein Cntn2 23

1.6 Directed Differentiation of CPC into the VCS lineage **23**

1.6.1 Effects of Sodium Nitroprusside on VCS Cell Differentiation 24

1.6.2 Beta-Adrenergic Stimulation 25

1.6.3 Beta-Adrenergic Agonists and Antagonists 26

1.6.4 Beta-Adrenergic Agonist Isoproterenol 28

1.6.5 Beta-Adrenergic Antagonist Metoprolol 28

1.7 Antioxidant Ascorbic Acid 29

Chapter 2: Materials and Methods 30

2.1 Animal Maintenance, Mouse strain and Timed Pregnancies 30

2.2 Heart Isolation 30

2.3 Cryosections 31

2.4 Immunostaining of Cryosections 31

2.5 Total RNA Extraction from Ventricular Tissue 34

2.6 Embryonic Ventricular Cell Isolation 35

2.7 Embryonic Ventricular Cell Primary Cultures and Drug Treatments 36

2.8 Total RNA Extraction from Ventricular Cells 39

2.9 RNA Purity and cDNA Reverse Transcription 40

2.10 Real Time Quantitative Polymerase Chain Reaction (RT-qPCR) and Primers 40

2.11 RT-qPCR Analysis 42

2.12 Immunostaining and Cell Proliferation Assay 42

2.13 EdU and Cell Count Quantification 44

2.14 Second Messenger cAMP Assay 45

2.15 Statistical Analysis 47

Chapter 3: Results 49

3.1 Gene expression analysis of conduction system markers (Cx40, Cntn2 and HCN4) in the developing mouse ventricles 49

3.2 Immunodetection of conduction system proteins Cx40, HCN4, and Cntn2 in E11.5 and Adult cardiac cross-sections 52

3.3 Identification of proliferating ventricular conduction system cardiac progenitor cells (VCS CPCs) and ventricular conduction system cardiomyocytes (VCS CMs) 55

3.4 Characterizing the effect of Isoproterenol on the proliferation of ventricular conduction system cardiac progenitor cells (VCS CPCs) and ventricular conduction system cardiomyocytes (VCS CMs) 57

3.5 Characterizing the effect of Isoproterenol on the differentiation of E11.5 ventricular cells into the ventricular conduction system cell lineage 59

3.6 Characterizing the effect of Metoprolol on the differentiation of E11.5 ventricular cells into the ventricular conduction system cell lineage 62

3.7 Characterizing the effects of isoproterenol, ascorbic acid, and metoprolol on production of second messenger cAMP in E11.5 ventricular cells 66

Chapter 4: Discussion 72

4.1 Summary of Results 72

4.2 Developmental expression of ventricular conduction system genes 76

4.3 Effect of Beta-adrenergic stimulation on conduction system cell development 77

4.4 The effect of Beta-adrenergic receptor inhibition on conduction system cell development 80

4.5 Effect of Ascorbic Acid 82

4.6 Effect of ISO, AA and METO on cAMP production through Beta-adrenergic receptor signaling 84

4.7 Limitations and Future Directions 89

4.8 Conclusion 91

References 92

LIST OF TABLES

Table 2.1 Primary antibodies and dilutions (in blocking buffer) used for immunofluorescence analysis. 33

Table 2.2 Secondary antibodies and dilutions (in blocking buffer) used for immunofluorescence analysis. 33

Table 2.3 Preparation of dose treatments for Isoproterenol (from 1mM ISO stock) and Metoprolol (from 1mM METO stock), with and without the supplementation of Ascorbic Acid (from 10mM AA stock) diluted in 10 % FBS-DMEM to make a total volume of 10 ml. 38

Table 2.4 Primers used in Real-time quantitative polymerase chain reaction (RT-qPCR), primer sequence from (5' to 3'), and expected amplicon size (bp) 41

Table 3.1 Relative fold change in Cx40 gene expression with treatments of Isoproterenol, Ascorbic Acid and Metoprolol 64

Table 3.2 Relative fold change in Cntn2 gene expression with treatments of Isoproterenol, Ascorbic Acid and Metoprolol 64

Table 3.3: Assessment of changes in endogenous cAMP in E11.5 ventricular cells treated with metoprolol in combination with/without isoproterenol and ascorbic acid. 68

Table 4.1: Summary of key findings 74

Table 4.1: Summary of key findings (Cont.) 75

LIST OF FIGURES

Figure 1.1: Differentiation of Cardiac Progenitor Cells. 13

Figure 1.2: Mesodermal derivation of Cardiac Progenitor cells 15

Figure 1.3: Cardiomyocyte contraction 18

Figure 1.4: The cardiac conduction system within the heart 21

Figure 1.5: Beta-Adrenergic Receptor Activation-induced cardiac contractility 27

Figure 2.1: Generation of the cAMP standard curve 48

Figure 3.1: RT-qPCR analysis of Conduction system gene expression for markers Cx40, Cntn2, HCN4 and GAPDH in the developing mouse ventricles from E11.5, E14.5, E16.5, Neonatal, and Adult hearts 51

Figure 3.2: Immunostaining analysis of conduction system gene expression for HCN4, Cx40, and Cntn2 from E11.5 whole mouse heart cross-sections 53

Figure 3.3: Immunostaining analysis of Cntn2 expression in adult mouse heart cross-sections ..54

Figure 3.4: Identification of proliferating ventricular conduction system cardiomyocytes (VCS CMs) and ventricular conduction system cardiac progenitor cells (VCS CPCs) in E11.5 mouse ventricular cells. 56

Figure 3.5: Proliferation analysis of ventricular conduction system cardiomyocytes (Cx40+/MF20+/EdU+) and ventricular conduction system cardiac progenitor cells (Cx40+/MF20-/EdU+) from E11.5 murine ventricular cells treated with or without isoproterenol and ascorbic acid. 58

Figure 3.6: Differentiation analysis of ventricular conduction system marker gene expression of Cx40, Cntn2, HCN4 and GAPDH from isoproterenol and ascorbic acid treated E11.5 murine ventricular cells 61

Figure 3.7: Differentiation analysis of ventricular conduction system marker gene expression of Cx40, Cntn2, and HCN4 from metoprolol treated E11.5 murine ventricular cells 65

Figure 3.8: Assessment of changes in endogenous cAMP in E11.5 ventricular cells treated with varying doses of ascorbic acid 69

Figure 3.9: Assessment of changes in endogenous cAMP in E11.5 ventricular cells treated with varying doses of isoproterenol with/without ascorbic acid supplementation. 70

Figure 3.10: Assessment of changes in endogenous cAMP in E11.5 ventricular cells treated with metoprolol in combination with/without isoproterenol and ascorbic acid. 71

Figure 4.1: Proposed signaling pathway for increased VCS gene expression 88

ABSTRACT

Myocardial regenerative treatments with cardiac progenitor cells (CPCs) have been emerging as viable treatment options for myocardial injury. CPCs have the potential to differentiate into working cardiomyocytes and conduction system cardiomyocytes, however mechanisms of differentiation have yet to be studied. In this study the effect of β -adrenergic stimulation, with Isoproterenol (ISO), and inhibition, with metoprolol (METO), were analyzed on ventricular conduction system (VCS) generation from embryonic day 11.5 mice ventricles (containing populations of CPCs). The effects of supplementation of a reducing agent, ascorbic acid (AA), were also studied on enhancement of ISO actions on VCS gene expression. This study showed that both ISO-alone and in combination with AA was able to enhance VCS marker gene expression, through an increase in cAMP. Furthermore, METO was able to negate the ISO-induced increases in VCS gene expression and cAMP levels. This study indicates a role for β-adrenergic receptor signaling in VCS cell development.

LIST OF ABBREVIATIONS AND SYMBOLS USED

α	Alpha
β	Beta
β-AR	Beta -adrenergic receptor
Δ	Change
°	Degree
µL	Microliter
µm	Micrometer
µM	Micromolar
%	Percent
ACE	Angiotensin converting enzyme
AHF	Anterior heart-forming field
AB/AM	Antibiotic and antimycotic
AV	Atrioventricular
AP	Action potential
ATP	Adenosinetri-phosphate
AC	Adenylyl cyclase
BMSC	Bone marrow stem cells
BMPs	Bone morphogenetic proteins
BMSCs	Bone Marrow-Derived Stem Cells
CABG	Coronary artery bypass graft
Ca^{2+}	Calcium
cAMP	Cyclic adenosine 3', 5'-monophosphate
CCS	Cardiac conduction system
CDSCs	Cardiac-Derived Stem Cells
COMT	Catechol-o-methyltransferase
CPCs	Cardiac Progenitor cells
CMs	Cardiomyocytes
Cl^-	Chloride
cDNA	Complementary DNA

CHF	Congestive heart failure
Cx40	Connexin-40
Cx43	Connexin-43
Cntn2	Contactin-2
DCM	Dilated cardiomyopathy
DMEM	Dulbecco's modified eagle medium
E	Embryonic day
ERK	Extracellular signal-regulated kinases
ESC	Embryonic stem cell
FGF2	Fibroblast growth factor 2
FHF	First heart field
g	Grams
GAPDH	Glyceraldehyde 3-phosphate dehydrogenase
GDP	Guanosine diphosphate
GMP	Guanine monophosphate
GPCRs	G-protein-coupled receptors
GPI	Glycosyl phosphatidylinositol
GTP	Guanine triphosphate
H_2O	Water
H_2O_2	Hydrogen Peroxide
HCN4	Potassium/sodium Hyperpolarization-activated cyclic nucleotide-gated channel
hESC	Human embryonic stem cell
HMG-coA	3-Hydroxy-3-methylglutaryl-coenzyme
HPSCs	Human pluripotent stem cells
IBMX	1-Methyl-3-(2-methylpropyl)-7H-purine-2,6-dione
ICI	ICI-118,551
iPSC	Induced pluripotent stem cell
ISO	Isoproterenol
K^+	Potassium

LDL-C	Low-density lipoprotein cholesterol
LTCC	L-type Ca^{2+}channels
LV	Left ventricle
LVEF	Left ventricular ejection fraction
MAO	Monoamine oxidase
MAPK	Mitogen activated protein kinase
METO	Metoprolol
MF20	Sarcomeric myosin heavy chain
MI	Myocardial Infraction
MLC	Myosin light chain
MSC	Mesenchymal stem cell
Na^{+}	Sodium
NE	Norepinephrine
Nkx2.5	NK2 transcription-factor related, locus 5
nM	Nano molar
PBS	Phosphate buffered saline
PCR	Polymerase chain reaction
PF	Purkinje Fiber
PKA	Protein Kinase A
PLB	Phospholamban
PS	Primitive streak
qPCR	Quantitative polymerase chain reaction
RNA	Ribonucleic acid
RyR	Ryanodine receptor
SA	Sinoatrial
T-Tubules	Transverse tubules
SDS	Sodium dodecyl sulfate
SHF	Second heart field
SKM	Skeletal Myoblasts
SNP	Sodium nitroprusside

SERCA	Sarco/endoplasmic reticulum Ca^{2+}-ATPase SL Sarcolemma
SR	Sarcoplasmic reticulum
TAG-1	Transiently expressed axonal glycoprotein 1
VCS	Ventricular conduction system
VEGF	Vascular endothelial growth factor
VT	Ventricular tachycardias

ACKOWLEDGMENTS

First and foremost, I would like to thank my supervisor Dr. Kishore Pasumarthi for his guidance, support and understanding throughout my study. His enthusiasm and dedication towards research and science inspired me to work passionately over the last two years. His teaching style and instruction, allowed for me to better grow my own abilities as a researcher. I am forever thankful and grateful for his advice and encouragement.

I would also like to extend my thanks toward all members of the Pasumarthi lab, past and present, for their assistance, insight and friendship. A special thanks to Dr. Mark Baguma, and Sarita Chinni for their guidance and assistance throughout my endeavor. Furthermore, a special thanks to Abhishek Mishra for his support, guidance and friendship that allowed me to grow as a scientist.

I would like to thank my advisory committee, Dr. Susan Howlett, and Dr. Keith Brunt, as well as our graduate coordinators Dr. Morgan Langille and Dr. Denis Dupre for their valuable support and advice over the last two years. I would also like to express my gratitude to the administrative staff in the Department of Pharmacology, Luisa Vaughan, Sandi Leaf, and Lori Lawson for all of their assistance.

I would also like to express my sincere appreciation to my thesis examining committee, Dr. Susan Howlett, and Dr. Ketul Chaudhary for reviewing my thesis work.

Lastly, I would like to thank my family and friends for their encouragement and support throughout my graduate studies.

Chapter 1: Introduction

1.1 Thesis Overview

The cardiovascular system is responsible for distributing oxygen through vessels to every living cell in our body. A myocardial infarction or heart attack occurs when the blood and oxygen flow to the heart are blocked due to occlusions in one or more blood vessels. Lack of oxygen and blood supply to the heart leads to ischemia and myocardial cell death. Despite a successful reperfusion, the damage to myocardial tissue may persist leading to cardiac dysfunction. Stem and progenitor cell-based transplantation therapies are emerging as supplemental strategies for myocardial repair (Liu et al., 2018; Shiba et al., 2016). However, life-threatening ventricular arrhythmias are frequently reported as adverse side effects of cell transplantation in both preclinical and clinical studies possibly due to the formation of ectopic pacemaking cells (Liu et al., 2018; Shiba et al., 2016). Therefore, it is important to understand the mechanisms regulating cardiac conduction system (CCS) cell development. While the nodal cells within the CCS are considered the fastest pace making cells, many slow pacemaker cells are found within the His bundle and Purkinje fibers which form the ventricular conduction system (VCS). My master's research will focus on the identification of activators and inhibitors that play a role in the VCS cell development through the analysis of Purkinje cell (PC) generation in embryonic mouse ventricular cell cultures.

A previous study by Tsai et al. noted that sodium nitroprusside (SNP) promotes Purkinje like cell differentiation through activation of cAMP signaling pathway in embryonic stem cell (ESC) cultures (Tsai et al., 2015). Although SNP is a nitric oxide donor known to activate soluble guanylyl cyclase and increase cGMP levels, it was also shown to activate protein kinase

A and increase cAMP through an iron dependent mechanism (Hottinger et al., 2014). Furthermore, Tsai et al. demonstrated loss of Purkinje fibre (PF) phenotype in stem cell cultures treated with inhibitors of cAMP pathway (Tsai et al., 2015). Studies from the Pasumarthi laboratory found that a nonselective β-adrenergic receptor (β-AR) agonist, isoproterenol (ISO) can increase cAMP levels in both embryonic day 11.5 (E11.5) ventricular cell cultures (Feridooni et al., 2017) and fractionated E11.5 cardiac progenitor cells (CPC) and cardiomyocytes (CMs) (Feridooni & Pasumarthi, 2019). Whereas, β1-AR antagonist, metoprolol (METO) abolished the stimulatory effects of ISO on cAMP levels (Feridooni et al., 2017). Chronic stimulation of recipient mice with ISO after E11.5 ventricular cell transplantation significantly reduced the graft size, while METO protected the grafts from the inhibitory effects of ISO (Feridooni et al., 2017).

My project examined the effects of ISO on E11.5 mouse ventricular cell cultures with a focus on VCS cell development. Sympathetic neurons were first detected between E12.5 and E14.5 stages in rat and mouse hearts (Chen et al., 2006; Gomez, 1958). Notably, development of VCS components begins only after E11.5 and a fully functional VCS appears after E17.5 (Christoffels & Moorman, 2009; Viragh & Challice, 1977) and these reports collectively suggest a role for sympathetic nervous system, catecholamines and β-AR signaling in the formation of VCS cells. Thus, ISO a non-selective β-AR agonist and E11.5 ventricles which do not have Purkinje fibers would serve as tools to study the role of β- AR signaling in VCS development. Advancements in treatments for myocardial tissue specific injury with transplantable CPCs while preventing ectopic arrythmias requires the understanding of the effect of β- AR signaling on the proliferation and differentiation of VCS cells. The following will entail the hypotheses and corresponding objectives of this study:

1.) The first hypothesis addressed is that β-AR stimulation with ISO can increase the generation of VCS cells by simultaneously promoting differentiation of both CPC and CM fractions into a VCS cell lineage.

Objective 1: Measure VCS marker gene expression in Murine cardiac development [Connexin 40 (Cx40), Hyperpolarization Activated Cyclic Nucleotide gated potassium channel 4 (HCN4) and Contactin2 (Cntn2)].

Objective 2: Test the effects of ISO on proliferation and differentiation of E11.5 ventricular cells.

Objective 3: Determine the mechanisms responsible for β-AR mediated effects of ISO on VCS cell development through the analysis of cAMP production.

2.) The second hypothesis is that Ascorbic Acid will increase the efficacy of ISO effects on VCS cell proliferation and differentiation by preventing oxidation of ISO.

Objective 4: Test the effects of ISO with and without Ascorbic Acid supplementation on proliferation and differentiation of VCS cells.

Objective 5: Determine the mechanisms responsible for ISO and ascorbic acid mediated effects on VCS development through the analysis of cAMP production

3.) The third hypothesis is that β blockers can prevent antiproliferative and pro-VCS differentiation effects of ISO.

Objective 6: Examine the effects of β -AR inhibition with metoprolol on differentiation of VCS cells.

Objective 7: Determine the mechanisms responsible for β -AR inhibition mediated effects of Metoprolol on VCS development through the analysis of cAMP production

Through the completion of these objectives, further insight will be gained as towards whether (i) adrenergic receptor stimulation will lead to the formation of ectopic pace making

cells (ii) β-blockers can improve the efficacy of cell-based therapies by preventing the incidence of arrhythmias.

1.2 Cardiac Injury and Healing

In 2015, the World Health Organization reported that the leading cause of mortality was coronary heart disease (CHD), with approximately 7.4 million deaths throughout the world (Chadwick et al., 2019). Myocardial infarction (MI) is the most common form of CHD and is defined as ischemic death of myocardial tissue (Frangogiannis, 2015; Thygesen et al., 2007). Infarcts are most frequently caused by the rupture of atherosclerotic plaque, which builds up in arteries, and subsequent thrombosis leads to the occlusion of coronary vessels (Frangogiannis, 2015; Thygesen et al., 2007). Occluded vessels impede the flow of blood and result in decreased oxygen and nutrient supply, without which ischemia and cell death occurs in myocardial tissue (Frangogiannis, 2015; Thygesen et al., 2007). Myocardial tissue has limited regenerative potential and following cardiac injury, the innate inflammatory response is activated and scaring replaces dead/injured tissue (Prabhu & Frangogiannis, 2016; Richardson et al., 2015).

1.2.1 Myocardial wound healing

As illustrated by Richardson et al., Myocardial wound healing occurs in three stages; early inflammatory phase, fibrotic phase, and long-term remodeling phase (Richardson et al., 2015).

The early inflammatory phase, depicts the infiltration of neutrophils, macrophages, and lymphocytes at the ischemic site in the heart, resulting in resorption of necrotic tissue (Richardson et al., 2015). The necrotic tissue is further degraded by proteinases and replaced by

an initial temporary matrix of fibrin, fibronectin, laminin, and glycosaminoglycans, which is later structurally fixed with collagen (Richardson et al., 2015). Inflammation is upregulated by inflammatory mediators and complex signaling leading to the upregulation of fibroblasts and the beginning of the fibrotic phase (Richardson et al., 2015). Fibrotic phase is the increased accumulation of collagen and continued proliferation and differentiation of myofibroblasts (Richardson et al., 2015). The long-term remodeling phase is depicted by maturation of scar tissue as it is stabilized by accumulation of collagen (Richardson et al., 2015).

1.2.2 Scar formation

The collagen scar is stiffer than myocardial tissue making ventricular filling harder and based on the location of the scar it can further interfere with electrical conduction within the heart (Azevedo et al., 2016; Richardson et al., 2015). The collagen scar can interrupt the electrical conduction within the heart resulting in possible arrythmias, sustained tachycardia and/or fibrillation (Azevedo et al., 2016; Richardson et al., 2015). In addition to the development of possible arrhythmogenesis, cardiac injury results in cardiac remodeling. Cardiac remodeling is defined as cellular and morphological changes in size (atrial/ventricular cavity diameter), mass (hypertrophy and atrophy), geometry (heart wall thickness and shape), leading to negative functional consequences in the heart (Azevedo et al., 2016). The original thickness of the heart is altered after a myocardial injury as a scar forms and results in progressive thinning and lengthening of the infarcted area leading to both dilation and expansion of the heart cavity (Azevedo et al., 2016). The expanded and dilated regions of the cavity then become vulnerable to the possibility of a fatal rupture of the cardiac wall (Azevedo et al., 2016). The stiff scaring and adverse cardiac remodeling affect overall heart function and can progress to cardiac dysfunction

and eventual heart failure as the scarring progresses and cardiac function decreases (Azevedo et al., 2016; van den Borne et al., 2010).

1.2.3 Post-MI Treatment

Immediately following an infarct, the primary aim is for successful reperfusion therapy by restoring blood flow to the occluded vessel through anticoagulant, antiplatelet and thrombolytic treatments (Boersma et al., 2003; Saleh & Ambrose, 2018). If reperfusion is not successful coronary angioplasty, stent placement or coronary artery bypass graft surgery will be considered to improve blood flow (Saleh & Ambrose, 2018; Weisse, 2011). While blood flow can be successfully reestablished in the injured myocardial tissue, scarring and cardiac remodeling are more difficult to address. Current therapeutic strategies focus on preventing further damage and maintaining cardiac function rather than repairing and regenerating the injured tissue. A few of the current interventions used in post-MI management include Aspirin, β-Blockers, Angiotensin-converting-enzyme inhibitors (ACE-inhibitors), Statins, and catheter-based tissue ablation (Boersma et al., 2003; Richardson et al., 2015).

Aspirin is administered as a method of secondary prevention as patients who have suffered a cardiac injury are at high risk for a repeat event (Ittaman et al., 2014). Aspirin works as an antithrombotic treatment as it is an irreversible cyclooxygenase (COX) inhibitor and additionally suppresses the production of prostaglandin (Ittaman et al., 2014). The side effects of continued use of aspirin are dose-dependent and can result in hypertension, gastrointestinal/ renal toxicity and in rare cases intracranial bleeding (Ittaman et al., 2014).

Post-MI management with ß-blockers helps to reduce the workload of the heart by decreasing heart rate, blood pressure and cardiac output (Kezerashvili et al., 2012). The

reduction in the workload prevents secondary infarction and early administration also helps prevent tachycardic arrhythmogenesis and limits infarct size (Kezerashvili et al., 2012). The side effects of continued use of ß-blockers include bradycardia, hypotension, depression and onset of diabetes (Kezerashvili et al., 2012).

ACE-inhibitors are also effective in reducing remodeling, ventricular dysfunction and heart failure associated with an atherosclerotic infarction (Bonarjee & Dickstein, 2001; Khalil et al., 2001; Yoshiyama et al., 2005). Secondary MI prevention through ACE-inhibitors works by preventing the conversion of angiotensin-1 into angiotension-2 (Bonarjee & Dickstein, 2001; Khalil et al., 2001; Yoshiyama et al., 2005). Angiotensin-2 binds to AT_1 receptors and increases blood pressure through direct vasoconstriction and stimulates the secretion of aldosterone from the adrenal cortex which in turn promotes the retention of sodium and water (Benigni et al., 2010). ACE-inhibitors prevent the conversion of angiotensin-1 into angiotension-2 and thus reduce blood pressure and systemic vascular resistance, both of which aid in post-MI management (Bonarjee & Dickstein, 2001; Khalil et al., 2001; Yoshiyama et al., 2005). ACE-inhibitors additionally regulate and reduce the hypertrophic response seen during cardiac remodeling (Bonarjee & Dickstein, 2001; Khalil et al., 2001; Yoshiyama et al., 2005). Adverse effects of continued ACE-inhibitor use are possible hyperkalemia, jaundice, and renal impairment (Parish & Miller, 1992).

After a myocardial infarct, Statins also known as 3-hydroxy-3-methylglutaryl-coenzyme A (HMG-coA) reductase inhibitors are primary-line treatments in the reduction of low-density lipoprotein cholesterol (LDL-C) (Ross et al., 1999; Wang et al., 2018). LDL-C is reduced as statins inhibit HMG-coA, a hepatic enzyme responsible for the synthesis of cholesterol (Ross et al., 1999). LDL-C levels have been shown to have a direct correlation with atherosclerosis and

cardiovascular disease, reductions of which can prevent the further build-up of arterial plaque and a secondary infarct (Ross et al., 1999; Wang et al., 2018). Side effects of continued statin use are possible myositis, myopathy, myalgia, glycemia, hepatotoxicity, peripheral neuropathy, impaired myocardial contractility, and autoimmune diseases (Beltowski et al., 2009; Golomb & Evans, 2008).

Following a myocardial infarct, the damage to conductive tissue can result in the development of ventricular tachycardias (VT) and catheter-based tissue ablations are considered as treatment options (Stevenson et al., 1998). Single VTs are easier to rhythm and pace map irregular conduction sites for catheter ablations with radiofrequency, however, multiple morphological VTs occur with MI and become more difficult to manage (Stevenson et al., 1998). Even with successful ablations often antiarrhythmic drug management with amiodarone may be required (Stevenson et al., 1998). Arrhythmias left untreated can be fatal, and sometimes the implementation of pace-making devices becomes necessary in order to properly manage the irregular rhythm (Xiao, 2011).

1.3 Potential Cardiac Cell-based Therapy

Cardiac injury results in irreparable damage to the myocardial tissue, in part due to the limited regenerative potential of cardiac cells. While post-MI maintenance with medication can aid in the prevention of a secondary infarct, the adverse effects of continued treatments can have detrimental effects to the systemic health of the patient. Additionally current therapeutic strategies can work to reduce ongoing damage, however lost myocardial tissue and function are unable to be recovered. If the goal for MI treatment were to repair and heal instead of treating symptoms, then a different approach must be considered. An ideal alternative treatment must

successfully address the loss of myocardial cells caused by ischemic death, revascularize injured regions and prevent cardiac remodeling (Dai et al., 2005). Cell-based therapies have shown to be competent in addressing these concerns through the secretion of cardioprotective and scar-limiting paracrine factors, and induction of myogenesis to replace and induction of angiogenesis to revascularize the injured tissue (Dai et al., 2005; van den Bos et al., 2008). Furthermore, cell-based therapies have been shown to be capable of improving the mechanical properties of the ischemic tissue, and reduce the adverse cardiac remodeling (van den Bos et al., 2008). Currently there are a variety of transplantable cells being considered for cell-based therapies, such as Skeletal Myoblasts (SkM), Bone Marrow-Derived Stem Cells (BMSCs), Embryonic Stem Cells (ESCs), Cardiac-Derived Stem Cells (CDSCs)/ Cardiac Progenitor cells (CPCs)(Barreto et al., 2019; Chang et al., 2020; Leite et al., 2015; Parmacek, 2006; van den Bos et al., 2008).

1.3.1 Skeletal Myoblasts

SkMs have been shown to be capable of increasing contractility of scarred tissue, and differentiating into cardiomyocytes to increase wall thickness in dilated ventricles (van den Bos et al., 2008). However, the ability of SkMs to differentiate into cardiomyocytes has been questioned, as transplanted SkMs could possibly be fusing with native cardiomyocytes rather than converting into true cardiomyocytes (van den Bos et al., 2008). SkMs do not raise ethical concerns as they are available in large numbers from a small host muscle biopsy and not from embryos (van den Bos et al., 2008). However, there is controversy regarding effective electromechanical coupling between myoblasts and host myocardium (van den Bos et al., 2008). Myoblasts in skeletal muscles are individually innervated by their own motor unit, whereas myocardium relies on the propagation of action potentials via cell-cell contact through channels

of gap junction proteins such as Connexin-43 (Cx43) and Connexin-40 (Cx40) (van den Bos et al., 2008). Furthermore, preliminary clinical studies noted the development of tachycardic arrythmias with myoblast transplantation (Cleland et al., 2007).

1.3.2 Bone Marrow-Derived Stem Cells

There are a multiple cell populations within BMSCs such as BMSCs expressing cell antigen c-kit, endothelial progenitor cells (angioblasts), and Mesenchymal stem cells (MSCs) (van den Bos et al., 2008). c-kit BMSCs were effective in increasing global heart function, as they were able to restore myocardial contractility within the infarcted scar and vascular tissue (van den Bos et al., 2008). However, the regenerative potential of these cells is in question because of possible fusion with native cardiomyocytes and decreased overall plasticity (van den Bos et al., 2008). Angioblasts were shown to decrease apoptosis of cardiomyocytes and improve cardiac function, however the incorporation of transplanted cells into the vasculature of injured tissue has been questioned (van den Bos et al., 2008). These cells were shown to secrete pro-arteriogenic factors that develop new or collateral vessels for vasculature (van den Bos et al., 2008). MSCs are capable of differentiating, increasing heart function and inducing angiogenesis (van den Bos et al., 2008).

1.3.3 Embryonic Stem Cells

ESCs are pluripotent and as such can differentiate into all three germ layers of ectoderm, endoderm, and mesoderm (Singla, 2009). Consequently, transplanted ESCs have the potential to differentiate into cardiomyocytes, but to enhance differentiation requires the exposure to growth factors/cytokines such as TGF- β2, bone morphogenic protein (BMP2) or fibroblast growth

factor 2 (FGF2) (Singla, 2009). Undifferentiated ESCs can be transplanted as well and both undifferentiated and differentiated ESCs have been shown to increase heart function (Singla, 2009). However, in graft transplantation treatments, the limitations of ESCs become apparent as both differentiation and regeneration are reduced (Singla, 2009). Additionally there is a high risk associated with the use of ESCs as their very pluripotent nature makes them prone to develop teratomas (Singla, 2009). Many studies have focused on the techniques of differentiating ESCs into the cardiomyocyte lineage, and of the cell populations that have been popularly studied are the human embryonic stem cells (HESCs) and induced pluripotent stem cell (iPSCs), collectively called human pluripotent stem cells (HPSCs)

HPSCs are effective treatment for cardiac regeneration as they can differentiate into various tissue specific cell types to repair injured myocardial tissues (Almeida et al., 2015). However, isolation of specific cell types is required from the heterogenous populations of atrial, nodal, and ventricular cardiomyocytes (Almeida et al., 2015). Purification of cell types is important as atrial, nodal, and ventricular cardiomyocytes differ in their electrophysiological properties and their excitation-contraction coupling mechanisms (Ng et al., 2010).

Successful integration of HPSCs in injured myocardial tissue, must consider these differences to function properly without the formation of arrhythmias (Almeida et al., 2015; Ng et al., 2010).

1.3.4 Cardiac-Derived Stem Cells/ Cardiac Progenitor cells

Over the numerous years of study of stem cells, the criteria to be classified as a Cardiac-Derived Stem Cell (CDSC) has become defined (Parmacek, 2006). A stem cell must meet the following four conditions to be considered a CDSC: 1) ability to sequentially self-renew through

cell division; 2) the daughter cell from the stem cell must be able to differentiate into more than one cell type; 3) in damaged tissue, the cells must replicate and recapitulate the function and lineage of the original tissue; and 4) in the absence of damaged tissue cells must be able to produced differentiated progeny (Parmacek, 2006). CDSCs are multipotent and can differentiate into various mesodermal cells including cardiomyocytes, smooth muscle cells, and endothelial cells.

CPCs have not been strictly classified as CDSCs, however CPCs are fated towards the cardiac lineage and can be distinguished by the expression of cardiac markers and transcription factors such as GATA4, Nkx2.5 and MEF2C (Cambria et al., 2016). CDSCs and CPCs have the potential to differentiate into both working cardiomyocytes (CMs) and ventricular conduction system cells (VCS) (Figure 1.1) (Cambria et al., 2016). CMs are contractile and thus express sarcomeric myosin and can be distinguished in culture by staining with Monoclonal Antibody MF20 (López-Unzu et al., 2019). VCS cells on the other hand can be distinguished through the expression of conduction system markers such as Connexin-40 (Cx40), Contactin-2 (Cntn2) and Hyperpolarization Cation-Selective Nucleotide Gated Cation Channel (HCN4)(Liang et al., 2015; Ng et al., 2010; B. Pallante et al., 2010). Treatment with these CPCs increased overall heart function by increasing left ventricular ejection fraction (LVEF), decreasing scar size, and reducing adverse remodeling (Cambria et al., 2016). While CDSCs and CPCs have demonstrated their regenerative potential, the complete mechanisms of proliferation and differentiation are still unknown (Cambria et al., 2016). The use of CPCs in cardiac regeneration requires controlling the differentiation of transplanted cells as unregulated differentiation and proliferation of conduction system cells can result in the formation of ectopic arrhythmogenic foci (Liu et al., 2018). Inappropriate growth of conduction system cells can result in spontaneous ectopic beats in

cardiac locations that do not follow the natural rhythm set by the heart and result in cardiac dysfunction. Understanding how transplanted cells can be induced into a specific cell-lineage can be beneficial in targeting tissue and cardiac region-specific regeneration. In this regard, it becomes imperative to examine cardiac development and factors that influence growth and differentiation of conduction system cells.

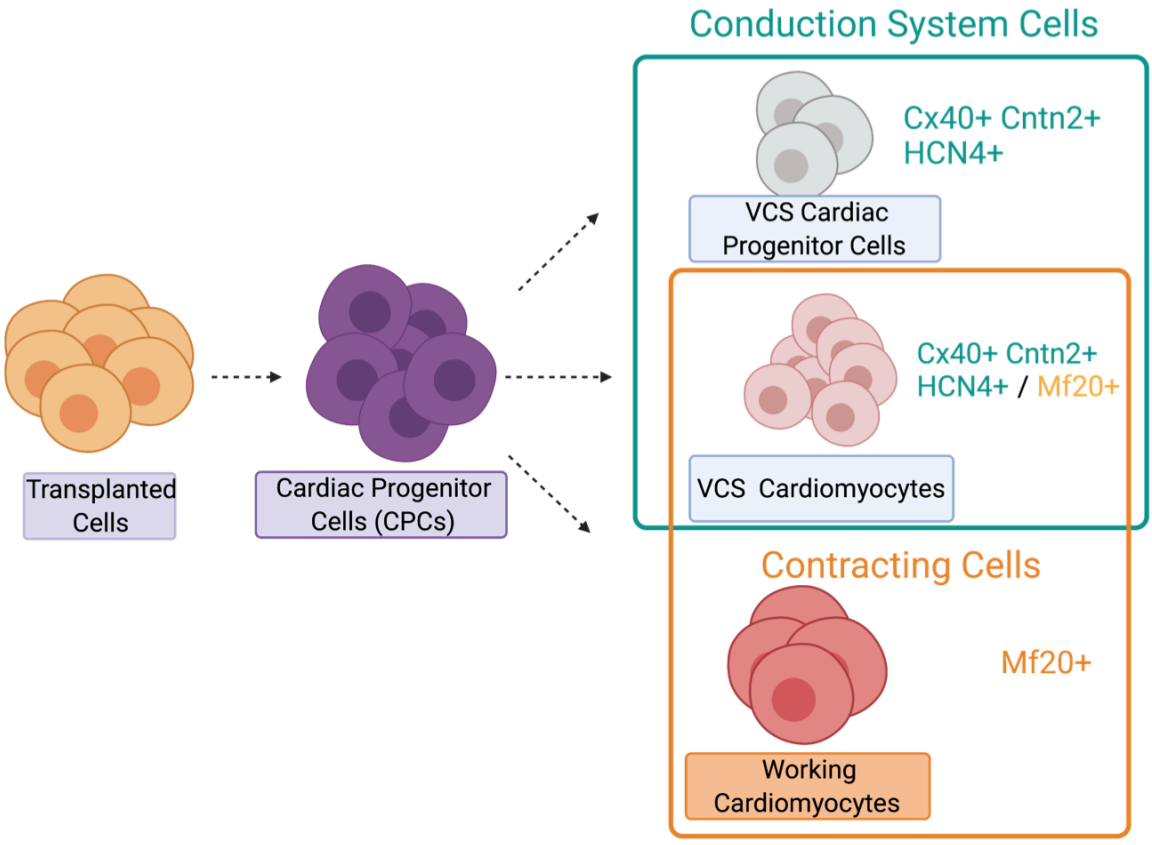

Figure 1.1: Differentiation of Cardiac Progenitor Cells.
Cardiac progenitor cell (CPC) population from transplanted cells can differentiation into working cardiomyocytes (positive for MF20 expression, negative for CCS markers Cx40, Cntn2, HCN4 expression), or ventricular conduction system (VCS) cardiomyocytes (positive for MF20, Cx40, Cntn2, HCN4 expression), or VCS CPCs (positive for Cx40, Cntn2, HCN4 expression, negative for MF20 expression) (Created with BioRender.com).

1.4 Cardiac Development

The heart is one of the most vital organs in the human body, being central to the cardiovascular system and responsible for oxygen and nutrient distribution. While passive oxygen diffusion is initially adequate in utero, with increased cellular demand the necessity of the cardiovascular system requires that the heart be the first organ to form (Tan & Lewandowski, 2020). Favorably, the mechanism of embryonic cardiogenesis remains conserved from species to species (Srivastava & Olson, 2000). Through analysis of cardiac systems from various species, commonly fruit fly, newt, zebrafish, boar, dog, rat, mouse and fowl, our understanding of the inner workings of cardiovascular development began to grow (Srivastava & Olson, 2000). The heart consists of three layers, the outer epicardium, middle myocardium, and inner endocardium (Smith & Bader, 2007). The outer epicardium consists of mesothelial cells, connective and adipose tissue that surround and protect the inner heart. The endocardium consists of endothelial cells that line the interior of the heart walls. The myocardium can be considered the thickest layer composed of cardiac muscle tissue. The myocardium originates from the primary heart tube and CPCs from the myocardium have the capacity to differentiate into working cardiomyocytes (CM) and cardiac conduction system cardiomyocytes (CCS CM) (Figure 1.2) (Gittenberger-de Groot et al., 2005; Zhang & Pasumarthi, 2007).

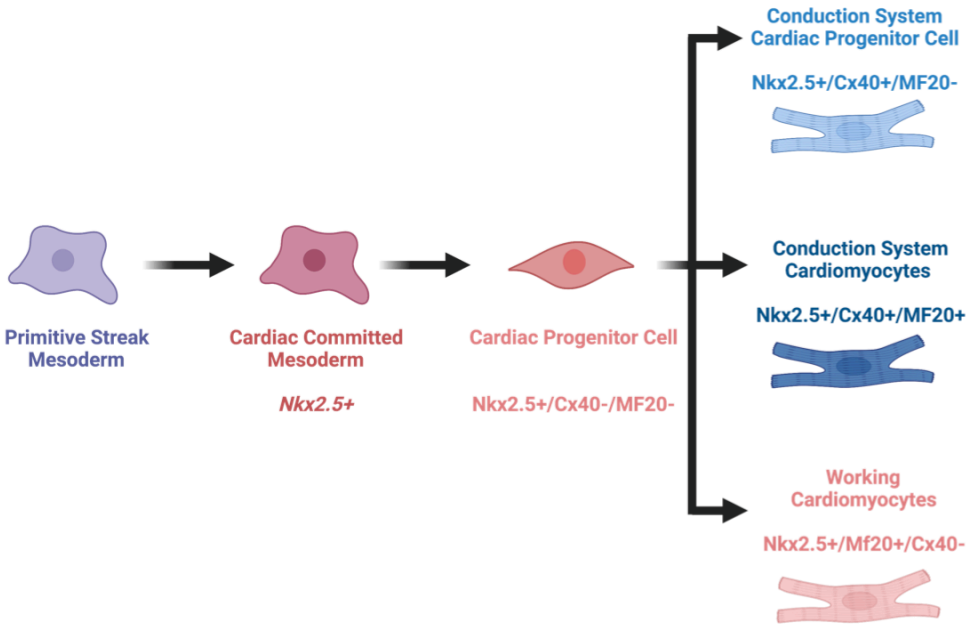

Figure 1.2: Mesodermal derivation of Cardiac Progenitor cells
Mesodermal cells originating from the primitive steak can commit to the cardiac lineage. One of the populations of cardiac committed mesodermal cells are the Cardiac progenitor cells. Cardiac progenitor cells can commit to the early cardiomyocyte lineage with expression of Nkx2.5. The early cardiac-fated Cardiac progenitor cell can then differentiate into either conduction system cardiac progenitor cells (Nkx2.5+/Cx40+/ MF20-), conduction system cardiomyocytes (Nkx2.5+/Cx40+/ Mf20+) or working cardiomyocytes (Nkx2.5+/Cx40-/ Mf20+). (Jeziorowska et al., 2015) (Created with BioRender.com)

1.4.1 Working Cardiomyocytes and Cardiac Contractions

The function of a working cardiomyocyte is to contract the individual chambers of the heart (Mikawa et al., 2003; Poelmann & Gittenberger-de Groot, 1999; Sedmera et al., 2000). The components that allow for this contraction are the intercalated disks, cell membrane (sarcolemma), T-tubules (invagination of the sarcolemma), sarcoplasmic reticulum, nucleus and the main contractile unit the sarcomere (Eisner et al., 2017). A complete contraction is initiated by the cardiac conduction system cell which generates and propagates an action potential (Eisner et al., 2017). An action potential is initiated by nodal cells in the sinoatrial node, and leads to

rapid depolarization in atrial and ventricular myocytes, followed by transient repolarization, a slowly decaying plateau, rapid repolarization, and then back to the resting state (Ng et al., 2010).

The action potential then results in excitation-contraction coupling (E-C coupling) with cardiomyocytes. E-C coupling refers to the propagation of an action potential with a rise in Ca^{+2} transient leading to myocardial contraction (Ng et al., 2010). An excitation from an action potential results in the opening of the L-type Ca^{+2} channels in the plasma membrane/ sarcolemma causing an influx of Ca^{+2} into the cardiomyocyte, sequentially triggering a contraction (Figure 1.3) (Ng et al., 2010). The voltage-gated calcium channels (VGCCS) on the sarcolemma are held within invaginations of the membrane referred to as T-tubules (Ng et al., 2010).

The opening of the voltage-gated calcium channels results in a calcium-induced calcium release in the cytoplasm, as calcium influx triggers opening of ryanodine receptors (RyR) and subsequent release of calcium stored within the sarcoplasmic reticulum (Eisner et al., 2017). The large increase in cytoplasmic calcium then interacts with the sarcomere (Eisner et al., 2017). The sarcomere is the contractile unit within the cardiomyocyte which is composed of thin-filament actin and thick-filament myosin contractile proteins, and regulated by proteins troponin and tropomyosin (Eisner et al., 2017). Calcium binding to troponin unblocks the actin sites allowing for the thick myosin filament to interact with thin actin filament causing the cell to shorten (Eisner et al., 2017). Multiple cardiomyocytes shortening in succession results in the larger contraction of the atria or ventricle and leads to the circulation of blood (Eisner et al., 2017). Between cardiomyocytes are intercalated disks containing desmosomes that anchor adjacent cardiomyocytes and gap-junction proteins responsible for maintaining transmission of the action potential (Eisner et al., 2017).

There are electrophysiological differences and differences in E-C coupling between nodal, atrial and ventricular cardiomyocytes. Starting with electrophysiological differences in humans, the transient outward current (I_{to}) in atrial myocytes has a greater amplitude and there are lower, shorter action potentials in comparison to ventricular myocytes (Ng et al., 2010). Another noticeable electrophysiological difference is that atrial myocytes have strong ultrarapid delayed rectifier potassium channels (I_{KUR}), characterized by rapid activation and slow inactivation of the outward current during the plateau phase; these channels are not expressed in ventricular myocytes (Ng et al., 2010). The presence of I_{KUR} in atria myocytes results in a faster activation and slower plateau than in ventricular myocytes (Ng et al., 2010). In regards to main differences in E-C coupling, E-C coupling in atrial myocytes differs from ventricular myocytes due to a difference in abundance of T-tubules (Ng et al., 2010). Spatially, atrial myocytes have fewer T-tubules than ventricular myocytes (Ng et al., 2010). Furthermore, due to the lack of T-tubules the calcium influx from VGCCs only originates at the periphery of the atrial cardiomyocyte as there is no protrusion of T-tubules into the center of the cardiomyocyte (Ng et al., 2010). Thus, atrial myocytes rely heavily on calcium-induced calcium release (CICR) from the sarcoplasmic reticulum (SR) to contract the centers of cardiomyocytes (Ng et al., 2010). Due to the difference in calcium patterning seen in atrial cardiomyocytes in comparison to ventricular cardiomyocytes, there is an overall temporal difference in depolarization and contraction (Ng et al., 2010).

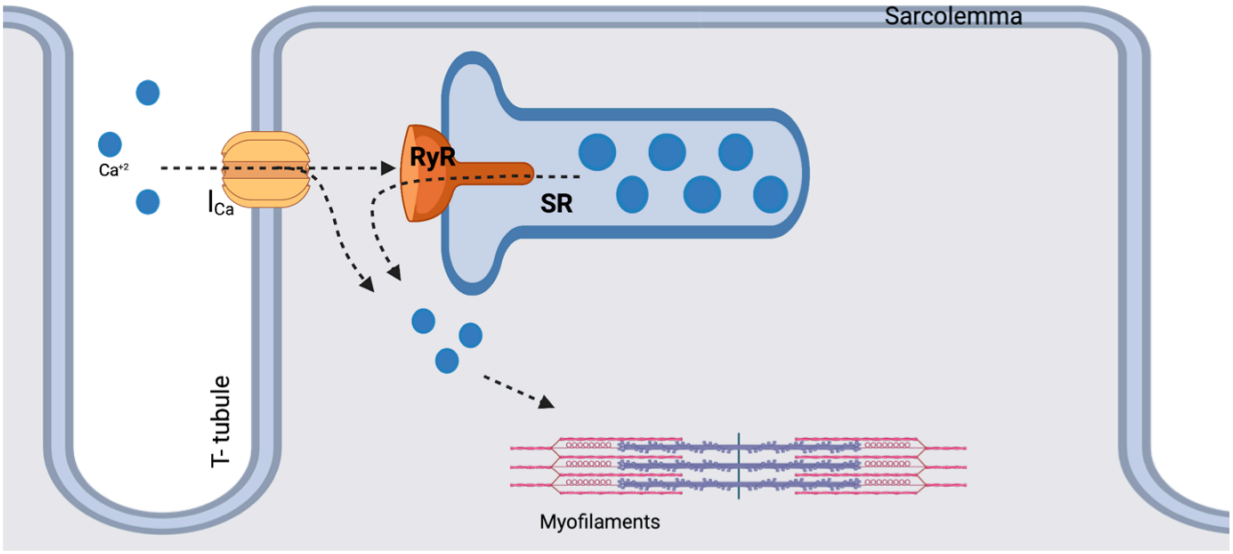

Figure 1.3: Cardiomyocyte contraction
An action potential results in the increase of calcium ion (Ca^{+2}) entering through the voltage-gated L-type Ca^{+2} channel in the sarcolemma. The increase in Ca^{+2} results in the opening of ryanodine receptors (RyR) and the further release of more Ca^{+2} from the sarcoplasmic reticulum (SR). A large presence of Ca^{+2} binds to troponin and activates cardiomyocyte contraction. (Bers, 2002) (Created with BioRender.com)

1.4.2 Conductive Cardiomyocytes and CCS development

Not all cardiomyocytes are equally conductive and, as previously mentioned, differential expression of genes with chamber specific functions is also seen in conduction specific proteins, such as connexin gap junction protein (Cx40), hyperpolarization cation-selective nucleotide gated cation channel (HCN4), and cell adhesion molecule Contactin-2 (Cntn2) (Liang et al., 2015; Mezzano et al., 2014; Monfredi et al., 2010; Pallante et al., 2010). Conductive cardiomyocytes differ from working cardiomyocytes in their electrophysiological properties and expression of cardiac conduction system (CCS) genes that are responsible for E-C coupling (Mezzano et al., 2014). Both CCS cardiomyocytes and progenitor cells can express conduction specific proteins contributing to the CCS development, however pathways regulating VCS development are still being investigated.

Current factors/ pathways investigated in regulating VCS development include endothelin-1 (ET-1), neuregulin-1 (NRG-1), notch-1, atrial natriuretic peptide (ANP), and SNP. ET-1 and NRG-1 have both been associated in the transition of avian and murine embryonic cardiomyocytes into the CCS lineage (Patel & Kos, 2005). In a previous study, NRG-1 and ET-1 when supplemented into embryonic mice cardiomyocyte cultures induced upregulation of CCS-specific gene expression of gap junction proteins Cx40 and Cx45, and transcription factors Nkx2.5, GATA4, Irx4, HF-1b and the K^+ channel modulator MinK (Patel & Kos, 2005). Additionally, immunofluorescence analysis of NRG-1 and ET-1 treated cardiomyocytes indicated increased fluorescence of Cx40 protein with treatments (Patel & Kos, 2005). Excluding upregulation of Nkx2.5, ET-1 induced similar upregulation in avian models (Patel & Kos, 2005; Takebayashi-Suzuki et al., 2001). Purkinje fibers, which have a primary role in impulse propagation, also consist of VCS cells expressing high levels of Nkx2.5 and GATA4 (Takebayashi-Suzuki et al., 2001).

Notch-1 signaling, through fibroblast influence, has also been shown to upregulate Purkinje-like phenotype in cardiomyocytes (Ribeiro da Silva et al., 2020). Fibroblasts have a primary role in maintenance of the extracellular matrix, however they are also seen enriched in VCS environments (Ribeiro da Silva et al., 2020). The activation of the Notch-1 pathway in rat embryonic cardiomyocytes by factors secreted from fibroblasts was shown to induce expression of VCS markers NAV1.5, Contactin-2 (Cntn2), and Cx40 (all of which are seen as Purkinje-like phenotype) (Ribeiro da Silva et al., 2020).

ANP is a natriuretic peptide with a primary role of regulating cardiovascular homeostasis, however it has also been seen expressed in the VCS forming regions (Evrard et al., 1999; Govindapillai et al., 2018). Additionally, ANP has also been shown to induce expression of VCS

genes HCN4 and Cx40 in E11.5 mice ventricular cell cultures, known to contain both populations of CPC and CMs (Govindapillai et al., 2018). The mechanisms behind how ANP stimulates the generation of cells expressing Purkinje fibre-phenotype remains to be studied (Govindapillai et al., 2018).

Another study characterized the effects of Sodium Nitroprusside on VCS development in ES cell cultures which will be further discussed below (Tsai et al., 2015).

1.5 The Cardiac Conduction System

The cardiac conduction system (CCS) functions to initiate and propagate rhythmic electric signals through the heart to induce synchronized contractions of the atria and ventricles (Christoffels & Moorman, 2009). The CCS can be further classified as the Atrioventricular Conduction system consisting of the Sinoatrial node (SAN), Atrioventricular node (AVN), and Atrioventricular bundle (AVB), and the Ventricular Conduction System (VCS) consisting of the His bundle, Left and Right bundle branches (LBB and RBB), and then the Purkinje fibers (PF) (Figure 1.4). The SAN is the pacemaker of the heart with autorhythmic cells that spontaneously depolarize to generate an action potential that propagates toward the AVN (Mezzano et al., 2014; Monfredi et al., 2010). The role of the AVN is to propagate action potentials down the bundle branches so that the PF can transmit and induce an excitation-contraction coupling with ventricular cardiomyocytes (Mezzano et al., 2014; Monfredi et al., 2010). Within the CCS, conduction specific proteins have various roles that contribute to the proper functioning of the CCS and have differential expression through the heart.

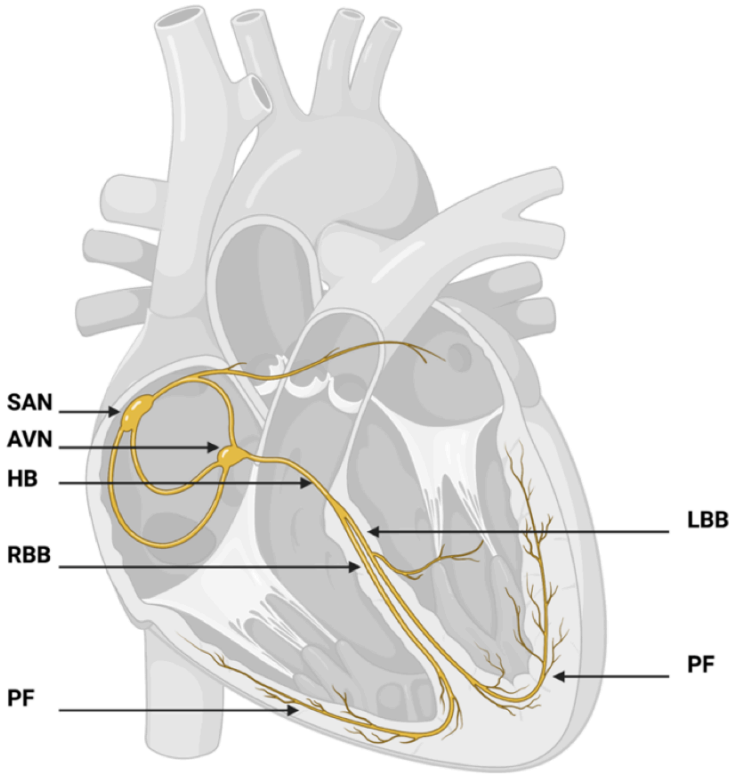

Figure 1.4: The cardiac conduction system within the heart
Action potential is initiated at the Sino-Atrial Node (SAN) and carried to the Atrioventricular Node (AVN). The AVN then propagates the action potential to the ventricular conduction system through the His-bundles (HB) which branch into the left bundle branch (LBB) and right bundle branch (RBB) and then finally to the Purkinje fibers (PF). The PF distribute the action potential to the ventricles of the heart. (DiFrancesco, 2010) (Created with BioRender.com).

1.5.1 Conduction system protein Cx40

The Gap junction protein Cx40 is responsible for cell-cell conduction of action potentials, necessary for E-C coupling (Giepmans, 2004; Willecke et al., 2002). Each Cx40 gap junction protein consists of six protein subunits (referred to as a hemichannel), and each subunit consistent of four-transmembrane proteins (Giepmans, 2004; Willecke et al., 2002). Two hemichannels in line/ contact allow for the permeation of small ions and molecules for one cell to another, including ions such as Ca^{+2}, molecules including second-messengers like cAMP, IP3 and nucleotides like ATP, and ADP (Giepmans, 2004; Willecke et al., 2002). Additionally, Cx40

has been found to be responsible for AVN conduction, without which AVN conduction is slowed (Verheule & Kaese, 2013). There are multiple connexin isoforms expressed in the murine heart, and Cx40 can be seen expressed in a mature heart in the atria and in the VCS (bundle branches, and PF) (Liang et al., 2015; Verheule & Kaese, 2013). The earliest expression of Cx40 in mice can be seen as early as embryonic day 11 (E11) and strictly conserved in the CCS after E14 (Verheule & Kaese, 2013). Cx40 expression is not seen in the SAN (Verheule & Kaese, 2013). Cx40 expression has been increased by transcription factors Nkx2.5 and Tbx5 meanwhile expression is decreased by Tbx2 and Tbx3 (Verheule & Kaese, 2013). Mutation or loss of Cx40 proteins reduces conduction and incidence of atrial fibrillation (Johnson & Camelliti, 2018).

1.5.2 Conduction system protein HCN4

HCN4 is one the earliest markers of the CCS lineage in progenitor cells during cardiogenesis (Liang et al., 2015). The role of HCN4 is in impulse initiation, essential for proper pacemaker functioning and as such HCN4 expression is primarily seen in the SAN (Liang et al., 2015). HCN4 generates spontaneous action potentials through a non-selective cation current (I_h). The earliest expression of HCN4 in mice is seen in E6 and in the First Heart Field (FHF) (Liang et al., 2015). In mature hearts, HCN4 expression can be seen throughout the entire CCS (Liang et al., 2015). As HCN4 expression is spread throughout the CCS, the specific function of HCN4 in working cardiomyocytes remains debatable (Liang et al., 2015). Upregulation of HCN4 can increase susceptibility to spontaneous excitation resulting in ectopic arrythmias (DiFrancesco, 2010). A single ectopic beat from distal PF could lead to the formation of re-entrant tachycardia and current mechanisms underlying development of ectopic/ pacemakers or induction of premature beats are not well understood (Deo et al., 2010).

1.5.3 Conduction system protein Cntn2

Cntn2 is a cell adhesion molecule, and in mice is known as transiently expressed axonal glycoprotein 1 (TAG-1) (Gurung et al., 2018; Pallante et al., 2010). Cntn2 was shown to be responsible for neuronal patterning and ion channel clustering (Pallante et al. (2010). The expression patterns of Cntn2 remain to be analyzed throughout murine cardiac development as Cntn2 is still a novel marker. However, Cntn2 is highly expressed in the SAN and in the distal portion of VCS in PF in the postnatal heart (Pallante et al., 2010). Cntn2 is a Glycosyl phosphatidylinositol (GPI)-anchored cell adhesion molecule expressed on the sarcolemma of PF myocardium (Pallante et al., 2010).

1.6 Directed Differentiation of CPC into the VCS lineage

Common to Cx40, HCN4 and Cntn2 proteins is that they are all expressed in the VCS in the distal PF tissue (B. Pallante et al., 2010; Smith & Bader, 2007; Verheule & Kaese, 2013). Understanding how to regulate expression of VCS proteins like Cx40, HCN4 and CNTN2 will allow for advancements in the field of cardiac cell transplantation by allowing us to control the growth and differentiation of transplanted CPCs. CPCs are an ideal candidate for cell transplantation therapy as they, unlike embryonic stem cells, are already cardiac fated and thus will not form teratomas (Cambria et al., 2016). CPCs can differentiate into multiple cell types including VCS cardiomyocytes, working cardiomyocytes, endothelial cells, and smooth muscle cells allowing for directed differentiation and tissue specific growth in damaged regions of the heart (Govindapillai et al., 2018; McMullen et al., 2009; Wu et al., 2006). At embryonic day 11.5 (E11.5), mouse ventricles showed to contain a significant number of undifferentiated CPCs,

which can be observed to express marker Nkx2.5 indicative of potential for myocardial differentiation (Feridooni & Pasumarthi, 2019). Additionally, in E11.5 mice ventricles cultures there was a minimal presence of endothelial cells, observed through the absence of CD31 endothelial marker expression (Feridooni & Pasumarthi, 2019). The findings indicate that E11.5 ventricular cells can be used as a tool to study the differentiation potential of E11.5 ventricular cells into VCS and working cardiomyocytes. In this regard, it is important to analyze the effect of sodium nitroprusside (SNP) on the increased expression of CCS markers (Tsai et al., 2015).

1.6.1 Effects of Sodium Nitroprusside on VCS Cell Differentiation

SNP is conventionally used as a short acting arterial and venous vasodilator, being comprised of nitric oxide (NO) and iron (Hottinger et al., 2014). The mode of action of SNP initiates with spontaneous generation of NO, and NO activates soluble guanylate cyclase in vascular smooth muscles which then catalyzes increased turnover of cyclic guanosine monophosphate (cGMP) from GTP (Friederich & Butterworth, 1995). The increased cGMP then inhibits Ca^{+2} uptake into the vascular smooth muscle while upregulating the increased uptake of Ca^{+2} into the smooth endoplasmic reticulum (SR) (Friederich & Butterworth, 1995). Collectively, reduction of Ca^{+2} results in vasodilation, however another direct mechanism has been suggested the effect of NO directly on myocardium (Friederich & Butterworth, 1995). NO may decrease Ca^{+2} sensitivity of contractile elements and increase dephosphorylation of myosin light chains (MLC) leading to vasodilation (Karaki et al., 1997).

Additionally, a high-throughput screening of 5000 chemicals on a Cntn2+: egfp ESC line revealed that, in the presence of 100 μM SNP, there was increased Cntn2+ expression (Tsai et al., 2015). The proposed mechanism of action is that the iron from SNP increased cAMP which

in turn activates PKA and leads to increased transcription of CCS genes (Kim et al., 2006; Tsai et al., 2015). This raises the question as to whether cAMP increased by β-AR stimulation also increases the expression of CCS genes.

1.6.2 Beta-Adrenergic Stimulation

β-agonists have been proven as beneficial in treatments for chronic heart failure (CHF) and dilated cardiomyopathy (DCM) (Talan et al., 2011). CHF is characteristic of reduced systolic and diastolic functioning and as such β-agonists function to aid in contraction and achieve an increased cardiac output (Talan et al., 2011). Although β-agonists are effective in increasing cardiac contraction, caution must be held when administering them as chronic stimulation can lead to down-regulation of β- ARs, and lead to electrophysiological disturbances (Stöckigt et al., 2012). When analyzing causes for CHF, a preceding increase in catecholamine outflow was seen leading to sustained and elevated activation of β- ARs causing abnormalities in the β- AR signaling system and ultimately leading to CHF (Madamanchi, 2007). In cases as such the popular treatment became the use of β-blockers which actively bind and prevent the activation of β-adrenergic signaling (Lucia et al., 2018). β-adrenergic signaling has been studied at an organ level and at a cellular level on the influence on CHF and arrythmias, however the induction and effect of differential patterning of CCS cell proliferation and cell fate has not been expansively studied.

1.6.3 Beta-Adrenergic Agonists and Antagonists

β- ARs are G-coupled-protein receptors that function to regulate second messenger molecules, which in turn activate downstream signaling (Madamanchi, 2007). There are four subtypes of β-ARs, of which β1-ARs are the most prominent within the heart and comprise 75-80% of total receptors (Madamanchi, 2007). The presence of β1-ARs was shown to be expressed as early as E11.5 in mice ventricles (Feridooni et al., 2017). Natural agonists of β- ARs are catecholamines such as Norepinephrine (NE), that upon binding to β1- ARs induce exchange of guanine monophosphate (GMP) for guanine triphosphate (GTP) on the α-Gs protein subunit and dissociation of Gα subunit from the G-β and G-γ subunits (Figure 5) (Cotecchia et al., 2012). The disassociated and activated α-Gs protein leads to the activation of adenyl cyclase, and catalyzes turnover of cyclic adenosine monophosphate (cAMP) from ATP (Morris et al., 2009). cAMP is one of the primary second messenger molecules regulated by β-ARs, which when elevated activate protein kinase A (PKA) by binding to the regulatory protein attached to PKA and dissociating it (Morris et al., 2009). Activated PKA then leads to the phosphorylation of 1. L-type Ca^{+2} channels 2. RyR (ryanodine receptors) 3. PLB (phospholamban) 4. Troponin- I. Phosphorylation of L-type Ca^{+2} channels result in increased permeability of Ca^{+2} (Madamanchi, 2007). Phosphorylation of RyR results in modulation of Ca^{+2} release from the SR(Lanner et al., 2010). Phosphorylation of PLB results in the released inhibition of PLB on SERCA and increased reuptake of Ca^{+2} into the SR thus accelerating reuptake of Ca^{+2} during the relaxation phase of contraction (Li et al., 2002). Phosphorylation of Troponin-I also increases the rate of relaxation (Zhang et al., 1995). Collectively, phosphorylation from PKA increases cardiac contractility and speeds cardiac muscle relaxation (Madamanchi, 2007).

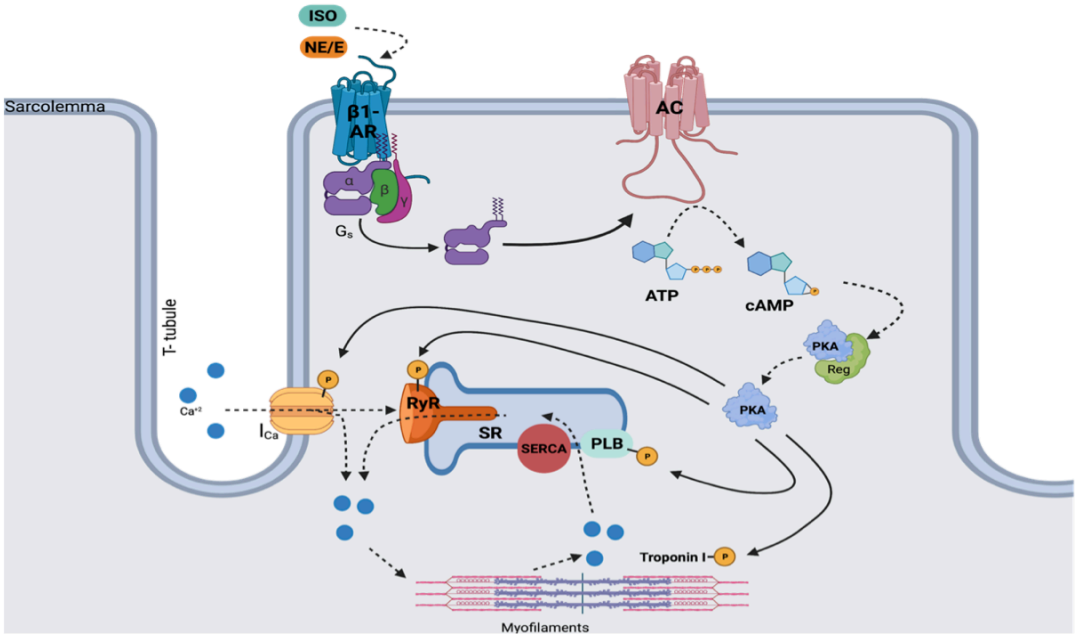

Figure 1.5: Beta-Adrenergic Receptor Activation-induced cardiac contractility
Activation of the β-1 Adrenergic Receptor (β-1 AR), results in activation of the G-coupled protein and dissociation of the activated α-subunit of the G-protein. The activated α-subunit activates the effector enzyme adenylate cyclase (AC) leading to the increased conversion of cAMP from ATP. cAMP binds to and activates Protein Kinase A (PKA), and the activated PKA phosphorylates Troponin 1 and Phospholambin (PLB) leading to increased contractility within the cardiomyocytes. (Created with BioRender.com) (Bers, 2002; Rehsia & Dhalla, 2010)

After the activation of a β-AR the agonist catecholamine gets oxidized or metabolized in the cytosol by catechol-o-methyltransferase (COMT) or in the outer mitochondrial membrane by Monoamine oxidase (MAO) into inactive metabolites (Paravati et al., 2021). To regulate proper cardiac output and contractility, β -adrenergic signaling can be targeted based on the type of cardiac arrythmias. β-agonists, such as Isoproterenol (ISO), have been used in cases of bradycardia to enhance contractility (Vavetsi et al., 2008). Meanwhile, β- AR Antagonists (often referred to as β-Blockers) such as Metoprolol (METO) are a primary line of treatment in cases of hypertension, CHF, and tachycardia, by reducing cardiac contractility and decreasing heart rate (Bonet et al., 2000). The expression of β2- ARs are more prominently seen in the pulmonary system and vascular beds, with a function of bronchodilation and pulmonary vasodilation

(Sturgill et al., 2011). β2- ARs activation becomes beneficial in treatments for asthma, which is typically symptomatic of airway obstruction and hyperresponsiveness (Pillai et al., 2011). Proper regulation of β-adrenergic signaling is required, to direct an effect towards either the pulmonary or the cardiac system.

1.6.4 Beta-Adrenergic Agonist Isoproterenol

ISO is a non-selective β-agonist, being capable of binding and activating both β1 and β2 ARs, leading to both enhanced cardiac contractility and vasodilation (Sturgill et al., 2011). Treatment with ISO, like SNP, results in increased turnover of cAMP, however the mechanisms involved in cAMP increase differ. As previously mentioned, SNP was proposed to activate PKA through Fe-induced cAMP increase, while ISO activates PKA through β- AR activated cAMP increase ((Hottinger et al., 2014; Tsai et al., 2015). The effect of β- AR signaling and its effects on the differentiation patterns of embryonic mouse ventricles has not been extensively studied, however some effects on proliferation and differentiation have been studied. Treatment with ISO decreases proliferation of E11.5 ventricular cells and reduces the graft size of transplanted cardiac cells (Feridooni et al., 2017). Additionally, ISO treatment in E11.5 ventricular cells reduces the number of CPCs, while increasing the number of CMs (Feridooni et al., 2017). It is not clear whether the ISO-induced increase in CMs are working CMs or VCS CMs.

1.6.5 Beta-Adrenergic Antagonist Metoprolol

METO is a selective β1- AR antagonist, and as previously mentioned is used in treatments of tachycardia, and post-MI management to reduce infarct size, heart rate, blood

pressure and cardiac output (Kezerashvili et al., 2012). METO acts through competitive antagonistic binding of β1- AR (Feridooni et al., 2017). METO treatment results in reduced cAMP turnover in E11.5 ventricular cells (Feridooni et al., 2017) . Additionally, treatment of METO in E11.5 ventricular cells, negates the anti-proliferative effects of ISO on graft size of transplanted cardiac cells (Feridooni et al., 2017). The effects of β1- AR inhibition on VCS development in the mouse have not been studied.

1.7 Antioxidant Ascorbic Acid

Ascorbic Acid (AA) is a water-soluble vitamin necessary for growth and development with anti-oxidant properties, donating electrons obtained through free radicles (Moskowitz et al., 2018). Supplemented in solution, AA is shown to stabilize drugs like ISO through cyclic redox reactions to maintain ISO in its active form (Wong et al., 1987). ISO was hypothesized to activate β- ARs through oxidation and electron transfer of ISO to reduce β- ARs and in turn stimulate adenylate cyclase (Wong et al., 1987). ISO is oxidized into an o-quinone intermediate and then into adrenochrome, both of which are unable to stimulate the activation of adenylate cyclase (Wong et al., 1987). However, in the presence of AA the o-quinone intermediate was reduced back into the ISO active state and was able to stimulate adenylate cyclase activity (Wong et al., 1987). Additionally, AA has been shown to promote the differentiation of cardiomyocytes from ESCs (Perino et al., 2017). Through modulation of SMAD1/TGF-β receptor signaling, AA was able to induce cardiomyogenesis at 10 and 100 μM concentrations (Perino et al., 2017). However, whether enhanced CMs are of the CCS phenotype (Perino et al., 2017) is unclear and whether AA treatment can also induce VCS differentiation in E11.5 ventricular cultures is unknown.

Chapter 2: Materials and Methods

2.1 Animal Maintenance, Mouse strain and Timed Pregnancies

CD1 mice were purchased from Charles River Laboratories (Sherbrooke, Quebec, Canada) and used for all experimental procedures. Experimental protocols dictating the use of animals were approved by the Dalhousie University Committee on Laboratory Animals (Protocol# 18-044 and 20-052) and were performed in agreement with the Canadian Council on Animal Care Guide to Care and Use of Experimental Animals (CCAC, Ottawa, ON: Vol.1.1, 2nd edition, 1993; Vol 3, 1984). Mice were maintained on a 12-hour light/dark cycle and housed inside the Carleton Animal Care Facility at Dalhousie University. Timed Pregnant CD1 mice of the gestational ages embryonic day 11.5 (E11.5), E14.5, and E16.5 were purchased from Charles River, Sherbrooke, Quebec, Canada. E11.5 embryos from timed pregnant CD1 mice were utilized for all experimental procedures unless otherwise stated.

2.2 Heart Isolation

Mice were anesthetized using 4% isoflurane and were sacrificed by cervical dislocation. Timed Pregnant CD1 mice were used to isolate embryonic hearts from E11.5, E14.5 and E16.5 developmental stages with the help of a Leica MZ16SF stereomicroscope (Leica Microsystems, Richmond Hill, Ontario, Canada). Neonatal (Neo) mouse hearts, 1 day after birth, and Adult mouse hearts, 3-5 months after birth, were also harvested. Atria were removed and only ventricles (left and right) were used for developmental gene expression analysis. For cell culture and drug treatment studies, multiple ventricles from E11.5 mice were pooled together, and

ventricular cells were used after tissue digestion as described in sections 2.6 and 2.7. Whole embryos from E11.5 stage or whole hearts from the adult CD1 mice were used for cryosections.

2.3 Cryosections

E11.5 embryos and whole hearts from adult mice (3-5 months) were placed on a rocker in a 30% sucrose cryoprotectant solution overnight at 4°C. The next day, whole embryos or hearts were retrieved and embedded in OCT medium (Sakura Finetek, Torrance, California, USA) with the use of plastic embedding rings and then frozen at -80°C. The frozen hearts were then cut into thin 10µm tissue sections using a CM3050 S cryostat (Leica) and placed onto Superfrost® Plus slides (Fisher Scientific). E11.5 and adult cryosections were then used for immunostaining.

2.4 Immunostaining of Cryosections

E11.5 embryos and adult mouse heart cryosections were fixed in 4% paraformaldehyde (4 grams of paraformaldehyde in 100ml of PBS, pH adjusted to 7.4, using NaOH) for 10 minutes and then PBS rinses were done consisting of three consecutive 2-minute PBS washes. Sections were next permeabilized in 0.1% v/v Triton X-100 (Sigma) for 5 minutes and then again washed with PBS. After the rinses, sections were placed in a blocking buffer solution [10% v/v goat serum (Gibo), 1% w/v bovine serum albumin (BSA; Thermo Fisher Scientific) in PBS] for one hour. Sections were then incubated in a blocking buffer solution containing primary antibodies for markers Cx40, Cntn2, HCN4 and MF20, at dilutions listed in Table 2.1. Sections were incubated in primary antibodies for 24 hours at 4 °C and then washed again with PBS at room temperature. After the PBS rinses, slides were incubated with secondary donkey anti-rabbit

antibodies conjugated to Alexa Fluor 488 (1:150) and goat anti-mouse antibodies conjugated to Alexa Fluor 555 (1:150) or goat anti-rabbit antibodies conjugated to Alexa Fluor 555 (1:150) and goat anti-mouse antibodies conjugated to Alexa Fluor 488 (1:150) in blocking buffer for one hour at room temperature, at dilutions listed in Table 2.2. After one hour, the sections were washed again with PBS and then nuclei staining was performed with a solution of 1µg/mL of Hoechst 33258 (Sigma) in PBS for 5 minutes. Sections were rinsed again with PBS and the slides were mounted with 0.1% propyl gallate (Sigma) solution [(0.1% w/v propyl gallate, 50% v/v glycerol (Thermo Fisher Scientific), 50% v/v PBS]. Immunofluorescence was then examined using the Leica DM2500 Fluorescence microscope, images were captured using a Leica DFC 500 digital acquisition system, and images were analyzed with Adobe Photoshop 7.0 software.

Table 2.1 Primary antibodies and dilutions (in blocking buffer) used for immunofluorescence analysis.

Primary Antibody	Dilution	Source/ Catalogue #
Connexin 40 (Cx40) **Rabbit polyclonal**	1:150	Alpha Diagnostics Catalogue #: Cx40-A
Contactin- 2 (Cntn2) (2D4M7G) **Rabbit mAb**	1:150	Cell Signaling Technology Cat# 26372S
Hyperpolarized Cyclic Nucleotide Gated Channel- 4 (HCN4) **Rabbit polyclonal**	1:150	Alomone Laboratories Catalogue #: APC-052
Sarcomeric myosin (MF20) **Mouse monoclonal**	1:75	Developmental Studies Hybridoma Bank Catalogue #: MF-20

Table 2.2 Secondary antibodies and dilutions (in blocking buffer) used for immunofluorescence analysis.

Secondary Antibody	Dilution	Source/ Catalogue #
Donkey anti-rabbit conjugated to Alexa Fluor 488	1:150	Invitrogen Thermofisher Scientific/ Cat# A21260
Goat anti-mouse conjugated to Alexa Fluor 555	1:150	Invitrogen Thermofisher Scientific/ Cat# A21425
Goat anti-rabbit conjugated to Alexa Fluor 555	1:150	Invitrogen Thermofisher Scientific/ Cat# A21430
Goat anti-mouse conjugated to Alexa Fluor 488	1:150	Invitrogen Thermofisher Scientific/ Cat# A11017

2.5 Total RNA Extraction from Ventricular Tissue

Ventricles from developmental stages (E11.5, 14.5, 16.5, Neo, and Adult) were used for developmental gene expression analysis and total RNA from ventricular tissues was isolated using the Trizol (Invitrogen) method. Sex of the embryos and neonates could not be determined due to the smaller size. Although Y-chromosome specific PCR can be performed on individual embryos, preserving individual ventricular tissue until the PCR results are obtained is extremely time consuming and also requires sacrificing a large number of pregnant mice to obtained sufficient quantities of RNA from each sex at each stage. All adult hearts were collected from the sacrificed pregnant females. For E11.5 and E14.5 stages, multiple ventricles were pooled. For each developmental stage, approximately 25-50 mg of ventricular tissue was minced and homogenized in 1ml TRIzol and then incubated for 5 minutes at room temperature. Then 0.2 ml of chloroform was added to each sample and these were incubated for 3 minutes, and then centrifuged at 16,612 rcf for 15 minutes at 4ºC. The supernatant was then transferred to a tube containing 0.5ml isopropyl alcohol and incubated for 10 minutes at room temperature to precipitate RNA. The tube was then centrifugation at 16,612 rcf rpm for 10 minutes at 4ºC, and then the RNA pellet was washed with 70% ethanol and solubilized in nuclease free H_2O (Ambion). The concentration of RNA and purity was then measured through absorbance readings at 260nm and 280nm using a spectrometer (SmartSpecTM Plus, Bio-Rad, Mississauga, Ontario, Canada). Samples with 260:280 ratios >1.8 were considered pure and used for further analysis. The RNA was then used to generate cDNA for RT-qPCR and gene expression analysis was performed for Cx40, Cntn2, HCN4 and GAPDH as described in sections 2.9 to 2.11.

2.6 Embryonic Ventricular Cell Isolation

After ventricles (both left and right) were dissected from multiple E11.5 embryos, the ventricles were pooled and placed in a 0.2% collagenase solution (Worthington Biochemical Corp, Lakewood, NJ, USA). Ventricles in solution were then incubated for 45 minutes at 37°C to digest ventricular tissue and a 200 µl pipette was used to mechanically dissociate cells from digested tissue. Cells in solution were then allowed to sit for 5 minutes to gravity separate the tissue for disassociated cells, and the cells in the upper layer were separated from the lower tissue layer. The solution containing the cells was centrifuged for 4 minutes at 4,000 rpm, 4°C, and supernatant was discarded. The pellet was re-suspended in DMEM (Dulbecco's Modified Eagles Medium; Wisent, Saint Bruno, Quebec, Canada) containing 10% fetal bovine serum (FBS; Wisent, Saint Bruno, Quebec, Canada) and 1% antibiotic and antimycotic solution (Ab/Am, Thermofisher Scientific). Cell number was counted with a hemocytometer and then 2.5 x 10^5 cells in 1 ml media was seeded per well on a 4-chamber slide (Cat# 154917, Nunc, Rochester, New York, USA), or a 35mm culture dish (Cat# 353001, Corning, New York, USA). Prior to seeding, chamber slides and 35mm culture dishes were coated with fibronectin (1:1000 dilution in PBS, Cat# F1141-2MG, Millipore Sigma) for 30 min in an incubator at 37°C. Cells seeded onto chamber slides were used for cell proliferation and immunofluorescence analysis, while cells seeded onto culture dishes were used for RNA extraction and gene expression analysis. E11.5 ventricular cells cultured under these conditions for a period of 1-2 days were shown to contain predominantly CPCs and differentiated CMs with very few endothelial and smooth muscle cells (<1%)(Hotchkiss et al., 2015)

2.7 Embryonic Ventricular Cell Primary Cultures and Drug Treatments

β- AR agonist and antagonist drugs were used to examine the effect of β- AR signaling on the proliferation and differentiation of E11.5 cells into the ventricular conduction system lineage. Ventricular cells were seeded onto the 4-chambered slide or 35mm culture dish (2.5 x 10^5 cells per well/35 mm dish) for 6 hours in an incubator at 37°C for cell attachment and then fresh media with or without drugs was added. In brief, cells treated with either Isoproterenol (ISO; Sigma, Cat#: I6504), Metoprolol (METO; Sigma, Cat#: M5391-1G), Ascorbic Acid (AA; Sigma, Cat#: A4544-25G) or with a combination containing two or more drugs. Drug treatments of ISO, METO and AA were prepared by solubilizing powder with nuclease free H_2O (Ambion, Cat# AM9937), and then diluted to make 1mM stock solutions for ISO and METO and 10mM stock solution for AA, and stocks were diluted in 10%FBS-DMEM. A 100 mM ISO stock was made by solubilizing 0.0123 g of ISO in 500 µl of nuclease-free H_2O, and then a 1 mM stock of ISO was made by mixing 1 µl of 100 mM ISO stock with 99 µl nuclease-free H_2O. A100 mM METO stock was made by solubilizing 0.0342 g of METO in 500 µl of nuclease-free H_2O, and then a 1 mM stock of METO was made by mixing 1 µl of 100 mM METO stock with 99 µl nuclease-free H_2O. A 10 mM AA stock was made by solubilizing 0.01g AA in 5670 µl nuclease-free H_2O.

Dosages of 0, 1, 2.5, 5, and 10 µM ISO, and/or 0, 1, 10 µM METO with and without supplementation of AA were prepared by mixing 0, 10, 25, 50, and 100 µl of ISO, and/or METO respectively from the 1 mM drug stock solution with supplementation of 0, 10, 100 µl AA from the 10 mM drug stock solution into 10 % FBS-DMEM for a total of 10 ml, preparation of tested dosages are listed in Table 2.3. In addition to the drugs added during drug treatments, for analysis of cell proliferation, 1µl of 10X stock solution of Click-iT EdD buffer additive

(Component F) (ThermoFisher Scientific, Cat#: C10340) was added per chamber on the 4-chambered slides. Edu was added only for cell proliferation experiments and Edu experiments were conducted in cells grown on 4-well chamber slides (see section 2.16). For RNA extraction, cells were grown on 35mm culture dishes (see section 2.8). Cells treated with drug doses and EdU were incubated for 24 hours at 37°C and then washed twice with PBS rinses for 2-minute. After PBS rinses, cultures were used for RNA extraction and conduction system gene expression analysis or Edu cell proliferation assays.

Table 2.3 Preparation of dose treatments for Isoproterenol (from 1mM ISO stock) and Metoprolol (from 1mM METO stock), with and without the supplementation of Ascorbic Acid (from 10mM AA stock) diluted in 10 % FBS-DMEM to make a total volume of 10 ml.

Tested Dosage (µM)	(µl) ISO	(µl) METO	(µl) AA	(µl) 10% FBS-DMEM
0 ISO, 0 AA	**0**	0	0	10000
0 ISO, 10 AA	**0**	0	10	9990
0 ISO, 25 AA	**0**	0	25	9975
0 ISO, 50 AA	**0**	0	50	9950
0 ISO, 100 AA	**0**	0	100	9900
1 ISO, 0 AA	**10**	0	0	9990
1 ISO, 10 AA	**10**	0	10	9980
1 ISO, 100 AA	**10**	0	100	9890
2.5 ISO, 0 AA	**25**	0	0	9975
2.5 ISO, 10 AA	**25**	0	10	9965
2.5 ISO, 100 A	**25**	0	100	9875
5 ISO, 0 AA	**50**	0	0	9950
5 ISO, 10 AA	**50**	0	10	9940
5 ISO, 100 AA	**50**	0	100	9850
10 ISO, 0 AA	**100**	0	0	9900
10 ISO, 10 AA	**100**	0	10	9890
10 ISO, 100 AA	**100**	0	100	9800
0 ISO, 0 AA, 1 METO	**0**	10	0	9990
0 ISO, 10 AA, 1 METO	**0**	10	10	9980
1 ISO, 0 AA, 1 METO	**10**	10	0	9980
1 ISO, 10 AA, 1 METO	**10**	10	10	9970
2.5 ISO, 0 AA, 1 METO	**25**	10	0	9965
2.5 ISO, 10 AA, 1 METO	**25**	10	10	9955
0 ISO, 0 AA, 10 METO	**0**	100	0	9900
0 ISO, 10 AA, 10 METO	**0**	100	10	9890
1 ISO, 0 AA, 10 METO	**10**	100	0	9890
1 ISO, 10 AA, 10 METO	**10**	100	10	9880
2.5 ISO, 0 AA, 10 METO	**25**	100	0	9875
2.5 ISO, 10 AA, 10 METO	**25**	100	10	9865

2.8 Total RNA Extraction from Ventricular Cells

Next, total RNA was extracted from the ventricular cells that were seeded and treated on 35mm culture dishes, using the Aurum Total RNA Mini Kit (Bio-Rad; Cat# 732-6802). After rinsing the cells with PBS, 350 µl of lysis solution containing β-mercaptoethanol (Bio-Rad; Cat# 732-6802) was added to each dish. Cells were then scraped off the interior surface of the plate and an 18-gauge needle was used to homogenize the cell lysate. Cell lysates were then transferred to a 2ml capped tube and stored at -80°C for later use.

When ready for use, the frozen cell lysates were thawed and 350 µl of 70 % ethanol was added for each tube. The total of 700 µl cell lysate was then transferred to a RNA binding column placed within a tube (from the kit), and the lysate was spun for 60 seconds at 12,000 rcf and the flow-through was discarded from the wash tube. Then to remove genomic DNA, 700 µl of total RNA low stringency wash solution containing ethanol (Bio-Rad; Cat#: 732- 6804) was added to the binding column and then spun for 30 seconds at 12,000 rcf. The flow-through was once again discarded and then, the binding column was incubated with DNase mix. DNase mix consisted of 5 µl of DNase-in-Tris Stock solution with 75 µl of DNase dilution solution, and the 80 µl mix was transferred to each binding column and incubated for 25 minutes at room temperature. Next, 700 µl of total RNA high stringency wash solution (Bio-Rad; Cat#: 732-6803) was added into each column and spun for 30 seconds at 12,000 rcf. The flow-through was then discarded and 700 µl of low stringency wash solution was pipetted into each column and spun for 60 seconds at 12,000 rcf. The flow-through was once again discarded, and then the column was spun twice for 60 seconds at 12,000 rcf. Next, the binding column was transferred to a 1.5 ml capped microcentrifuge tube and 30 µl of Elution solution (Bio-Rad; Cat#: 732- 6801) was added and samples were incubated for 2 minutes. The purified RNA was then eluted out of

the binding columns by centrifuging for 2 minutes at 12,000 rcf. Next, purity of the RNA was analyzed, and a portion of the RNA was reverse transcribed into cDNA for real time quantitative PCR (RT-qPCR), while the remaining RNA was stored at -80°C.

2.9 RNA Purity and cDNA Reverse Transcription

RNA purity was measured using a nanodrop lite spectrophotometer (ThermoFisher Scientific), with a quality standard of a 260:280 ratio > 1.8. RNA was then converted into complementary DNA (cDNA) sequences using SuperScript VILO MasterMix reverse transcriptase kit (ThermoFisher Scientific). The revere transcription reaction consisted of 20 ng of purified RNA, 2 µl of SuperScript Vilo MasterMix, and Nuclease free H_2O (Ambion) to make a total reaction mixture of 20 µl. The reaction mixtures for all samples were transferred into Eppendorf tubes, and incubated at 25°C for 10 min, 42°C for 90 min, and heat inactivated at 85°C for 5 min using a thermal cycler (Eppendorf A22331G). The resulting cDNA was next used for RT-qPCR assays to analyze conduction system gene expression.

2.10 Real Time Quantitative Polymerase Chain Reaction (RT-qPCR) and Primers

cDNA obtained from 35mm culture dish samples were amplified by a real time quantitative polymerase chain reaction (RT-qPCR) using conduction system primers, listed in Table 2.4. Primers for Cx40, Cntn2, HCN4 and GAPDH were generated using the primer design tools (https://mouseprimerdepot.nci.nih.gov/) developed by (Cui et al., 2007)(Cui et al., 2007) or (https://pga.mgh.harvard.edu/primerbank/). The designed primers were made to span from exon-exon boundaries to ensure PCR reactions did not amplify genomic DNA.

Table 2.4 Primers used in Real-time quantitative polymerase chain reaction (RT-qPCR), primer sequence from (5' to 3'), and expected amplicon size (bp)

Primers	Primer Sequence (5'-3')	Expected Amplicon Size (bp)
Cx40-F	CAGAGCCTGAAGAAGCCAAC	137
Cx40-R	GACTGTGGAGTGCTTGTGGA	
Cntn2- F	GCACTGTCGTCAGCAAGGAA	152
Cntn2-R	CCAGCGGTAGGACAAACCT	
HCN4-F	CCTCCTGCGCCTCTTGAGGCTTT	119
HCN4-R	TGCCAATGAGGTTCACGATGCGT	
GAPDH-F	TCGTCCCGTAGACAAAATGG	132
GAPDH-R	TTGAGGTCAATGAAGGGGTC	

For the qPCR reaction, a mixture of 2µl of 5X EVOlution EvaGreen® qPCR mix (Montreal Biotech Inc., Quebec City, Canada), 2 µl Nuclease free H_2O (Ambion), 1 µl of the forward and reverse primers (2µM), and 1 µl of cDNA were added per well into a sample plate. For each sample of cDNA, primers for Cx40, Cntn2, HCN4 and GAPDH were added into separate wells, and duplicated twice for every primer pair/per sample. Samples were spun down for 2 minutes at 700 rpm, and then the sample plate was run on an ECO thermocycler (Illumina, San Diego, California, USA) set at 50°C for 2 min; 95°C – 10 min, followed by 40 cycles of amplification and a final melt curve analysis. Each amplification cycle consisted of 95°C – 15 sec and 60°C – 1 min, and the final melt curve cycle consisted of 95°C, 60°C, 95°C, for 15 sec steps. Melt curves were used to confirm the specific amplification of a single peak without any nonspecific amplifications.

2.11 RT-qPCR Analysis

Gene expression levels were normalized using housekeeping control gene glyceraldehyde 3-phosphate dehydrogenase (GAPDH) and with a cycle threshold (C_T) set at a value of 0.1. Gene expression was quantified using the $\Delta\Delta C_T$ method (Livak & Schmittgen, 2001), where C_T values represent the number of cycles required for a gene to cross a threshold that exceeds the background level.

The $\Delta\Delta C_T$ method for each sample and gene entailed the following calculations: 1. The ΔC_T values for each sample were determined as the difference between C_T values for each gene and the corresponding GAPDH C_T values. 2. $-\Delta\Delta C_T$ values were determined as the difference between ΔC_T values for each sample and the averaged ΔC_T value of all samples. 3. The average $2^{-\Delta\Delta C_T}$ value for the control groups were calculated. The control groups were determined as the no drug treatment samples, and their values were set to 1 and all other samples were compared relative to the control group for each gene expression assay. 4. Relative expression for each sample was determined by calculating $2^{-\Delta\Delta C_T}$ values for each sample and then dividing the result by the averaged $2^{-\Delta\Delta C_T}$ values from the control group. The $\Delta\Delta C_T$ method, normalized to the expression of GAPDH, represented the relative fold change in gene expression of samples to the no drug treatment control group.

2.12 Immunostaining and Cell Proliferation Assay

For analysis of cell proliferation, E11.5 ventricular cells seeded on 4-chamber slides (2.5 x 10^5 cells per well) and 1 µl of Click-iT Edu stock solution (ThermoFisher Scientific, Cat#:

C10340) was added per chamber on the 4-chambered slides. Cells were also treated simultaneously with or without ISO, METO and AA as described in section 2.7 for 24 hours at 37°C and then washed twice with PBS rinses for 2-minute. After PBS rinses, chamber slides were fixed with 4% w/v paraformaldehyde for 10 minutes at 4°C and then washed again twice with PBS rinses for 2-minute. After fixation and PBS rinses, the chamber slides were then used for proliferation and immunofluorescence analysis of Cx40 and saromeric myosin markers to track VCS cells. Simultaneously, Click-iT EdU proliferation assay was done for the analysis of VCS cell proliferation. After fixation and PBS rinses, cells were permeabilized with 0.1% v/v Triton X-100 (Millipore Sigma) for 5 minutes followed by 2 washes with PBS for 2 minutes each. Next, 150 µl of blocking buffer [10% v/v goat serum (Gibo), 1% w/v bovine serum albumin (BSA; Thermo Fisher Scientific) in PBS] was added per well for 1 hour at room temperature. After one hour, cells were then incubated in a blocking buffer solution containing primary antibodies for gap junction protein marker Cx40 and sarcomeric myosin marker MF20 at dilutions listed in Table 2.1. Cells were incubated with primary antibodies for 24 hours at 4 °C and then washed again with PBS at room temperature. After the PBS rinses, slides were incubated with secondary goat anti-rabbit antibodies conjugated to Alexa Fluor 555 (1:150) and goat anti-mouse antibodies conjugated to Alexa Fluor 488 (1:150) in blocking buffer for one hour at room temperature, listed in Table 2.2. After 1 hour, wells were rinsed again with PBS and then a Click-iT EdU proliferation assay was done.

Click-iT Plus EdU Alexa Fluor 647 Imaging Kit (ThermoFisher Scientific; Cat#: 10640) was used to assess cellular proliferation, and reagents from the kit were used to make a reaction cocktail. A reaction cocktail was made with 10x Click-iT EdU buffer (88 µl), copper protectant (20 µl), Alexa Flour picoyl azide (2.5 µl), 10 X Reaction buffer (10 µl) and Nuclease free H_2O

(880 µl). After the PBS rinses, 200 µl of the reaction cocktail was added per well of the chamber slide and left to incubate in the dark for 30 minutes at room temperature. After 30 minutes, the slides were rinsed twice with PBS for 2 minutes each, and then nuclei were stained with a solution of 1µg/mL of Hoechst 33258 (Millipore Sigma) in PBS for 5 minutes. The wells were rinsed again with PBS and then the chamber was removed from the slide and then the slides were mounted with 0.1% propyl gallate (Sigma) solution [(0.1% w/v propyl gallate, 50% v/v glycerol (Thermo Fisher Scientific), 50% v/v PBS]. Immunofluorescence staining was then examined using the Leica DM2500 Fluorescence microscope, and images were captured in 40 X magnification using a Leica DFC 500 digital acquisition system, and images were analyzed with Adobe Photoshop 7.0 software.

2.13 EdU and Cell Count Quantification

After immunostaining E11.5 ventricular cells from chamber slides, the proliferation capacity of the was assessed visually through images captured. Images of cells from 10 random fields were taken per well/ treatment dose, each being stained for nuclei, CMs ($Cx40^-$, $MF20^+$), VCS CPCs ($Cx40^+$, $MF20^-$), VCS CMs ($Cx40^+$, $MF20^+$), and EdU.

Proliferation was assessed based on the total number of VCS CPCs and VCS CMs that were stained positive for EdU florescence out of total cells counted per well. Each well (all 10 fields) was compared to all wells/ drug treatments and change in proliferation was examined relative to the control group of no drug treatment, and only cells that were stained positive for nuclei were considered.

2.14 Second Messenger cAMP Assay

The effect of drug treatments of ISO, METO, and AA on the production of cAMP was assessed in E11.5 ventricular cells with a cAMP competitive immunoassay, using a two-step protocol from the cAMP dynamic 2 htrf assay kit (Cisbio, Cat#: 62AM4PEB). Treated cells were left for 60 minutes and endogenous cAMP levels were assessed by measuring fluorescent resonance energy transfer (FRET) signals. FRET signals were produced when the supplemented d2-dye labelled cAMP analogue (d2-cAMP) bound to binding sites on anti-cAMP monoclonal antibodies (mAb-Cryptate). Excitation of mAB-Cryptate lead to a donor- acceptor energy transfer to the fluorophore on d2-cAMP and emission of signal. Both endogenous cAMP and added d2-cAMP analogue competed for binding sites on mAb-Cryptate, however only d2-cAMP was tagged with a fluorophore and produced FRET signals, endogenous cAMP did not produce FRET signals. FRET signal was inversely proportional to endogenous cAMP levels, as the larger concentrations of endogenous cAMP out-competed d2-cAMP for binding sites on mAb-Cryptate and produced lowed FRET signals. Endogenous cAMP concentrations of treated cells were then extrapolated and FRET signals produced during treatment were compared to known FRET signals on a cAMP standard curve.

The following steps were taken for measurement of d2-cAMP fluorophore emissions in treated ventricular E11.5 cells: 1.) A 384-well plate was obtained and 5,000 isolated E11.5 ventricular cells in 5 µl of 10% FBS-DMEM were pipetted into each well. 2.) Drug treatments diluted in 5 µl of 10 % FBS-DMEM were mixed into each well with a P20 pipette. Drug treatment combinations consisted of the following three groups: Group I. AA (0 µM, 10 µM, 25 µM, 50 µM, 100 µM). Group II. ISO (0 µM, 1 µM, and 2.5 µM) supplemented with or without AA (0 µM, 10 µM, 100 µM) Group III. ISO (0 µM, 1 µM, and 2.5 µM) supplemented with or

without AA (0 μM, 10 μM) and METO (0 μM, 1 μM, 10 μM). Negative control wells were also prepared with 5 μl of 10% FBS-DMEM with no drug additives. Each treatment was replicated into 3 wells. 3.) 0.3 μl of 500 μM phosphodiesterase inhibitor 3-isobutyl-1-methylxanthine (IBMX; Millipore Sigma) was added per well to prevent degradation of endogenous cAMP. After steps 1-3, the plate was then sealed and left to incubate for 30 minutes at room temperature. 4.) After 30 minutes, 5 μl of d2-cAMP analogue diluted in lysis buffer was added into every well, except for the negative controls. The omission of d2-cAMP from negative controls was done to show specificity in signal emission and the absence of non-specific fluorescent emissions. 5.) Next, 5 μl of mAb-Cryptate diluted in lysis buffer was added into all wells, including the negative wells. 6.) The plate was then sealed and left to incubate for 1 hour in the dark at room temperature. 7.) After 1 hour, d2-cAMP was excited at 337nm and emissions at wavelengths of 665nm and 620nm were recorded, using a POLARstar Omega plate reader (BMG, Labtech).

From the measured emissions, changes in FRET (ΔF) signaling per well/ treatment was calculated and endogenous cAMP concentrations were extrapolated through the following steps: 1.) The 665nm/620nm ratio per well was determined by dividing the 665nm emission by 620nm and then ratio was multiplied by 10^4. 2.) The ratios from the three replicates from every treatment were averaged, and to determine ΔF the averaged triplicate ratio for each treatment was subtracted by the averaged triplicate ratio from the negative control and then the total was multiplied by 100. 3.) ΔF values were plotted and compared to ΔF values from the known cAMP standard concentrations in order to extrapolate the cAMP concentration for treated cells (Figure 2.1).

2.15 Statistical Analysis

Statistical analysis was conducted using the Graphpad Prism Version 8.01 (Graphpad Software, San Diego, USA). Data are presented as mean ± standard error of the mean (SEM). Multiple group comparisons were analyzed by either one-way or two-way ANOVA with Sidaks multiple comparison post hoc test. Significance for all analyses was assessed at $p<0.05$. For each experiment, the number of experiments/replicates along with corresponding statistical analysis is represented in the corresponding figure legends.

A.

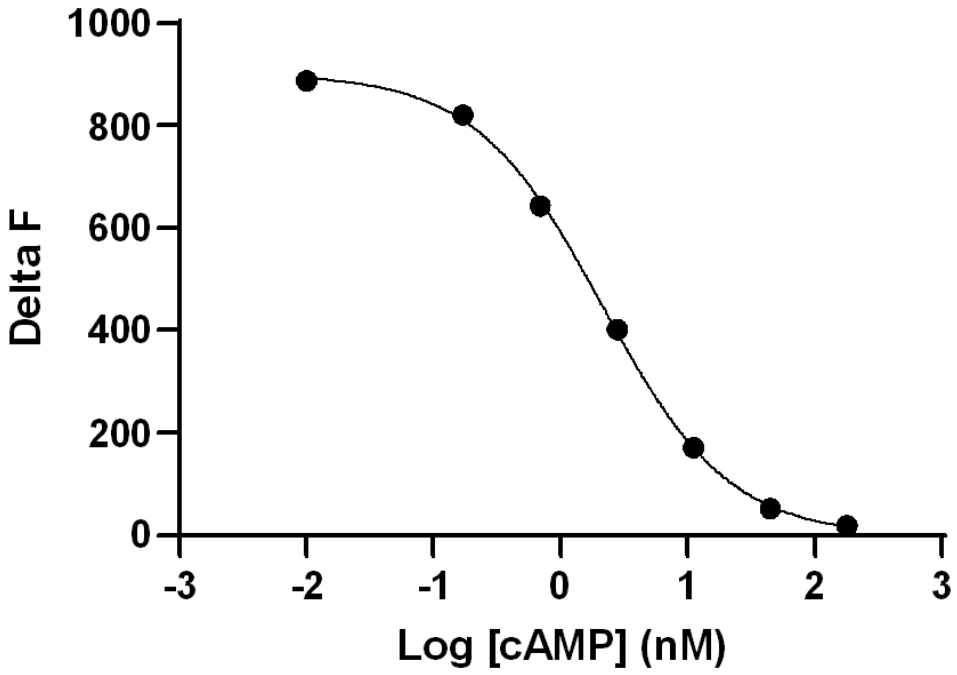

B.

Final [cAMP] (nM)	Delta F
178	18.6032
44.5	52.01435
11.1	171.632
2.78	402.4864
0.69	643.6106
0.17	821.5744
0.00	888.0494

Figure 2.1: Generation of the cAMP standard curve
A) A cAMP standard curve was generated using the Delta F values calculated from standards with known cAMP concentrations, ranging cAMP concentrations of 0- 178 nM. **B)** listed known standard final cAMP concentrations (nM) with corresponding calculated Delta F values.

Chapter 3: Results

3.1 Gene expression analysis of conduction system markers (Cx40, Cntn2 and HCN4) in the developing mouse ventricles

Although nodal tissues (SAN and AVN) are formed by E11.5 stage in the mouse heart, there is no clear evidence for ventricular conduction fiber formation at this stage (Miquerol et al., 2011). Notably, the relative VCS marker gene expression is not very well documented during different stages of ventricular development. To directly address this aspect, ventricular tissue was extracted from various stages of mouse heart development (E11.5, E14.5, E16.5, neonatal and adult) and relative gene expression levels of VCS marker genes (Cx40, Cntn2 and HCN4) were determined using RT-qPCR analysis. Gene expression was normalized to the levels of the house-keeping gene GAPDH which was shown to remain constant across all stages of heart development in a previous study (Fig. 3.1D) (Hotchkiss et al., 2014). RT-qPCR analysis showed expression of Cx40 at the E14.5 stage was significantly higher (2.7-fold) when compared to that of the E11.5 stage (Fig. 3.1A). At the neonatal stage of development, Cx40 expression was significantly decreased by 2.3-fold in comparison to the E14.5 stage (Fig. 3.1A). The adult ventricles showed the lowest level of Cx40 expression with a significant 3.5-fold decrease in comparison to the E14.5 stage (Fig. 3.1A).

Expression of Cntn2 was not detected in the E11.5 stage, so expression of Cntn2 was graphed relative to the E14.5 stage were Cntn2 expression is seen (Fig. 3.1B). The expression of Cntn2 had a 9.3-9.5-fold increase in the neonatal stage in comparison to the E14.5 and E16.5 stages (Fig. 3.1B). The expression of Cntn2 had a 5.9-fold decrease in expression in the adult stage in comparison to the neonatal stage (Fig. 3.1B). Additionally, the expression of Cntn2

showed a 3.7-fold increase in expression in the adult stage in comparison to the E16.5 stage (Fig. 3.1B).

Expression of HCN4 was detectable in the E11.5 stage ventricles, which was seen to increase in the E14.5 stage (Fig. 3.1C). The E14.5 stage had the highest expression level of HCN4 in comparison to all other stages, with a significant 2.4-fold higher expression in comparison to the adult cardiac developmental stage. The adult cardiac stage had the lowest level of HCN4 expression. Collectively, these results suggest that higher levels of Cx40 and HCN4 gene expression can be detected in the embryonic heart, whereas higher levels of Cntn2 gene expression can be detected in postnatal stages during mouse ventricular development.

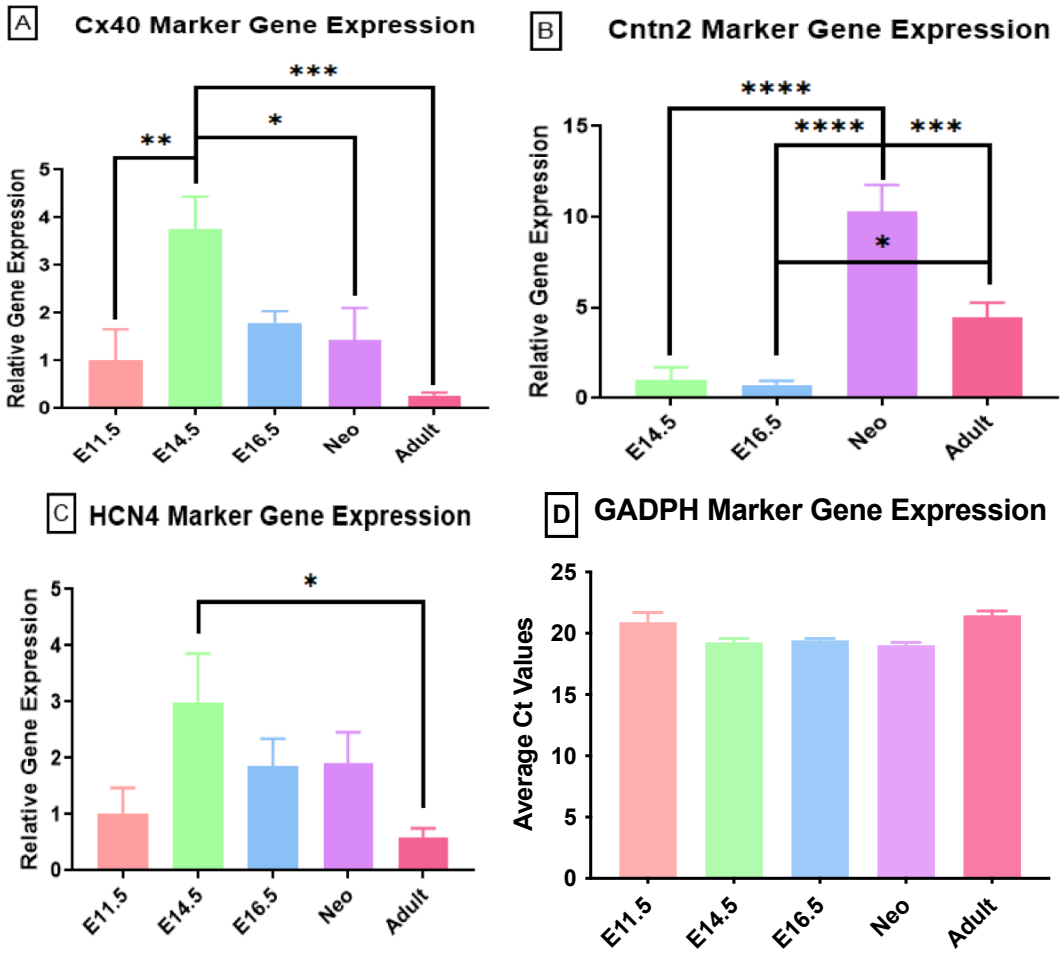

Figure 3.1: RT-qPCR analysis of Conduction system gene expression for markers Cx40, Cntn2, HCN4 and GAPDH in the developing mouse ventricles from E11.5, E14.5, E16.5, Neonatal, and Adult hearts

(A-C) Expression of all three conduction system markers were normalized to **(D)** the expression of GAPDH which had consistent mRNA expression throughout ventricular development. The expression of **(A)** Cx40 and **(C)** HCN4 was graphed and compared relative to the expression at the E11.5 stage. The expression of **(B)** Since Cntn2 transcripts were undetectable at E11.5 stage, Cntn2 gene expression was graphed and compared relative to the expression of the E14.5 stage. **(A)** ***P < 0.005 E14.5 Vs. Adult, **P < 0.05 E14.5 Vs. E11.5 or Neonatal **(B)** ****P < 0.0005 Neonatal Vs. E14.5 or E16.5, ***P < 0.005 Neonatal Vs. Adult, *P < 0.05 Adult Vs. E16.5 **(C)** *P < 0.05 E14.5 Vs. Adult. Bars represent mean ± SEM, N=5 independent RNA ventricular tissue extractions per developmental stage, analyzed in two technical replicates/primer pair for each sample. One-way ANOVA with Sidak's multiple comparison test.

3.2 Immunodetection of conduction system proteins Cx40, HCN4, and Cntn2 in E11.5 and Adult cardiac cross-sections

The developmental stages of E11.5 and adult were stained for expression of conduction system markers. Protein levels of all three VCS markers were determined in cryosections of E11.5 hearts using immunostaining methods. The rationale for using E11.5 cryosections was to visualization expression of conduction system markers in the early development of the conduction system. Additionally, E11.5 cells in the later part of this study were also treated and used to determine the effect of β-adrenergic signaling on conduction system gene expression, so early visualization would allow further insight. Adult cryosections were imunostained for conduction system proteins for a comparison with the immunostaining seen with the E11.5 cryosections. The presence of Cx40 and HCN4 proteins was readily detected with immunostaining of whole heart cross-sections in the E11.5 development stage (Fig. 3.2). HCN4 staining can be seen in the right common cardinal vein (RCCV, future superior vena cava) and the junction between RCCV and the dorsal wall of the right atrium where the primitive SA node is located (Fig. 3.2 1A). Notably, very low levels of HCN4 staining were detected in both left and right ventricles at E11.5 stage (not shown). Expression of Cx40 can also be detected in the trabecular compartment in E11.5 left ventricle cross-sections (Fig. 3.2B). In contrast to HCN4 and Cx40 immunostains, the expression of Cntn2 was not detected in E11.5 cardiac cross sections (Fig. 3.2C). However, the expression of Cntn2 was readily detected when adult whole heart cross-sections were stained with Cntn2 specific antibodies. Cntn2 staining was seen in the left bundle branch (Figure 3.3) and SAN/ AVN (not shown) in adult murine cardiac cross-sections. These results suggest that E11.5 mouse hearts express both Cx40 and HCN4 proteins, whereas the Cntn2 protein is absent or undetectable.

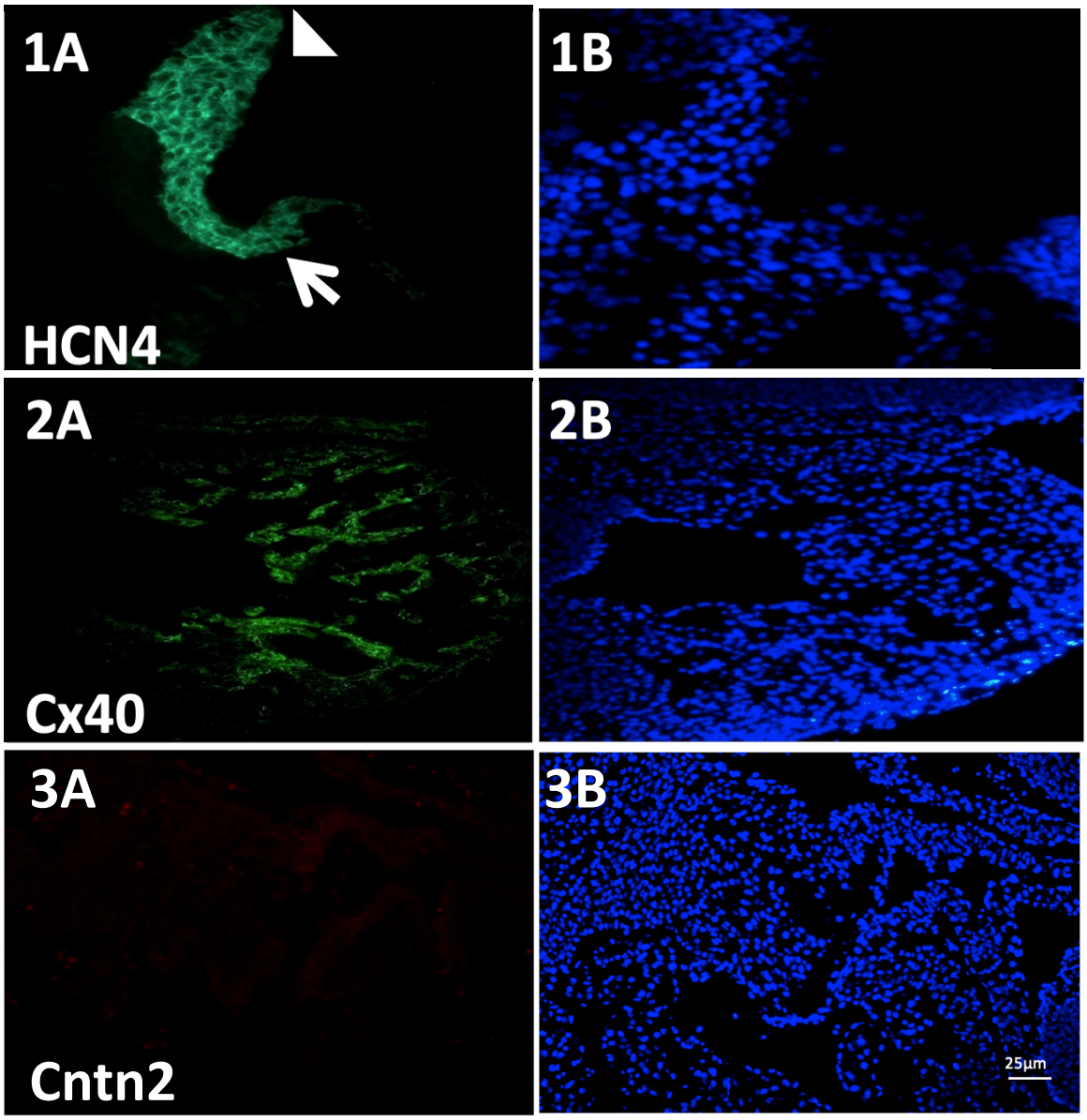

Figure 3.2: Immunostaining analysis of conduction system gene expression for HCN4, Cx40, and Cntn2 from E11.5 whole mouse heart cross-sections
(1A) HCN4 immunostaining of the right common cardinal vein (arrowhead) and SA node (arrow) is visible in green after staining with rabbit polyclonal HCN4 antibodies and secondary donkey anti-rabbit antibodies conjugated to Alexa Fluor 488 **(1B)** Hoechst nuclei staining for HCN4 stained cross-section. **(2A)** Cx40 staining of trabeculae in the left ventricle is visible in green after staining with rabbit polyclonal Cx40 antibodies and secondary donkey anti-rabbit antibodies conjugated to Alexa Fluor 488 **(2B)** Hoechst nuclei staining for Cx40 stained cross-section. **(3A)** Cntn2 staining in the ventricles was not detected after staining with rabbit polyclonal Cntn2 antibodies and secondary goat anti-rabbit antibodies conjugated to Alexa Fluor 555 **(3B)** Hoechst nuclei staining for Cntn2 stained cross-section. Fields were taken in 40X magnification with a scale bar of 25 µm for all fields.

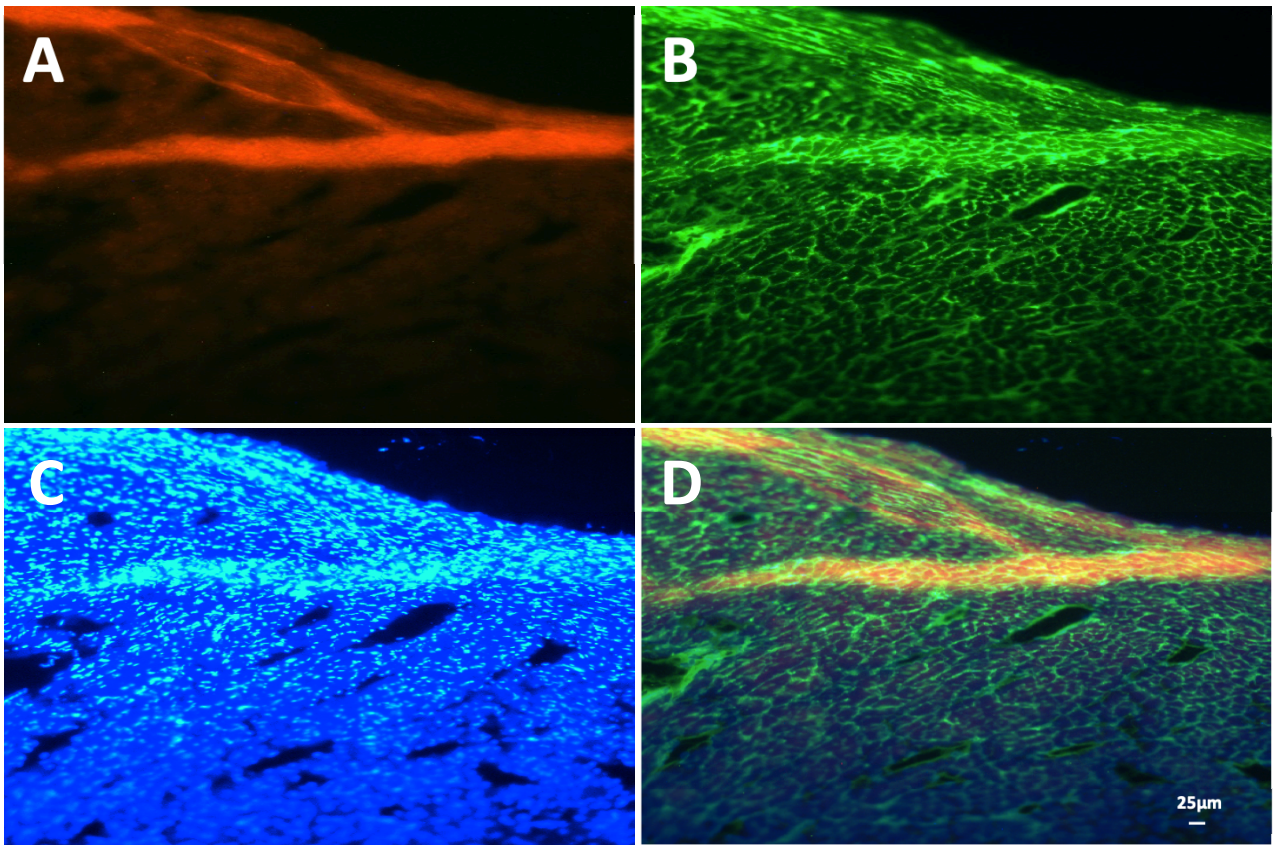

Figure 3.3: Immunostaining analysis of Cntn2 expression in adult mouse heart cross-sections

(A) Cntn2 stain of left bundle branch (LBB) was visible as red by staining with rabbit polyclonal Cntn2 antibodies and secondary goat anti-rabbit antibodies conjugated to Alexa Fluor 555 **(B)** Sarcomeric myosin was stained by mouse monoclonal MF20 antibodies and secondary goat anti-mouse antibodies conjugated to Alexa Fluor 488 **(C)** Hoescht nuclei staining **(D).** Merged overlay of Cntn2, Mf20 and Hoechst fields. Fields were taken in 10X magnification with a scale bar of 25 µm for all fields.

3.3 Identification of proliferating ventricular conduction system cardiac progenitor cells (VCS CPCs) and ventricular conduction system cardiomyocytes (VCS CMs)

The effects of ISO and β- AR signaling on cardiac conduction system development, proliferation or differentiation, have not been studied. In this study the effect of ISO on both murine cardiac conduction system proliferation and differentiation was assessed. For the cell proliferation analysis, E11.5 ventricular cells were seeded and treated with various concentrations of ISO and Ascorbic acid (AA) on 4-chamber slides. Specifically, the effect of ISO on Edu incorporation was determined. Slides were then imunostained for Cx40 and sarcomeric myosin (MF20) expression and Click-iT EdU and Hoechst staining were performed. Images of the assayed chamber slides were captured in blinded fashion (10 random fields per chamber/ treatment), using a Leica DM2500 fluorescence microscope and Leica DFC 500 digital acquisition system. Cells positive for both Cx40 and MF20 staining were designated as VCS CMs and cells positive for only Cx40 were designated as VCS CPCs (Figure 3.4). Edu is known to be incorporated into the newly synthesized DNA and thus Edu positive staining was used to identify proliferating cells in both VCS CMs and VCS CPCs populations (Figure 3.4D). In Figure 3.4E, proliferating VCS CMs were identified through the positive staining for Cx40, MF20 and EdU ($Cx40^{+}/Mf20^{+}/EdU^{+}$). Proliferating VCS CPCs were identified through the positive staining for Cx40 and EdU and negative staining for MF20 ($Cx40^{+}/Mf20^{-}/EdU^{+}$), shown in Figure 3.4F.

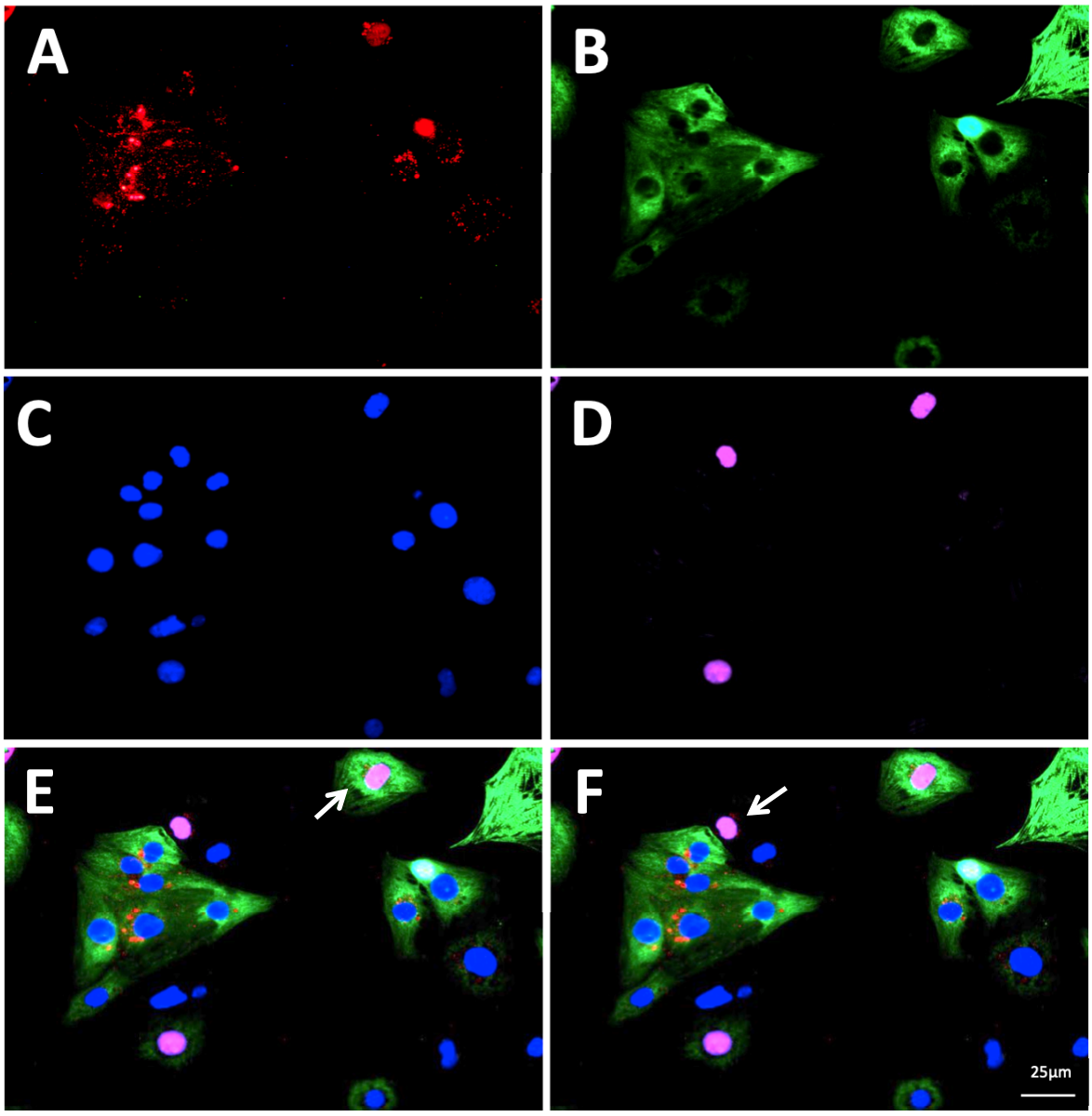

Figure 3.4: Identification of proliferating ventricular conduction system cardiomyocytes (VCS CMs) and ventricular conduction system cardiac progenitor cells (VCS CPCs) in E11.5 mouse ventricular cells.
(A) Cells were stained with Cx40 specific polyclonal antibodies and the Cx40 protein visible in red was visualized by secondary antibodies conjugated to Alexa Fluor 555 (B) Cells in panel A were co-stained with Sarcomeric myosin antibodies (Mf20) and myosin was visualized by secondary antibodies conjugated to Alexa Fluor 488 (C) Nuclei were visualized by Hoechst staining (D) Proliferating cells were visualized through a Click-IT EdU assay (pseudo-colored purple) (E) Merged image with arrow indicating proliferating ventricular conduction system cardiomyocyte ($Cx40^{+}/Mf20^{+}/EdU^{+}$) (F) Merged image with arrow indicating proliferating ventricular conduction system cardiac progenitor cell ($Cx40^{+}/Mf20^{-}/EdU^{+}$). Images of the same field were taken in 40X magnification with a scale bar of 25 µm for all fields.

3.4 Characterizing the effect of Isoproterenol on the proliferation of ventricular conduction system cardiac progenitor cells (VCS CPCs) and ventricular conduction system cardiomyocytes (VCS CMs)

VCS CPC and VCS CM proliferation rates in E11.5 ventricular cell cultures treated with various concentrations of ISO, with and without supplementation with AA, were determined by counting number of EdU positive VCS CM ($Cx40^{+}/MF20^{+}/EdU^{+}$) and EdU positive VCS CPC ($Cx40^{+}/MF20^{-}/EdU^{+}$) populations out of total cells from all 10 fields per treatment (Figure 3.5). ISO treatments of 1 μM, 2.5 μM, 5 μM, and 10 μM did not significantly affect the proliferation rates of VCS CMs (figure 3.5A) or VCS CPCs (figure 3.5B) in comparison to the control group (0 μM ISO treatment group). AA was supplemented for two reasons; the first reason was to prevent oxidation of ISO and increase its bioavailability. ISO is a catecholamine that has a very short half-life of 2.5-5 minutes, and it can get oxidized into its inactive o-quinone intermediate and then into adrenochrome (Procaccini et al., 2019; Wong et al., 1987). AA when added in combination with ISO is able to act as a reducing agent to reduce o-quinone back into its active ISO state (Wong et al., 1987). The second reason was to analyze the effect of AA on conduction system expression as AA had previously been studied to induce cardiomyogensis in ES cell cultures (Perino et al., 2017). AA concentrations used in this study were selected based on the previously published study (Cui et al., 2007) as well as based on the fact that a 10-fold molar excess of AA is required to prevent ISO oxidation (Perino et al., 2017). Supplementation of AA at 10 μM and 100 μM with ISO treatments also did not affect the percentage of EdU positive VCS CMs (figure 3.5A) or VCS CPCs (figure 3.5B) out of total cells in comparison to the ISO treatments alone. AA treatments alone at concentrations of 10 μM and 100 μM also did not significantly affect the percentage of EdU positive VCS CMs (figure 3.5A) or VCS CPCs (figure 3.5B) out of total cells, seen in comparison to the 0 μM ISO 0 μM AA group.

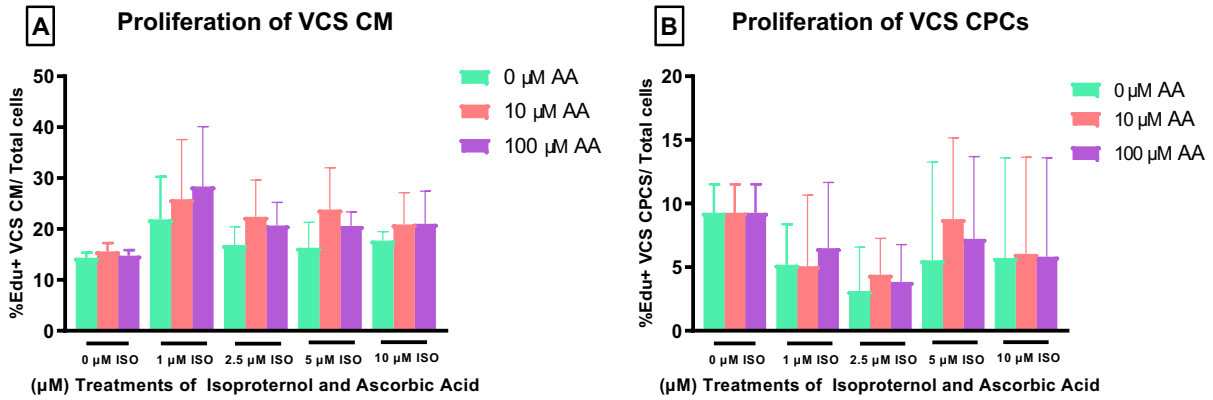

Figure 3.5: Proliferation analysis of ventricular conduction system cardiomyocytes (Cx40+/MF20+/EdU+) and ventricular conduction system cardiac progenitor cells (Cx40+/MF20-/EdU+) from E11.5 murine ventricular cells treated with or without isoproterenol and ascorbic acid.

(A-B) E11.5 ventricular cells were treated for 24 hours with concentrations of 0, 1, 2.5, 5, and 10 µM ISO (green bars) and with or without supplementation of 10 µM AA (pink bars) or 100 µM AA (purple bars). The effect of treatments on cell proliferation was calculated in **(A)** VCS CMs (Cx40+/MF20+/EdU+) and **(B)** VCS CPCs (Cx40+/MF20-/EdU+). Each bar represents mean ± SEM, N=3 independent experiments per group (10 fields per treatment in each experiment). Total number of cells counted for the 0 ISO treatment group was 545 (0 AA), 571 (10 AA), 765 (100 AA). Total number of cells counted for the 1 ISO treatment group was 765 (0 AA), 812 (10 AA), 656 (100 AA). Total number of cells counted for the 2.5 ISO treatment group was 753 (0 AA), 906 (10 AA), 694 (100 AA). Total number of cells counted for the 5 ISO treatment group was 785 (0 AA), 765 (10 AA), 808 (100 AA). Total number of cells counted for the 10 ISO treatment group was 832 (0 AA), 656 (10 AA), 601 (100 AA). Two-way ANOVA with Sidak's multiple comparisons test.

3.5 Characterizing the effect of Isoproterenol on the differentiation of E11.5 ventricular cells into the ventricular conduction system cell lineage

The effect of ISO on murine ventricular conduction system differentiation was assessed by RT-qPCR analysis of VCS gene expression in E11.5 ventricular cell cultures. Cells were seeded on 35-mm dishes and treated for 24 hours with concentrations of 0, 1, and 2.5 μM ISO with and without supplementation of 10 μM AA. Higher dosages of ISO at 5 μM and 10 μM were also tested but were not included for two reasons. Firstly, treatments of 5 μM and 10 μM were not tested on the effects of β- AR signaling on VCS gene expression. Secondly, the treatments of 5 μM and 10 μM had similar trends to 1 and 2.5 μM ISO treatment. After 24 hours, the total RNA was extracted from the treated cells, reverse transcribed and a RT-qPCR analysis was performed to determine the relative fold change in conduction system gene expression. Gene expression of Cx40 (Figure 3.6A), Cntn2 (Figure 3.6B), and HCN4 (Figure 3.6C) were measured and normalized to the expression levels of GAPDH, which has consistent gene expression and does not increase or decrease with treatments (Fig. 3.6 D). The gene expression of Cx40, Cntn2, HCN4 and GAPDH was then compared relative to the 0 μM ISO 0 μM AA treatment group (Figure 3.6).

Cx40 gene expression significantly increased by 2.2-fold when treated with 2.5 μM ISO 10 μM AA in comparison to 0 μM ISO 0 μM AA (Fig. 3.6A). Expression of Cx40 significantly increased by 1.9-fold with treatments of 2.5 μM ISO 10 μM AA μM when compared to 0 μM ISO 10 μM AA (Fig. 3.6A). Expression of Cx40 also significantly increased by 1.4-fold with treatments of 1 μM ISO 0 μM AA μM when compared to 0 μM ISO 0 μM AA (Fig. 3.6A).

Gene expression of Cntn2 significantly increased by 3.1-fold with treatments of 2.5 μM ISO 10 μM AA in comparison to 0 μM ISO 0 μM AA (Fig. 3.6B). Gene expression of Cntn2

also significantly increased by 2.9-fold with treatments of 2.5 μM ISO 0 μM AA in comparison to 0 μM ISO 0 μM AA (Fig. 3.6B).

Gene expression of HCN4 was not significantly increased or decreased by treatments of ISO and/or AA (Fig. 3.6C). Notably, gene expression of GAPDH remained constant after treatments with ISO and/or AA as indicated by no changes in the threshold cycle values (Ct) between groups (Fig 3.6D). Collectively, these findings indicate that ISO treatment of E11.5 ventricular cells can increase VCS gene expression in a dose dependent manner both with and without AA supplementation.

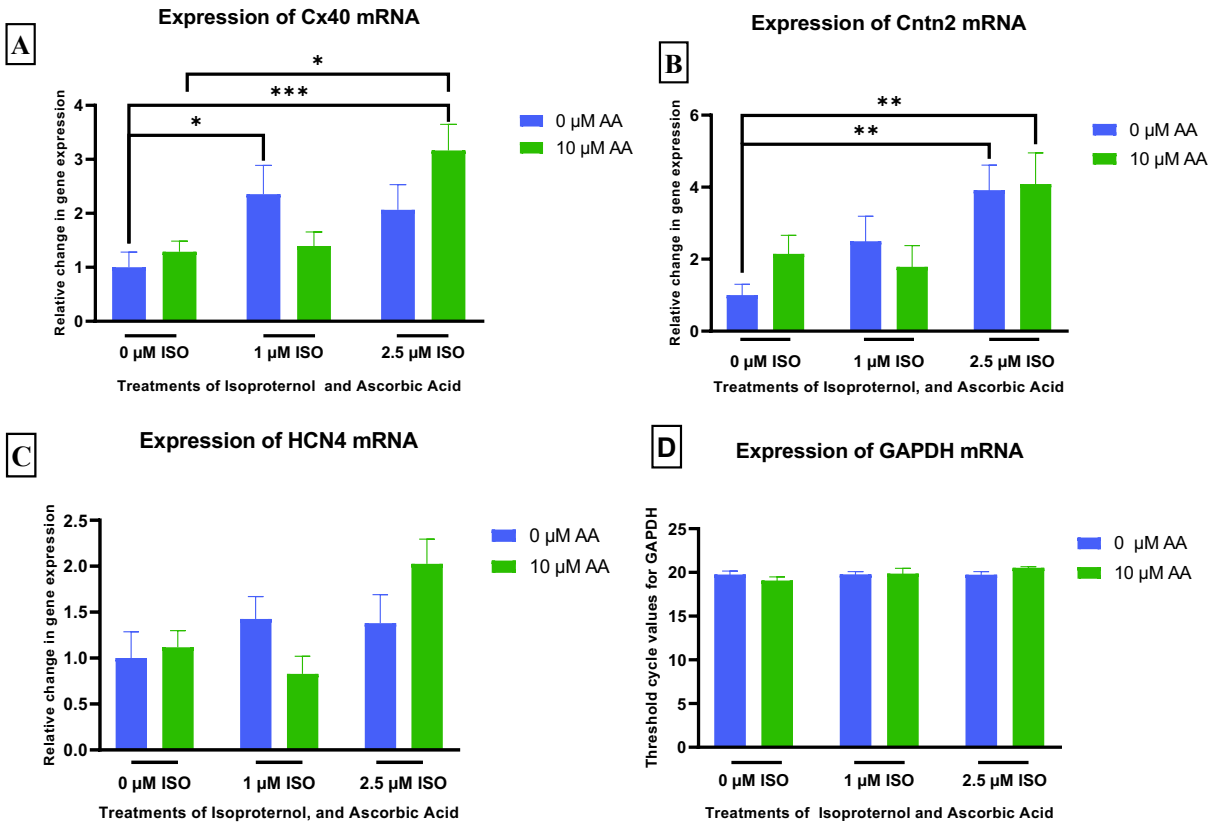

Figure 3.6: Differentiation analysis of ventricular conduction system marker gene expression of Cx40, Cntn2, HCN4 and GAPDH from isoproterenol and ascorbic acid treated E11.5 murine ventricular cells

(A-D) E11.5 ventricular cells were treated for 24 hours with concentrations of 0, 1 and2.5µM ISO without AA supplementation (blue bars) and with 10 µM AA supplementation (green bars). The effect of treatments on conduction system differentiation was assessed through RT-qPCR analysis for **(A)** Cx40 **(B)** Cntn2 **(C)** HCN4. Analyzed gene expression was normalized to the expression of housekeeping gene GAPDH and relative fold-change in gene expression was compared to the 0 ISO 0 AA treatment group. **(D)** Changes in the threshold cycle values (Ct) for GAPDH were plotted for each treatment group. **(A)** *$P < 0.05$ 1 µM ISO 0 µM AA Vs. 0 µM ISO 0 µM AA, 2.5 µM ISO 10 µM AA Vs. 0 µM ISO 10 µM AA. ***$P < 0.005$ 2.5 µM ISO 10 µM AA Vs. 0 µM ISO 0 µM AA **(B)** **$P < 0.01$ 2.5 µM ISO 10 µM AA Vs. 0 µM ISO 0 µM AA, 2.5 µM ISO 0 µM AA Vs. 0 µM ISO 0 µM AA. Each bar represents mean ± SEM, N=4-5 separate cell cultures, treatments and extractions for each treatment group. Two-way ANOVA with Sidak's multiple comparisons test.

3.6 Characterizing the effect of Metoprolol on the differentiation of E11.5 ventricular cells into the ventricular conduction system cell lineage

The effect of METO on the differentiation of E11.5 murine ventricular cells into the ventricular conduction system was assessed by RT-qPCR analysis of Cx40, Cntn2, and HCN4 gene expression. E11.5 cells were seeded on 35-mm dishes and treated for 24 hours with concentrations of 0, 1, and 2.5 μM ISO with and without supplementation of 10 μM AA, and with and without supplementation of 1 μM METO. After 24 hours, the total RNA was extracted from the treated cells, reverse transcribed and a RT-qPCR analysis was performed to determine the relative fold changes in conduction system gene expression. Gene expression of Cx40 (Figure 3.7A) (Table 3.1), Cntn2 (Figure 3.7B) (Table 3.2), and HCN4 (Figure 3.7C) were measured and normalized to the expression levels of GAPDH, which has consistent gene expression and does not increase or decrease with treatments.

Cx40 gene expression significantly increased by 2.2-fold when treated with 2.5 μM ISO/ 10 μM AA/ 0 μM METO in comparison to 0 μM ISO/ 0 μM AA/ 0 μM METO (Table 3.1) (Fig. 3.7A). The same treatment of 2.5 μM ISO/ 10 μM AA/ 0 μM METO also increased Cx40 gene expression by 1.9-fold when compared to 0 μM ISO/ 10 μM AA/ 0 μM METO (Fig. 3.7A). With the addition of METO, expression of Cx40 significantly decreased by 2.1-fold with treatments of 2.5 μM ISO/ 10 μM AA μM/ 1 μM METO when compared to 2.5 μM ISO/ 10 μM AA/ 0 μM METO (Fig. 3.7A). Expression of Cx40 significantly increased by 1.3-fold with treatments of 1 μM ISO/ 0 μM AA/ 0 μM METO when compared to 0 μM ISO/ 0 μM AA/ 0 μM METO (Fig. 3.7A). With the addition of METO, expression of Cx40 significantly decreased by 1.4-fold with treatments of 1 μM ISO/ 0 μM AA/ μM 1 μM METO when compared to 1 μM ISO/ 0 μM AA/ 0 μM METO (Fig. 3.7A).

Gene expression of Cntn2 also significantly increased by 3.1-fold with treatments of 2.5 μM ISO/ 10 μM AA/ 0 μM METO in comparison to 0 μM ISO/ 0 μM AA/ 0 μM METO (Table 3.1)(Fig. 3.7B). With addition of METO, expression of Cntn2 did not significantly decrease with treatments of 2.5 μM ISO/ 10 μM AA/ 1 μM METO when compared to 2.5 μM ISO/ 10 μM AA/ 0 μM METO (Fig. 3.7B). Furthermore, treatments of 2.5 μM ISO/ 10 μM AA/ 1 μM METO still significantly increased Cntn2 by 2.8-fold in comparison to 0 μM ISO/ 0 μM AA/ 0 μM METO (Fig. 3.7B). Gene expression of Cntn2 also significantly increased by 2.9-fold with treatments of 2.5 μM ISO/ 0 μM AA/ 0 μM METO in comparison to 0 μM ISO/ 0 μM AA/ 0 μM METO (Fig. 3.7B). With addition of METO, expression of Cntn2 significantly decreased by 2.4-fold with treatments of 2.5 μM ISO/ 0 μM AA/ 1 μM METO when compared to 2.5 μM ISO/ 0 μM AA/ 0 μM METO (Fig. 3.7B).

Gene expression of HCN4 was not significantly increased or decreased by treatments of ISO, METO and/or AA (Fig. 3.7C).

Table 3.1 Relative fold change in Cx40 gene expression with treatments of Isoproterenol, Ascorbic Acid and Metoprolol

Treatments	In comparison to	Relative change in gene expression
2.5 µM ISO 10 µM AA µM 0 µM METO	0 µM ISO 0 µM AA 0 µM METO	2.2-Fold Increase
2.5 µM ISO 10 µM AA 0 µM METO	0 µM ISO 10 µM AA 0 µM METO	1.9-Fold Increase
2.5 µM ISO 10 µM AA µM 1 µM METO	2.5 µM ISO 10 µM AA 0 µM METO	2.1- Fold Decrease
1 µM ISO 0 µM AA µM 0 µM METO	0 µM ISO 0 µM AA 0 µM METO	1.3-Fold Increase
1 µM ISO 0 µM AA µM 1 µM METO	1 µM ISO 0 µM AA 0 µM METO	1.4-Fold Decrease

Table 3.2 Relative fold change in Cntn2 gene expression with treatments of Isoproterenol, Ascorbic Acid and Metoprolol

Treatments	In comparison to	Relative change in gene expression
2.5 µM ISO 10 µM AA µM 0 µM METO	0 µM ISO 0 µM AA 0 µM METO	3.1-Fold Increase
2.5 µM ISO 10 µM AA µM 1 µM METO	2.5 µM ISO 10 µM AA µM 0 µM METO	N.S.
2.5 µM ISO 10 µM AA µM 1 µM METO	0 µM ISO 0 µM AA 0 µM METO	2.8-Fold Increase
2.5 µM ISO 0 µM AA µM 0 µM METO	0 µM ISO 0 µM AA 0 µM METO	2.9-Fold Increase
2.5 µM ISO 0 µM AA µM 1 µM METO	2.5 µM ISO 0 µM AA 0 µM METO	2.4-Fold Decrease

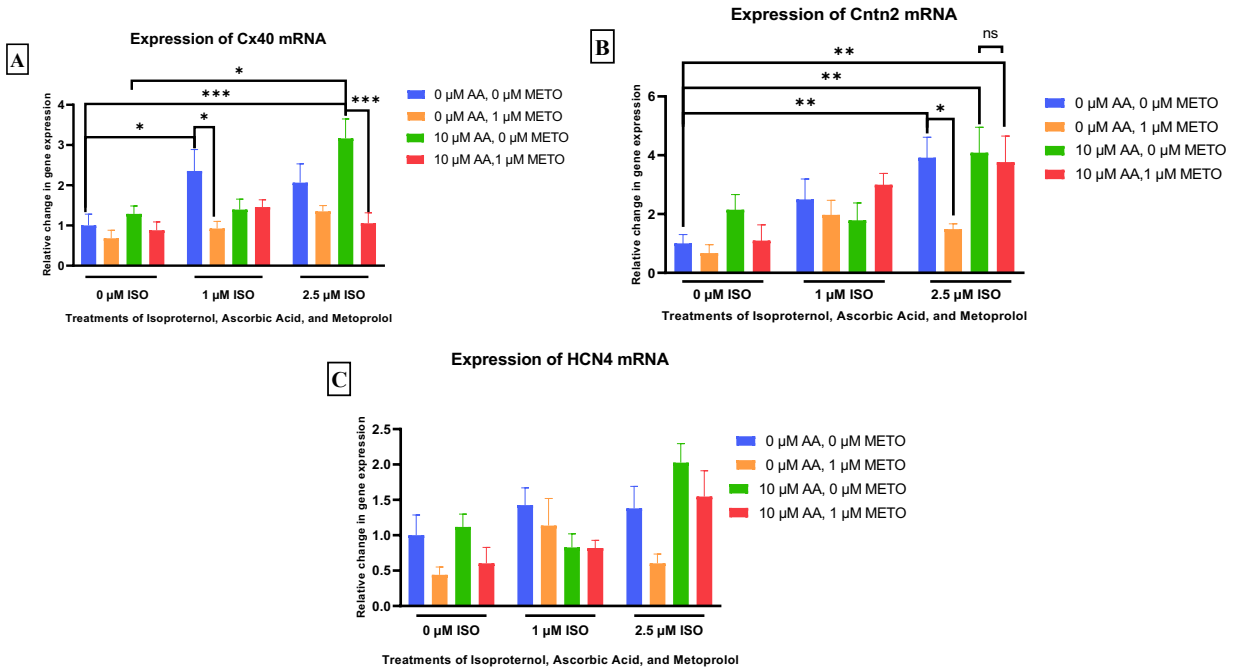

Figure 3.7: Differentiation analysis of ventricular conduction system marker gene expression of Cx40, Cntn2, and HCN4 from metoprolol treated E11.5 murine ventricular cells

(A-C) E11.5 ventricular cells were treated for 24 hours with concentrations of 0, 1, and 2.5 µM ISO (Blue bars) with supplementation of 10 µM AA alone (Green bars) and 1 µM METO alone (red bars), and 10 µM AA + 1 µM METO (Red bars). The effect of treatments on conduction system differentiation was determined through RT-qPCR analysis of gene expression for **(A)** Cx40 **(B)** Cntn2 **(C)** HCN4. Analyzed gene expression was normalized to expression of housekeeping gene GAPDH and relative fold-changes in gene expression was compared to the 0 ISO 0 AA 0 METO treatment group. **(A)** ***$P < 0.005$ 2.5 µM ISO 10 µM AA 0 µM METO Vs. 0 µM ISO 0 µM AA 0 µM METO, 2.5 µM ISO 10 µM AA 0 µM METO Vs. 2.5 µM ISO 10 µM AA 1 µM METO, *$P < 0.05$ 1 µM ISO 0 µM AA 0 µM METO Vs. 0 µM ISO 0 µM AA 0 µM METO, 2.5 µM ISO 10 µM AA 0 µM METO Vs. 0 µM ISO 10 µM AA 0 µM METO, 1 µM ISO 0 µM AA 0 µM METO Vs. 1 µM ISO 0 µM AA 1 µM METO. **(B)** **$P < 0.01$ 2.5 µM ISO 0 µM AA 0 µM METO Vs. 0 µM ISO 0 µM AA 0 µM METO, 2.5 µM ISO 10 µM AA 0 µM METO Vs. 0 µM ISO 0 µM AA 0 µM METO, 2.5 µM ISO 10 µM AA 1 µM METO Vs. 0 µM ISO 0 µM AA 0 µM METO, *$P < 0.05$, 2.5 µM ISO 0 µM AA 0 µM METO Vs. 2.5 µM ISO 0 µM AA 1 µM METO. Each bar represents mean ± SEM, N=5-6 separate cell cultures, treatments and extractions for each treatment group. Only ΔCq values within 2 SD ± mean for each treatment group were considered. Two-way ANOVA with Sidak's multiple comparisons test.

3.7 Characterizing the effects of isoproterenol, ascorbic acid, and metoprolol on production of second messenger cAMP in E11.5 ventricular cells

The change in endogenous cAMP production was studied in E11.5 ventricular cells treated with ISO, AA, and METO to determine possible mechanistic actions of ISO on ventricular conduction system gene expression. In previous sections, concentrations of 1 and 2.5 μM ISO with and without supplementation of 10 μM AA increased the gene expression of Cx40 and Cntn2 (Figure 3.6). Similar concentrations of ISO and AA were used to treat ventricular cells for 1 hour and the endogenous production of cAMP was assessed through a cAMP competitive immunoassay. These experiments were performed to assess if changes in conduction system gene expression were dependent on changes in cAMP production. Three groups of treatments were performed to analyze effects of ISO with or without AA on endogenous cAMP production in E11.5 ventricular cells. Group I consisted of varying doses of AA and analyzed whether AA alone had an effect on endogenous cAMP production. Group II analyzed the effect of ISO with and without supplementation of AA on endogenous cAMP, with a particular focus on concentrations that increased expression of conduction system genes Cx40 and Cntn2. Group III analyzed the effect of METO alone and in combination with ISO and AA on cAMP production.

For group I, E11.5 ventricular cells treated with 10, 25, 50, and 100 μM AA did not significantly alter production of cAMP relative to the control group (0 μM AA) (Figure 3.8).

For group II, cells treated with doses of ISO (1 and 2.5 μM) significantly increased cAMP production in comparison to 0 μM ISO treatment group, seen in the pink bars in figure 3.9. Supplementation of 10 μM and 100 μM AA with varying doses of ISO did not significantly increase or decrease production of cAMP relative to the respective ISO treatments alone, seen in figure 3.9 (paired green and blue bars Vs. red bar). These findings indicate that ISO and AA

concentrations that increased expression of conduction system genes Cx40 and Cntn2 also increased the endogenous production of cAMP. Treatments of 2.5 μM ISO /10 μM AA which increased Cx40 and Cntn2 gene expression, had a 5.3-fold increase in cAMP in comparison to 0 μM ISO/ 0 μM AA. Treatments of 2.5 μM ISO/ 10 μM AA which increased Cx40 gene expression had a 4.9-fold increase in cAMP in comparison to 0 μM ISO/ 10 μM AA. Treatments of 2.5 μM ISO/ 0 μM AA which increased Cntn2 gene expression, had a 6.5-fold increase in cAMP in comparison to 0 μM ISO/ 0 μM AA. Treatments of 1 μM ISO/ 0 μM AA, which increased Cx40 gene expression, had a 3.6-fold increase in cAMP in comparison to 0 μM ISO/ 0 μM AA.

For group III, treatments of METO alone (1 and 10 μM doses) in the absence of ISO and AA, did not significantly decrease cAMP compared to the no drug treatment group (0 μM ISO and 0 μM AA) (Table 3.3). Treatments of 1 μM METO with 1 μM ISO/ 0 μM AA decreased cAMP by 4.3-fold, and 10 μM METO with 1 μM ISO/ 0 μM AA decreased cAMP by 4.7-fold in comparison to the 1 μM ISO/ 0 μM AA treatment group (Table 3.3). Treatment of cells with 1 μM METO with 1 μM ISO/ 10 μM AA significantly decreased cAMP by 3.5-fold in comparison to the 1 μM ISO/ 10 μM AA treatment group (Table 3.3). Treatment of 10 μM METO with 1 μM ISO/ 10 μM AA significantly decreased cAMP by 3.6-fold in comparison to the 1 μM ISO/ 10 μM AA treatment group (Table 3.3). Treatment of 10 μM METO with 2.5 μM ISO/ 0 μM AA significantly decreased cAMP by 3.3-fold in comparison to the 0 μM METO 2.5 μM ISO/ 0 μM AA group (Table 3.3). However, a lower dose treatment of 1 μM METO with 2.5 μM ISO 0 μM AA did not significantly decrease cAMP in comparison to the 2.5 μM ISO/ 0 μM AA (Table 3.3). Additionally, treatments of 1 or 10 μM METO with 2.5 μM ISO/ 10 μM AA did not significantly decrease cAMP in comparison to the 2.5 μM ISO/ 10 μM AA group (Table 3.3).

Table 3.3: Assessment of changes in endogenous cAMP in E11.5 ventricular cells treated with metoprolol in combination with/without isoproterenol and ascorbic acid.

Treatments	In comparison to	Change in cAMP
0 µM ISO 0 µM AA 1 µM METO	0 µM ISO 0 µM AA 0 µM METO	N.S
0 µM ISO 0 µM AA 10 µM METO	0 µM ISO 0 µM AA 0 µM METO	N.S
0 µM ISO 10 µM AA 1 µM METO	0 µM ISO 10 µM AA 0 µM METO	N.S
1 µM ISO 10 µM AA 10 µM METO	0 µM ISO 10 µM AA 0 µM METO	N.S
1 µM ISO 0 µM AA 1 µM METO	1 µM ISO 0 µM AA 0 µM METO	4.3-Fold Decrease
1 µM ISO 0 µM AA 10 µM METO	1 µM ISO 0 µM AA 0 µM METO	4.7-Fold Decrease
1 µM ISO 10 µM AA 1 µM METO	1 µM ISO 10 µM AA 0 µM METO	3.5-Fold Decrease
1 µM ISO 10 µM AA 10 µM METO	1 µM ISO 10 µM AA 0 µM METO	3.6-Fold Decrease
2.5 µM ISO 0 µM AA 1 µM METO	2.5 µM ISO 0 µM AA 0 µM METO	N.S
2.5 µM ISO 0 µM AA 10 µM METO	2.5 µM ISO 0 µM AA 0 µM METO	3.3-Fold Decrease
2.5 µM ISO 10 µM AA 1 µM METO	2.5 µM ISO 10 µM AA 0 µM METO	N.S
2.5 µM ISO 10 µM AA 10 µM METO	2.5 µM ISO 10 µM AA 0 µM METO	N.S

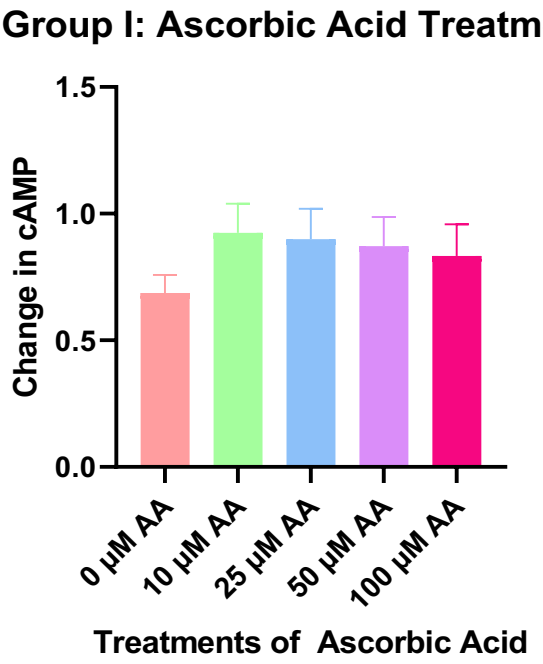

Figure 3.8: Assessment of changes in endogenous cAMP in E11.5 ventricular cells treated with varying doses of ascorbic acid
Cells were treated with 0,10, 25, 50, and 100 µM AA and a cAMP competitive immunoassay was conducted to examine changes in endogenous cAMP production. No significant changes were observed in treatment groups relative to the 0 µM AA group. Each bar represents mean ± SEM, N=5 independent experiments per group. One-way ANOVA with Sidak's multiple comparisons test.

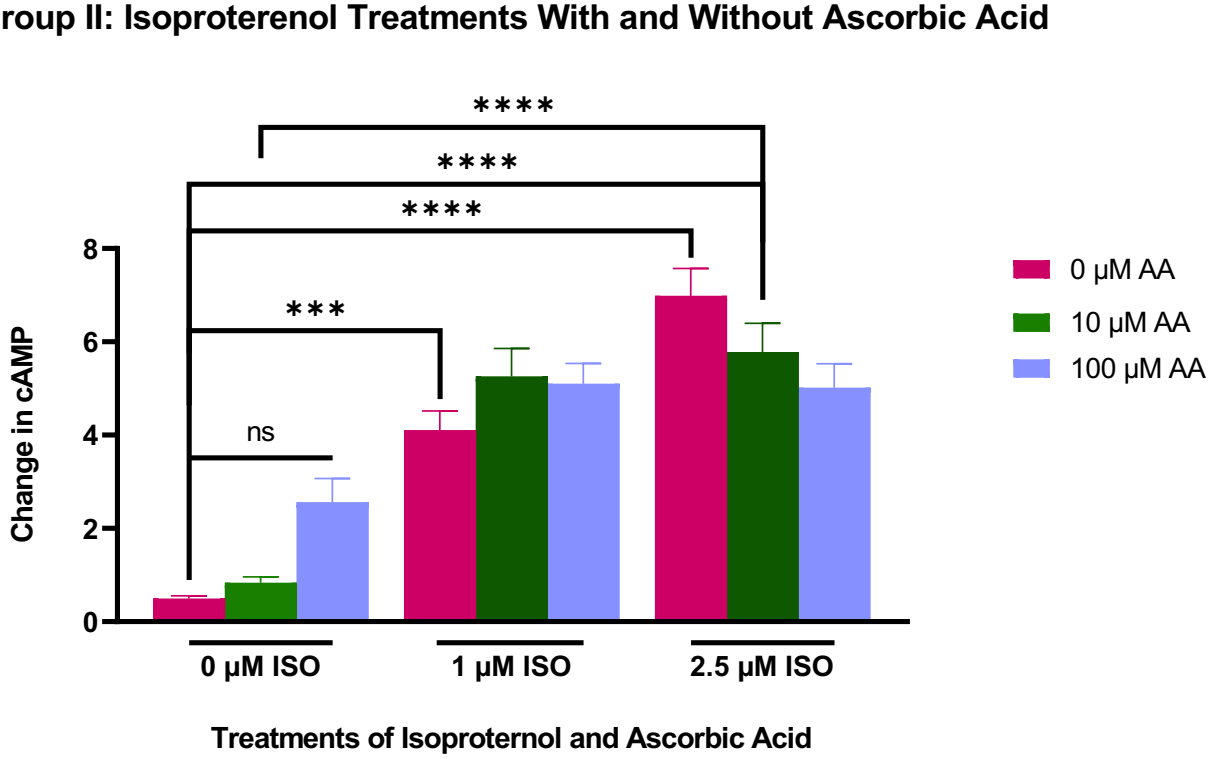

Figure 3.9: Assessment of changes in endogenous cAMP in E11.5 ventricular cells treated with varying doses of isoproterenol with/without ascorbic acid supplementation.
E11.5 ventricular cells were treated with 0, 1, and 2.5 µM ISO and supplemented with 0 µM (red), 10 µM (green), 100 µM (blue) AA. A cAMP competitive immunoassay was conducted to examine change in endogenous cAMP production. ***P < 0.005 1 µM ISO 0 µM AA Vs. 0 µM ISO 0 µM AA, ****P < 0.0001 2.5 µM ISO 10 µM AA Vs. 0 µM ISO 0 µM AA and 0 µM ISO 10 µM AA, 2.5 µM ISO 0 µM AA Vs. 0 µM ISO 0 µM AA. Each bar represents mean ± SEM, N=4 independent experiments per group. Two-way ANOVA with Sidak's multiple comparisons test.

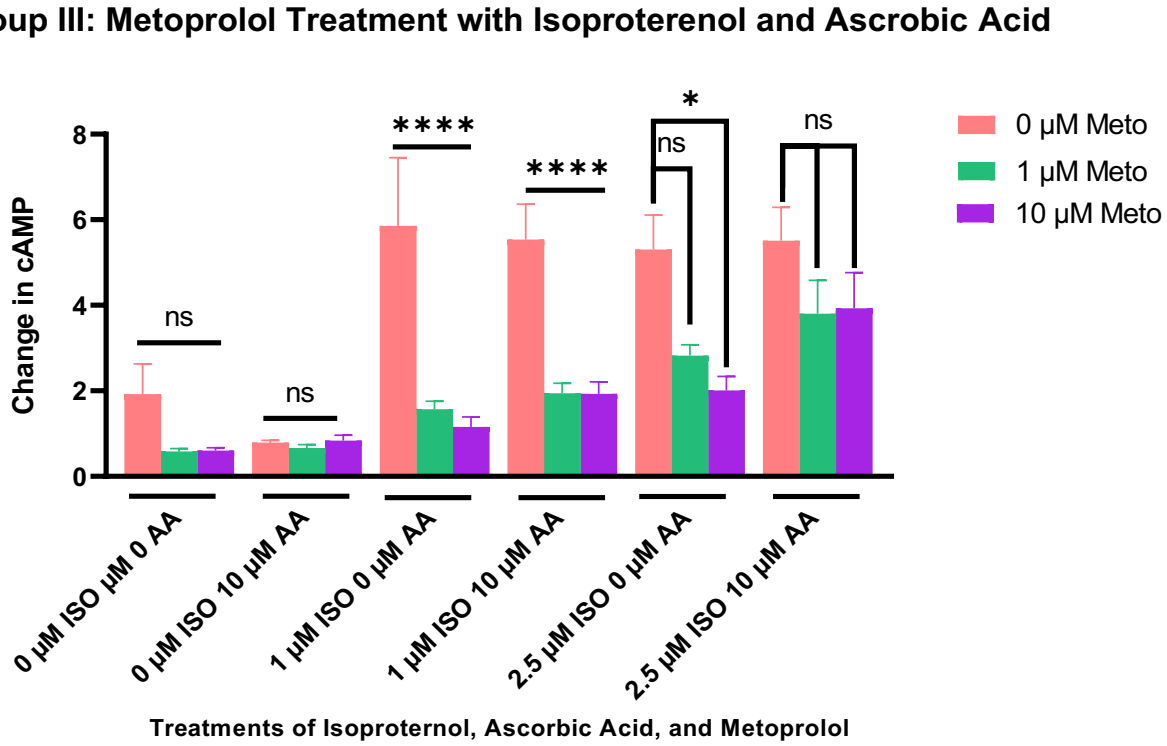

Figure 3.10: Assessment of changes in endogenous cAMP in E11.5 ventricular cells treated with metoprolol in combination with/without isoproterenol and ascorbic acid.
E11.5 ventricular cells were treated with 0, 1, 2.5, 5, and 10 µM ISO in the presence or absence of 1 and 10 µM METO and supplemented with 0 µM (red), 10 µM (green), 100 µM (blue) AA. A cAMP competitive immunoassay was conducted to examine changes in endogenous cAMP production. ****$P < 0.0001$ 1 µM ISO 0 µM AA 0 µM METO Vs. 1 µM ISO 0 µM AA 1 µM METO, 1 µM ISO 0 µM AA 0 µM METO Vs. 1 µM ISO 0 µM AA 10 µM METO, 1 µM ISO 10 µM AA 0 µM METO Vs. 1 µM ISO 10 µM AA 1 µM METO, 1 µM ISO 10 µM AA 10 µM METO Vs. 1 µM ISO 10 µM AA 10 µM METO. *$P < 0.05$ 2.5 µM ISO 0 µM AA 0 µM METO Vs. 2.5 µM ISO 0 µM AA 10 µM METO. Each bar represents mean ± SEM, N=5 independent experiments per treatment group. Two-way ANOVA with Sidak's multiple comparisons test.

Chapter 4: Discussion

4.1 Summary of Results

Understanding the effect of β- AR signaling on the differentiation and proliferation of CPC populations into the VCS lineage will allow for developments in the field of cardiac regenerative medicine. Additionally, by controlling the growth and differentiation of CPCs toward the VCS lineage, we can treat Purkinje fiber injured cardiac regions while controlling for the spontaneous generation of ectopic foci and arrythmias. There is little information about when conduction system markers Cx40, HCN4 and Cntn2 are expressed during murine cardiac development (Liang et al., 2015; Verheule & Kaese, 2013). Additionally, previous studies have indicated that higher cAMP levels, with sodium nitroprusside (SNP) treatment, resulted in increased conduction system gene expression in differentiating in ES cell cultures (Tsai et al., 2015). However, the effect of β- AR signaling, through agonistic and antagonistic binding, on conduction system expression has not been examined. The overall aim of this study was to examine when the conduction system genes Cx40, HCN4, and Cntn2 are expressed during murine development and investigate the impact of β- AR signaling on the proliferation and differentiation of conduction system cells.

In this study, the expression levels of Cx40, HCN4, and Cntn2 were analyzed in mouse ventricles obtained from various cardiac developmental stages (E11.5, E14.5, E16, Neonatal, and Adult). Next, the effect of β- adrenergic signaling through binding of Isoproterenol (ISO) and/or Metoprolol (METO) on conduction system gene expression were analyzed in E11.5 ventricular cells. ISO is a non-selective β-agonist commonly used in treatments of bradycardia to increase cardiac contractility (Vavetsi et al., 2008). In previous studies, ISO has shown to decrease the proliferation of E11.5 CPCs and CMs and reduce graft size (Feridooni et al., 2017). METO is a

selective- β1 antagonist which is commonly used in treatment of hypertension, CHF and tachycardia (Bonet et al., 2000). In previous studies, METO when combined in treatments with ISO negated the anti-proliferative effects of ISO on graft size (Feridooni et al., 2017). In this study, the effect of ISO and/ or METO on VCS marker gene expression of Cx40, HCN4 and Cntn2 was analyzed with and without the supplementation of ascorbic acid (AA). AA is an anti-oxidant that acts as a reducing agent for ISO in order to increase its bioavailability (Moskowitz et al., 2018; Wong et al., 1987). Additionally, AA has been shown to influence differentiation of ESC into CMs through SMAD1/ BMP signaling (Perino et al., 2017). Lastly, to gain mechanistic insight behind the effects on ISO and/or METO on possible changes in conduction system gene expression changes, changes in cAMP levels were analyzed. Results obtained from these experiments have been summarized in Table 4.1.

Table 4.1: Summary of key findings

Research Question/Experiments performed	Key Findings
Developmental Expression patterns of VCS gene markers	• Expression of Cx40 and HCN4 was highest in the E14.5 stage, and lowest in the Adult stage • Expression of Cntn2 was highest in Neo-natal stage, and lowest in E14.5 • In the E11.5 stage, Cntn2 expression was not seen • Immunostaining confirmed that in: • E11.5 cross-sections: Cx40 (left ventricle) and HCN4 (Sinoatrial node) were visible, Cntn2 was not visible • Adult cross-section: Cntn2 (left bundle branch, PF, SAN, AVN) was visible
Effect of beta-AR stimulation on VCS CPC and VCS CM proliferation	• Percent of proliferating (EdU^+) VCS CPCs ($Cx40^+/Mf20^-$)/ total cells were not changed with ISO and AA treatments compared to controls. • Percent of proliferating (EdU^+) VCS CMs ($Cx40^+/Mf20^+$)/ total cells were not changed with ISO and AA treatments compared to controls of no treatment.
Effect of beta-AR stimulation on VCS gene expression (ISO alone)	• ISO treatment alone was able to increase Cx40 and Cntn2 expression but not HCN4 expression: • This finding indicates that β-adrenergic stimulation with ISO alone can increase VCS gene expression in the embryonic mouse heart.
Effect of beta-AR stimulation on VCS gene expression (AA alone)	• AA alone was unable to increase Cx40, Cntn2 or HCN4 expression: • This finding indicates VCS gene expression is not enhanced or reduced by treatments of Ascorbic acid alone
Effect of beta-AR stimulation on VCS gene expression (ISO+AA supplementation)	• ISO at a higher concentration (2.5 μM) was able to increase Cx40 and Cntn2 gene expression when supplemented with AA • Expression of HCN4 was not changed with ISO stimulation with ISO and/or AA supplementation • These findings indicate that ascorbic acid supplemented with β-adrenergic stimulation has a positive effect on VCS gene expression in the embryonic mouse heart

Table 4.1: Summary of key findings (Cont.)

Research Question/Experiments performed	Key Findings
Effect of inhibition of beta-AR signaling on Cx40 gene expression (METO+ISO+ AA)	• ISO-induced increase in Cx40 gene expression (with and without) supplementation of AA was negated with treatments of β1-adrenergic inhibitor METO • These findings indicate that increase in Cx40 gene expression was negated with β-adrenergic inhibition that was previously increased by β-adrenergic stimulation with and without AA
Effect of inhibition of beta-AR signaling on Cntn2 gene expression (METO+ISO+ AA)	• ISO-induced increase in Cntn2 gene (2.5 μM) expression (without AA) was negated with treatments of METO (1 μM) • ISO-induced increase in Cntn2 gene (2.5 μM) expression was not negated with treatments of METO (1 μM), when supplemented with AA (10 μM AA) • Expression of HCN4 was not changed with treatments of METO with ISO and/ or AA • Additionally, these results show that AA can prevent the effects of β-adrenergic inhibition on Cntn2 gene expression that was previously increased by β-adrenergic stimulation with ISO
Effect of AA supplementation on cAMP levels (AA alone)	• Treatments of AA alone did not increase or decrease cAMP
Effect of beta-AR stimulation on cAMP levels (ISO and ISO+AA)	• Treatments of ISO with and without supplementation of AA increased cAMP for all groups that exhibited increase in Cx40 and Cntn2 gene expression • cAMP was not further increased with ISO supplemented with AA in comparison to ISO treatment alone
Effect of beta-AR inhibition on cAMP levels (ISO and ISO+AA)	• β-adrenergic inhibition with METO (1 and 10 μM) decreased levels of cAMP in co-treatments of 1 μM ISO with and without supplementation of AA • β-adrenergic inhibition with METO (1 μM) did not decrease levels of cAMP in co-treatments of 2.5 μM ISO with and without supplementation of AA • β-adrenergic inhibition with METO (10 μM) decreased levels of cAMP in co-treatments of 2.5 μM ISO without supplementation of AA, but did not decrease cAMP when AA was supplemented.

4.2 Developmental expression of ventricular conduction system genes

Ventricular conduction system genes Cx40, Cntn2 and HCN4 have been studied by several groups, however, there remain inconsistencies in which developmental stages these markers are expressed and which stage has the highest expression for each marker gene. In a mouse heart, Cx40 has been shown to be expressed as early as embryonic day 11.5 (E11.5) (Verheule & Kaese, 2013). In the gestation of a human heart, Cx40 has been shown to be expressed as early as 9 weeks gestation (Kaba et al., 2001). Cntn2 expression is a novel marker of VCS development, and expression in adult mouse and canine hearts has been seen on the sarcolemma of Purkinje fibre myocardium, however developmental expression patterns have yet to be thoroughly studied (B. Pallante et al., 2010). HCN4 has been found to be expressed earliest in the primary heart field in E6 mice hearts, primarily in the SAN, and spreads throughout the VCS as the heart matures (Liang et al., 2015).

Consistent with previous reports, the presence of Cx40 and HCN4 in the VCS was seen in the E11.5 stage in this study and developmental gene expression analysis revealed the highest expression at the E14.5 stage, and the lowest in the adult stage (Figure 3.1). Cntn2 expression was not seen in the VCS at the E11.5 developmental stage, instead the earliest expression was seen in the E14.5 developmental stage (Figure 3.1). Additionally, the Cntn2 marker gene was seen expressed the highest during the Neonatal developmental stage, and lowest in the E14.5 stage (Figure 3.1). Immunostaining analysis of E11.5 ventricular cross sections showed that expression of Cx40 was visible in the trabeculae of the left ventricle and HCN4 was visible in the SA node (Figure 3.2). These results correspond with RT-qPCR marker gene expression analysis from E11.5 ventricular tissue as both Cx40 and HCN4 were present in the E11.5 stage. Cntn2 expression was also not seen expressed in E11.5 cross-sections, however, was seen

expressed in the descending left bundle branch in Adult cross sections (Figure 3.3). These results also correspond with RT-qPCR marker gene expression analysis from E11.5 ventricular tissue as Cntn2 was not seen expressed in the E11.5 stage but was visible later as the heart matured and visible in the adult stage. Additional immunolocalization studies are required to confirm the expression patterns of VCS marker genes in other stages of cardiac development. This study describes the gene expression patterns of all three VCS markers at various stages of cardiac development.

4.3 Effect of Beta-adrenergic stimulation on conduction system cell development

In this study, the effects of β-adrenergic signalling on proliferation and differentiation of VCS populations were observed with treatment of ISO, a β1-AR agonist. The populations that were examined were VCS CPCs ($Cx40^{+}/MF20^{-}$) and VCS CMs ($Cx40^{+}/MF20^{+}$) through immunostaining. The proliferation of the VCS populations was assessed through a Click-IT EdU proliferation assay, that measures the incorporation of Edu (a thymidine analog) during DNA synthesis (S- phase). Both VCS CPC and VCS CM populations were observed with treatments of 1, 2.5, 5, and 10 μM ISO with and without supplementation of AA. However, the percentage of proliferating VCS CPCs and proliferating VCS CMs out of total cells per treatment did not vary in comparison to the no treatment 0 μM ISO group. These results were contrary to the finding by Feridooni et al, that found inhibitory effect of 1 μM ISO on proliferation rates of Nkx2.5+ CPCs (Nkx2.5+/MF20-) in E11.5 ventricular cell cultures (Feridooni et al., 2017). There are two possible reasons for the discrepancies observed between these studies. The first reason was the use of different proliferation assays. Feridooni et al used the [3H] thymidine autoradiography for monitoring changes in cell proliferation in their study (Feridooni et al.,

2017). In contrast, a fluorescence-based Click-IT EdU assay was performed in this study to eliminate the use of radioisotopes. The second noticeable difference is the use of different cell lineage markers to identify E11.5 CPCs. This study used Cx40 labeling to identify VCS CPCs and VCS CMs which represent a relatively smaller fraction of total ventricular myocardium at any given developmental stage. Whereas, Feridooni et al identified all ventricular cells using Nkx2.5 labeling and this approach marks all primary and secondary heart field derived CPCs which can give raise to working CMs, conduction system cells and vascular smooth muscle cells (McMullen et al., 2009; Wu et al., 2006). These differences in cell tracking methodologies (Nkx2.5+ Vs Cx40+) are further consistent with differences in the number of proliferating CPCs observed between studies. For example, in the 0 μM ISO no treatment control group, the percentage of proliferating Nkx2.5+ CPCs out of total cells was 54.1% for the Feridooni et al study, and only 9.28% for Cx40+ CPCs in this study. While β-AR stimulation decreased proliferation of Nkx2.5+ CPCs and Nkx2.5+ CMs in Feridooni's study, the results in this study showed that β-AR stimulation did not affect proliferation of VCS CPCs and VCS CMs. Taken together, these results may also suggest that inhibitory effects of ISO on cell proliferation observed in Feridooni's study may be restricted to non-VCS CPCs and non-VCS CMs and this notion needs to be further confirmed by additional cell labeling experiments (e.g. co-immunostaining with Nkx2.5 and Cx40 antibodies). Future studies should also be performed using [3H] thymidine autoradiography to confirm the absence of ISO effects on proliferation of VCS CPCs and VCS CMs.

The effect of β-adrenergic signalling on differentiation of VCS populations was assessed through RT-qPCR analysis of extracted total RNA from ISO treated E11.5 ventricular cells. Cells were treated with 1 and 2.5 μM ISO with and without supplementation of AA, and VCS

marker gene expression of Cx40, HCN4 and Cntn2 were assessed. Notably, when E11.5 ventricular cells were treated with 1 μM ISO alone, there was a significant increase (1.3-Fold) in the Cx40 expression, compared to the no treatment 0 μM ISO 0 μM AA control group. When E11.5 ventricular cells were treated alone with 2.5 μM ISO there was a significant increase (2.9-Fold) in Cntn2 gene expression compared to the no treatment 0 μM ISO 0 μM AA control group. These findings show that β-adrenergic stimulation with ISO alone can increase gene expression of both Cx40 and Cntn2, however at different treatment concentrations. The increase in Cntn2 expression required a larger concentration of ISO alone at 2.5 μM, while Cx40 was able to increase expression at a lower concentration of 1 μM ISO alone. Additionally, the expression of Cx40 and Cntn2 have both been increased with the supplementation of AA. The expression of Cx40 increased (by 2.2-Fold) with treatments of 2.5 μM ISO 10 μM ISO. The expression of Cntn2 increased (by 3.3-Fold) with treatments of 2.5 μM ISO 10 μM ISO. These results indicate that both ISO alone and ISO + AA can increase the expression of both Cx40 gene and Cntn2 in E11.5 ventricular cells. Furthermore, Cntn2 results indicate that the supplementation of AA (2.5 μM ISO 10 μM AA) with a 3.3-fold increase enhances gene expression in comparison to a 2.9-fold increase in ISO treatment alone (2.5 μM ISO 0 AA). HCN4 expression in E11.5 ventricular cells were not altered by treatments of ISO even in combination with AA. The collective findings from Cx40, and Cntn2 expression suggest that β- AR stimulation with ISO treatments in combination with AA can induce transcriptional changes in VCS marker genes and promote differentiation of E11.5 ventricular cells into the VSC lineage. However, it was seen that while Cx40 gene expression was increased by 1 μM ISO alone, this effect was not seen when cells were treated with 1 μM ISO 10 μM AA. This indicates that the role of AA is more complex than seen and further studies are required to isolate the effect of AA.

In a study conducted by Yan et al. stimulation of ESCs with ISO resulted in the generation of beating embryoid bodies, indicating the β-adrenergic stimulation played a role in cardiac differentiation (Yan et al., 2011). However, the study by Yan et al did not determine whether these generated beating embryoid bodies were a result of the increased differentiation of conduction system CMs/ CPCs or working CMS. Additionally, the cell populations used between the two studies differed as the Yan et al study used ESCs whereas this study used embryonic ventricular cells (Yan et al., 2011). The number of beating embryoid bodies, however did increase with treatments of ISO in a dose-dependent manner similar to this study (Yan et al., 2011). Our study shows that CPCs can be induced to differentiate towards the VCS lineage through treatments of ISO and ISO + AA. Furthermore, in cardiac regenerative treatments CPCs can be possibly used and induced with ISO to generate VCS cells in injured regions of the heart suffering from reduced conduction. The introduction of these cell can be done possibly through intravenous injection or through tissue grafts to specific injured regions, however the applicability of these methods remains to be well defined/ understood. Another possible concern with treating hearts to induce CPCs into VCS cells with β-adrenergic stimulation is that there is the possibility of generating ectopic foci in non-conducting regions of the heart. The ectopic growth of VCS cells in regions not responsible for rapid conduction can result in the presentation of arrythmias. A possible approach in addressing this concern is considering the effect of β-adrenergic inhibition in controlling VCS differentiation.

4.4 The effect of Beta-adrenergic receptor inhibition on conduction system cell development

The effect of β- AR signal inhibition on differentiation of E11.5 ventricular cells were analyzed through treatments with METO. While previous studies have noted METO's anti-

proliferative effects of ISO on graft size, little is known about the effect of METO on VCS differentiation. In this study, the ISO-induced increase in Cx40 expression was decreased with treatments of 1 μM ISO 0 μM AA 1 μM METO in comparison to 1 μM ISO 0 μM AA 0 μM METO. Additionally, the ISO+AA-induced increase in Cx40 expression (2.5 μM ISO 10 μM AA) was decreased with treatments of 1 μM METO (2.5 μM ISO 10 μM AA 1 μM METO). These results indicate that METO negated the ISO-induced increase in Cx40 gene expression that was previously seen from both ISO treatments alone at lower concentration and ISO at higher concentrations with supplementation of AA. The ISO-induced increase in Cntn2 expression was also decreased with treatments of 1 μM METO (2.5 μM ISO 0 μM AA 1 μM METO) in comparison to 2.5 μM ISO 0 μM AA 0 μM METO. However, the ISO+AA-induced increase in Cntn2 expression (2.5 μM ISO 10 μM AA) was not decreased when 1 μM METO was added (2.5 μM ISO 10 μM AA 1 μM METO). Furthermore, even with the added 1 μM METO treatment (2.5 μM ISO 10 μM AA 1 μM METO) Cntn2 expression still significantly increased. These results indicate that METO only negated the ISO alone-induced increase in Cntn2 gene expression and did not negate ISO + AA-induced increase in Cntn2 expression. HCN4 expression was not altered with treatments of METO in combination with ISO, and AA on E11.5 ventricular cells.

Previous studies from Yan et al, found that selective β1- adrenergic antagonist CGP20712A (CGP) when treated 1 hour prior to treatments of ISO, negated the generation of beating embryonic bodies from ESCs. While ISO-induced enhancement was negated by both CGP in the Yan et al study and METO in this study, the effect on the VCS was not studied in the former. Collectively, these findings suggest that as it is possible to upregulate VCS cell generation with β- AR stimulation, VCS cell generation can also be prevented with inhibition of

β- AR signaling. The applicability of β- AR inhibition in controlling/ preventing ectopic generation of VCS cells in tissue grafts remains to be studied. As seen in the Feridooni et al. study, treatments of METO were able to negate the antiproliferative effect of ISO on graft size, however the effect of METO co-treatments with ISO on VCS generation in tissue grafts have not been studied. Based on findings from this study, it is anticipated that β-AR inhibition in stem and progenitor cell transplantation studies can lead to formation of larger grafts with no or minimal number of VCS cells. The testing of β-adrenergic stimulation and inhibition on VCS generation within donor cell grafts would provide further insight into the application of CPCs in treating arrythmias as well as preventing arrythmias as a result of ectopic proliferation.

4.5 Effect of Ascorbic Acid

This study showed that β- AR stimulation was able to upregulate VCS gene expression with and without AA supplementation. While 10 μM AA alone is unable to increase gene expression of Cx40 or Cntn2, the supplementation of AA with ISO enhanced Cntn2 gene expression and prevented METO from negating the increase in Cntn2. Furthermore, from analyzing the change of Cx40 expression, the possible cardioprotective effects of AA can be seen. The treatment of ISO alone at a lower concentration (1 μM) is able to increase Cx40 expression, however the treatment of ISO alone at higher concentration (2.5 μM) is able to increase Cx40 expression. The reason why ISO at a higher concentration was not able to increase Cx40 expression is likely because ISO is cardiotoxic at a larger dose (Ramos & Acosta, 1983). The cardioprotective effect of AA can be seen when the higher concentration of ISO (2.5 μM ISO 0 μM) is supplemented with 10 μM AA (2.5 μM ISO 10 μM), and there is an increase in Cx40 expression. In a previous study by Ramos et al, the cardioprotective effect of AA was

studied in cultured rat myocytes treated with varying concentrations of ISO and AA (Ramos & Acosta, 1983). Lactate Dehydrogenase (LDH) production (released during cell death) and cell viability were assessed to determine the extent of myocyte injury (Ramos & Acosta, 1983). Cell injury increased in a dose-dependent manner with ISO concentrations as low as 10^{-4} M ISO (Ramos & Acosta, 1983). However, 5×10^{-4} M co-treatment with AA was able to prevent ISO-induced toxicity and decrease in cell viability (Ramos & Acosta, 1983). Additionally, a study by Feridooni et al showed there was increased cell death of E11.5 ventricular cell cultures with ISO treatments of 5 and 10 μM (unpublished work from Pasumarthi Lab). A study done by Buttros et al, noted that ISO at high concentrations can induce myocardial ischemia and injury in rats through production of free radicals as a result of increased oxidative metabolism and increased iNOS synthesis (Buttros et al., 2009). Additionally, the cardioprotective effect from ascorbic acid is seen by protecting against free radicals and by supressing iNOS synthesis (Buttros et al., 2009). The findings from these studies elaborate the cardioprotective effects of supplementation of AA, and prevention of cell viability when co-treated with ISO. Based on these studies, it can be further proposed that 10 μM AA supplementation may be effective in preventing myocyte injury in E11.5 ventricular cell cultures treated with 1 and 2.5 μM ISO. However, future studies are required to validate the levels of cell injury and cell death in embryonic ventricular cell cultures treated with different concentrations of ISO and determine the efficacy of AA in preventing cytotoxic effects of ISO.

In a study by Perino et al, the effect of AA on cardiomyogenesis was investigated (Perino et al., 2017). Treatments of AA were able to induce ESCs to differentiate into $TNNT2^{+}$-cardiomyocytes through modulation of SMAD1/BMP receptor signaling (Perino et al., 2017). These findings show that AA is more than a simple anti-oxidant and cytoprotective agent but can

also play an important role in the induction of embryonic cells into the cardiac lineage, however it was undetermined whether these generated CMs in ESC cultures displayed VCS expression (Perino et al., 2017). This study showed that AA can act synergistically with ISO to induce embryonic cell differentiation towards the VCS lineage. AA alone, however, was unable to induce differentiation of E11.5 ventricular cells into the VCS lineage. While mechanisms behind AA's inductive process are not fully understood, the effect of AA on β- AR signaling, and cAMP production was studied to provide further insights.

4.6 Effect of ISO, AA and METO on cAMP production through Beta-adrenergic receptor signaling

The analysis of cAMP production allows insight into mechanisms regulating synergistic effects of ISO and AA on VCS marker gene expression in E11.5 ventricular cell cultures. As previously mentioned, AA alone was unable to increase VCS gene expression. Additionally, E11.5 ventricular cells treated with 10, 25, 50, and 100 μM AA alone showed that there was no significant change in cAMP levels in comparison to 0 μM AA. These results suggest that AA alone is unable to activate adenylyl cyclase to produce cAMP, and this could possibly explain why VCS gene expression was not altered.

VCS gene expression was increased by 1 μM and 2.5 μM ISO concentrations with and without supplementation of 10 μM AA. The change in cAMP production was also measured in cells treated with ISO and AA at these concentrations and it was seen that the cAMP levels were upregulated by ISO treatments with and without AA in comparison to the 0 μM ISO 0 μM AA no treatment control group. While it was expected that treatments of ISO would increase cAMP production, it was interesting to note that AA when supplemented with ISO did not further increase cAMP in comparison to ISO alone. It is likely that AA works synergistically with ISO-

induced β-adrenergic stimulation to increase VCS gene expression, and thus these results suggest that in addition to β-adrenergic signalling an additional mechanism must be involved in the synergistic effect seen with AA treatment.

For Cx40 expression, the 1 μM ISO 0 AA treatment that induced an increase in gene expression was negated with the supplementation of 1 μM METO (1 μM ISO 0 AA 1 μM METO). The treatment of METO prevented the increase in cAMP that was previously seen through β-adrenergic stimulation of ISO alone, and the decrease in cAMP could possibly explain why Cx40 gene expression was not increased with treatments of 1 μM ISO 0 AA and 1 μM METO. This possibly suggests that β-adrenergic inhibition, through the decrease of cAMP can prevent the upregulation of Cx40 gene expression. This notion however changes in the presence of AA. It was seen that 1 μM METO was unable to decrease cAMP levels in cells co-treated with 2.5 μM ISO and 10 μM AA. However, the increase in Cx40 gene expression seen with 2.5 μM ISO and 10 μM AA treatment was prevented through 1 μM METO co-treatment. This suggests that as complex as the induction process is for the upregulation of VCS gene expression through β-adrenergic stimulation, the prevention process of this effect through β-adrenergic inhibition is also complex. Secondarily, the ratios of ISO: METO treatments and treatment durations must be considered in establishing patterns on β-adrenergic stimulation and inhibition. As treatment durations in gene expression analysis were 24 hours while change in cAMP was only measured after an hour of treatment of ISO, AA and/or METO.

The notion that β- AR inhibition with METO, through the decrease of cAMP can prevent the upregulation of VCS gene expression is also valid for the expression of Cntn2. This can be seen as Cntn2 gene expression which upregulated cAMP with β-adrenergic stimulation with ISO (2.5 μM), was negated by co-treatment with β-adrenergic inhibitor METO (1 μM). The same

negation of cAMP and Cntn2 gene expression that was seen with β-adrenergic inhibition of METO, was prevented when AA acid was supplemented. Collectively, analysis of the effect of ISO, METO and AA on changes in cAMP suggests that VCS gene expression is upregulated through β- AR stimulation and an increase in cAMP, which can be prevented by β- AR inhibition and reduction in cAMP. Additionally, the supplementation of AA has a secondary effect on VCS gene expression.

In Figure 4.1, a possible mechanism is proposed for VSC gene expression regulation through β-adrenergic signalling and the effect of AA. ISO binding to β- ARs leads to increase in cAMP and activation of Protein Kinase-A (PKA). The activated PKA, leads to phosphorylated activation of cAMP response element binding protein CREB. CREB is a transcription factor that has been understood to be involved in many cellular processes such as cell proliferation, differentiation and survival (Wen et al., 2010). Additionally, CREB is involved in the ventricular conduction system as cardiac-specific inactivation of CREB in mouse ventricles, leads to alterations in action potential shape and duration (Schulte et al., 2012). After phosphorylation of CREB, CREB-binding protein (CBP) interacts with CREB in the nucleus (Wen et al., 2010), and possibly leads to the upregulation of VCS gene expression. CBP is a co-factor that recruits transcription factors and helps stimulate gene transcription (Wen et al., 2010). In this study, ISO-alone was able to increase VCS expression through β- ARs and the mechanism behind this could be the result of activation of CREB-CBP. Furthermore, it was also seen that ISO in combination with AA also increased VCS expression, and this mechanism could be possibly a result of co-activation of SMAD1. Typically, activation of BMP receptor leads to the phosphorylated activation of SMAD1/5/9 (Chau et al., 2012). However, AA has also been shown to induce activation of SMAD1 through modulation of the bone morphogenic protein 2 (BMP2) signalling

(Perino et al., 2017). BMP signalling has important roles in cardiac development as well as cell proliferation, differentiation and migration during organ development and embryogenesis (Yuasa & Fukuda, 2008). SMAD1/5/9 are co-receptors from the SMAD protein family that bind to co-factor SMAD4 to increase gene expression of target genes (Duan et al., 2017). The activation of SMAD1 induces cardiomyocyte differentiation in mouse ESCs (Perino et al., 2017). We further propose that the combined activation of SMAD1 by AA binding with co-factors SMAD4 and CBP, and the activation of CREB-CBP synergistically induces expression of VCS genes. Additionally, AA can act as a reducing agent to reduce inactive ISO back into its active form, thus increasing ISO signaling and possibly increasing the induction of CREB and VCS gene expression. Furthermore, CBP could also possibly play an important role in enhanced VCS expression as CBP is bound as a cofactor by both CREB and SMAD1 (Pearson et al., 1999).

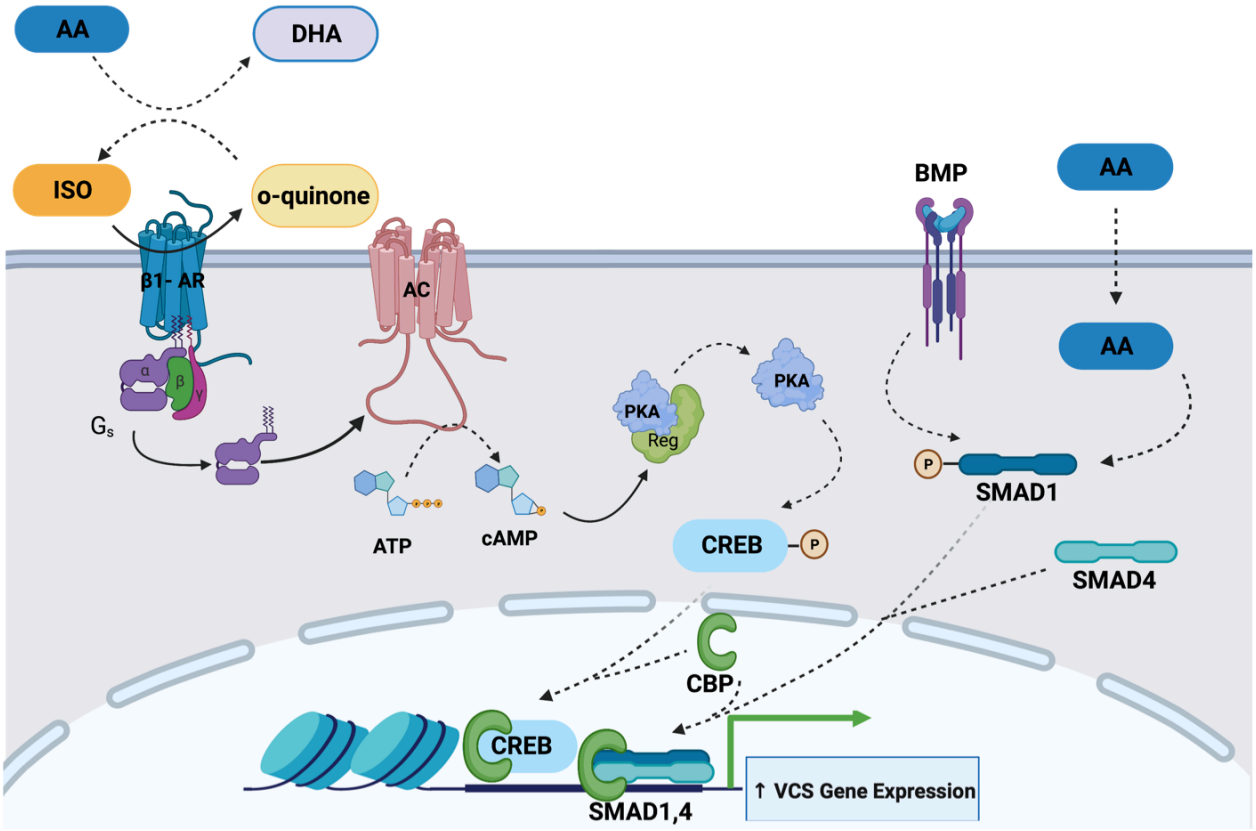

Figure 4.1: Proposed signaling pathway for increased VCS gene expression
Ascorbic acid (AA) acts as a reducing agent and is oxidized into dehydroascorbic acid (DHA) to reduce inactive ISO (o-quinone) back into its active state. Active ISO binds to β1- ARs to activate G-coupled proteins to induce activation of adenylate cyclase (AC). Activate AC leads to catalysis of ATP, to increase cAMP. Increased cAMP binds to the regulatory protein on PKA and release PKA from its inhibitor. Activate PKA then leads to the phosphorylation of CREB and CREB binds with co-factor CBP in the nucleus. CREB-CBP increases VCS gene expression. AA also modulates the increase in SMAD1 activation which is typically activated through the BMP receptor. Activated SMAD1 binds to cofactors SMAD4 and CBP to increase VCS gene expression when in combination with CREB-CBP.

4.7 Limitations and Future Directions

The findings in this study suggests the β-adrenergic stimulation with ISO can increase VCS gene expression of Cx40 and Cntn2, while β-adrenergic inhibition with METO can negate this effect. Supplementation of AA with ISO and METO has additionally revealed that AA can play a role in VCS gene expression with β-adrenergic signaling, through increasing bioavailability of ISO, and cardioprotective effects as well as synergistic effects on gene transcription. However, several limitations could be seen with this study. One of the limitations is that ISO is a non-specific β-agonist, so observed affects are not limited to β1-adrenergic signalling and β2-adrenergic signaling can also be influencing these effects. To further analyze specific β- AR function, a selective β1-agonist such as dobutamine, a selective β2-agonist such as albuterol, and a non-selective β- AR blocker such as propanolol should be individually tested on E11.5 ventricular cells for an effect on VCS gene expression.

Another limitation of this study is only METO was used to understand the effect of β-AR inhibition. METO is a specific β1-blocker, and while gene expression was reduced with METO treatments, there was a case when METO did not reduce Cntn2 expression. Treatments of 2.5 μM ISO 10 μM AA upregulated Cntn2 gene expression, which was not negated with added treatment of 1 μM METO. Future experiments should test the effects of β-adrenergic inhibition with larger doses of METO and examine if AA still exhibits an enhancing effect, or if gene expression is supressed by the increased METO.

A third limitation of this study is the limited treatment concentrations tested. While patterns of gene expression of Cx40 and Cntn2 were noted with treatments of ISO, AA and METO, the concentrations were limited to 1, and 2.5 μM ISO, 10 μM AA, and 1 μM METO. To

further elucidate and understand the effect of treatments of ISO, AA and METO on VCS gene expression, additional concentrations should be tested and analyzed.

Another limitation to this study is that the effect of β-adrenergic signaling was only analyzed on VCS marker gene expression. Additional experiments should be conducted to confirm changes in protein levels of VCS markers in embryonic ventricular cells treated with ISO and AA. Additionally, mechanisms responsible for synergistic effects of ISO and AA will need to be analyzed in future studies. Specifically, the effect of AA on the SMAD pathway and its potential interaction with the CREB pathway will need further validation. Future studies can examine the proposed mechanism of action through in-cell westerns or western blot analysis of SMAD phosphorylation and CREB-phosphorylation in the presence and absence of PKA inhibitors. No changes in HCN4 gene expression with ISO and AA treatment suggest the requirement of additional factors and pathways for VCS development.

A finding that was observed in this study was that results from ISO treatments on proliferation of VCS CPCs and VCS CMs measured through Click-IT EdU were contrary to the findings from Feridooni et al (Feridooni et al., 2017). This could be possibly explained due to difference in proliferation assays and differences in cell lineage tracking markers used. However a third proliferation assay such as a BrdU assay and combination of lineage markers (e.g. Cx40, Nkx2.5, MF20) should be used to reassess and confirm the effect of ISO on proliferation of different sub-lineages of CPC population (e.g. Nkx2.5+/Cx40^{-}/MF20^{-} Vs. Nkx2.5^{+}/Cx40^{+}/MF20^{-} CPCs).

4.8 Conclusion

β-adrenergic signalling has been shown to play a role in the VCS development as ISO induced β-adrenergic stimulation increased Cx40 and Cntn2 marker gene expression, and METO treatments negated this effect. Additionally, AA in this study was seen to exhibit cardioprotective effects and increased effectiveness of ISO-induced β- adrenergic stimulation on VCS expression. This study is relevant in cell-based regenerative treatment approaches to specifically regenerate injured conductive cells within the heart with VCS CPCs and β- AR stimulation. Furthermore, the potentially harmful ectopic arrythmias seen with the increased VCS gene expression and VCS cell differentiation in stem and progenitor cell-based interventions can be prevented with treatment of β-AR inhibition.

References

Almeida, S. O., Skelton, R. J., Adigopula, S., & Ardehali, R. (2015). Arrhythmia in stem cell transplantation. *Cardiac electrophysiology clinics, 7*(2), 357-370. https://doi.org/10.1016/j.ccep.2015.03.012

Azevedo, P. S., Polegato, B. F., Minicucci, M. F., Paiva, S. A. R., & Zornoff, L. A. M. (2016). Cardiac Remodeling: Concepts, Clinical Impact, Pathophysiological Mechanisms and Pharmacologic Treatment. *Arquivos brasileiros de cardiologia, 106*(1), 62-69. https://doi.org/10.5935/abc.20160005

Barreto, S., Hamel, L., Schiatti, T., Yang, Y., & George, V. (2019). Cardiac Progenitor Cells from Stem Cells: Learning from Genetics and Biomaterials. *Cells, 8*(12), 1536. https://doi.org/10.3390/cells8121536

Beltowski, J., Wojcicka, G., & Jamroz-Wisniewska, A. (2009, //). Adverse Effects of Statins - Mechanisms and Consequences. *Current Drug Safety, 4*(3), 209-228. https://doi.org/10.2174/157488609789006949

Benigni, A., Cassis, P., & Remuzzi, G. (2010). Angiotensin II revisited: new roles in inflammation, immunology and aging. *EMBO molecular medicine, 2*(7), 247-257. https://doi.org/10.1002/emmm.201000080

Bers, D. M. (2002, 2002/01/01). Cardiac excitation–contraction coupling. *Nature, 415*(6868), 198-205. https://doi.org/10.1038/415198a

Boersma, E., Mercado, N., Poldermans, D., Gardien, M., Vos, J., & Simoons, M. L. (2003, 2003/03/08/). Acute myocardial infarction. *The Lancet, 361*(9360), 847-858. https://doi.org/https://doi.org/10.1016/S0140-6736(03)12712-2

Bonarjee, V. V. S., & Dickstein, K. (2001). How long should angiotensin-converting enzyme inhibitors be given to patients following myocardial infarction: implications of the HOPE trial. *Current controlled trials in cardiovascular medicine, 2*(4), 151-155. https://doi.org/10.1186/cvm-2-4-151

Bonet, S., Agusti, A., Arnau, J. M., Vidal, X., Diogene, E., Galve, E., & Laporte, J. R. (2000, Mar 13). Beta-adrenergic blocking agents in heart failure: benefits of vasodilating and non-vasodilating agents according to patients' characteristics: a meta-analysis of clinical trials. *Arch Intern Med, 160*(5), 621-627. https://doi.org/10.1001/archinte.160.5.621

Buttros, J. B., Bergamaschi, C. T., Ribeiro, D. A., Fracalossi, A. C. C., & Campos, R. R. (2009, Jul 2009 2014-03-22). Cardioprotective Actions of Ascorbic Acid during Isoproterenol-Induced Acute Myocardial Infarction in Rats. *Pharmacology, 84*(1), 29-37. https://doi.org/http://dx.doi.org/10.1159/000222245

Cambria, E., Steiger, J., Günter, J., Bopp, A., Wolint, P., Hoerstrup, S. P., & Emmert, M. Y. (2016). Cardiac Regenerative Medicine: The Potential of a New Generation of Stem Cells. *Transfusion medicine*

and hemotherapy : offizielles Organ der Deutschen Gesellschaft fur Transfusionsmedizin und Immunhamatologie, 43(4), 275-281. https://doi.org/10.1159/000448179

Chadwick, J., Davatyan, K., Subramanian, S. S., & Priya, J. (2019). Epidemiology of Myocardial Infarction. In *Myocardial Infarction*. https://doi.org/10.5772/intechopen.74768

Chang, M.-L., Chiu, Y.-J., Li, J.-S., Cheah, K.-P., & Lin, H.-H. (2020). Analyzing Impetus of Regenerative Cellular Therapeutics in Myocardial Infarction. *Journal of Clinical Medicine, 9*(5). https://doi.org/10.3390/jcm9051277

Chau, J. F. L., Jia, D., Wang, Z., Liu, Z., Hu, Y., Zhang, X., Jia, H., Lai, K. P., Leong, W. F., Au, B. J., Mishina, Y., Chen, Y.-G., Biondi, C., Robertson, E., Xie, D., Liu, H., He, L., Wang, X., Yu, Q., & Li, B. (2012, 2012/05/15). A crucial role for bone morphogenetic protein-Smad1 signalling in the DNA damage response. *Nature Communications, 3*(1), 836. https://doi.org/10.1038/ncomms1832

Chen, F., Klitzner, T. S., & Weiss, J. N. (2006, May). Autonomic regulation of calcium cycling in developing embryonic mouse hearts. *Cell Calcium, 39*(5), 375-385. https://doi.org/10.1016/j.ceca.2005.12.004

Christoffels, V. M., & Moorman, A. F. (2009, Apr). Development of the cardiac conduction system: why are some regions of the heart more arrhythmogenic than others? *Circ Arrhythm Electrophysiol, 2*(2), 195-207. https://doi.org/10.1161/circep.108.829341

Cleland, J. G. F., Coletta, A. P., Abdellah, A. T., Nasir, M., Hobson, N., Freemantle, N., & Clark, A. L. (2007). Clinical trials update from the American Heart Association 2006: OAT, SALT 1 and 2, MAGIC, ABCD, PABA-CHF, IMPROVE-CHF, and percutaneous mitral annuloplasty. *European Journal of Heart Failure, 9*(1), 92-97. https://doi.org/https://doi.org/10.1016/j.ejheart.2006.12.001

Cotecchia, S., Stanasila, L., & Diviani, D. (2012). Protein-protein interactions at the adrenergic receptors. *Current drug targets, 13*(1), 15-27. https://doi.org/10.2174/138945012798868489

Cui, W., Taub, D. D., & Gardner, K. (2007, Jan). qPrimerDepot: a primer database for quantitative real time PCR. *Nucleic Acids Res, 35*(Database issue), D805-809. https://doi.org/10.1093/nar/gkl767

Dai, W., Hale, S. L., Martin, B. J., Kuang, J.-Q., Dow, J. S., Wold, L. E., & Kloner, R. A. (2005). Allogeneic Mesenchymal Stem Cell Transplantation in Postinfarcted Rat Myocardium. *Circulation, 112*(2), 214-223. https://doi.org/doi:10.1161/CIRCULATIONAHA.104.527937

Deo, M., Boyle, P. M., Kim, A. M., & Vigmond, E. J. (2010). Arrhythmogenesis by single ectopic beats originating in the Purkinje system. *Am J Physiol Heart Circ Physiol, 299*(4), H1002-H1011. https://doi.org/10.1152/ajpheart.01237.2009

DiFrancesco, D. (2010, 2010/02/19). The Role of the Funny Current in Pacemaker Activity. *Circulation Research, 106*(3), 434-446. https://doi.org/10.1161/CIRCRESAHA.109.208041

Duan, Y., Zhu, W., Liu, M., Ashraf, M., & Xu, M. (2017). The expression of Smad signaling pathway in myocardium and potential therapeutic effects. *Histology and histopathology, 32*(7), 651-659. https://doi.org/10.14670/HH-11-845

Eisner, D. A., Caldwell, J. L., Kistamás, K., & Trafford, A. W. (2017, 2017/07/07). Calcium and Excitation-Contraction Coupling in the Heart. *Circulation Research, 121*(2), 181-195. https://doi.org/10.1161/CIRCRESAHA.117.310230

Evrard, A., Hober, C., Racadot, A., Lefebvre, J., & Vantyghem, M. C. (1999, Mar-Apr). [Atrial natriuretic hormone and endocrine functions]. *Ann Biol Clin (Paris), 57*(2), 149-155. (Hormone natriurétique auriculaire et fonctions endocrines.)

Feridooni, T., Hotchkiss, A., Baguma-Nibasheka, M., Zhang, F., Allen, B., Chinni, S., & Pasumarthi, K. B. S. (2017). Effects of β-adrenergic receptor drugs on embryonic ventricular cell proliferation and differentiation and their impact on donor cell transplantation. *Am J Physiol Heart Circ Physiol, 312*(5), H919-H931. https://doi.org/10.1152/ajpheart.00425.2016

Feridooni, T., & Pasumarthi, K. B. S. (2019, 2019/01/01/). Fractionation of embryonic cardiac progenitor cells and evaluation of their differentiation potential. *Differentiation, 105*, 1-13. https://doi.org/https://doi.org/10.1016/j.diff.2018.11.001

Frangogiannis, N. G. (2015, Sep 20). Pathophysiology of Myocardial Infarction. *Compr Physiol, 5*(4), 1841-1875. https://doi.org/10.1002/cphy.c150006

Friederich, J. A., & Butterworth, J. F. (1995). Sodium Nitroprusside: Twenty Years and Counting. *Anesthesia & Analgesia, 81*(1).

Giepmans, B. N. G. (2004). Gap junctions and connexin-interacting proteins. *Cardiovascular Research, 62*(2), 233-245. https://doi.org/10.1016/j.cardiores.2003.12.009

Gittenberger-de Groot, A. C., Bartelings, M. M., Deruiter, M. C., & Poelmann, R. E. (2005, 2005/02/01). Basics of Cardiac Development for the Understanding of Congenital Heart Malformations. *Pediatric Research, 57*(2), 169-176. https://doi.org/10.1203/01.PDR.0000148710.69159.61

Golomb, B. A., & Evans, M. A. (2008). Statin adverse effects : a review of the literature and evidence for a mitochondrial mechanism. *American journal of cardiovascular drugs : drugs, devices, and other interventions, 8*(6), 373-418. https://doi.org/10.2165/0129784-200808060-00004

Gomez, H. (1958, Jan). The development of the innervation of the heart in the rat embryo. *Anat Rec, 130*(1), 53-71. https://doi.org/10.1002/ar.1091300106

Govindapillai, A., Hotchkiss, A., Baguma-Nibasheka, M., Rose, R. A., Miquerol, L., Smithies, O., Maeda, N., & Pasumarthi, K. B. S. (2018). Characterizing the role of atrial natriuretic peptide signaling in the development of embryonic ventricular conduction system. *Scientific Reports, 8*(1), 6939-6939. https://doi.org/10.1038/s41598-018-25292-0

Gurung, S., Asante, E., Hummel, D., Williams, A., Feldman-Schultz, O., Halloran, M. C., Sittaramane, V., & Chandrasekhar, A. (2018, Aug). Distinct roles for the cell adhesion molecule Contactin2 in the

development and function of neural circuits in zebrafish. *Mech Dev, 152*, 1-12. https://doi.org/10.1016/j.mod.2018.05.005

Hotchkiss, A., Feridooni, T., Baguma-Nibasheka, M., McNeil, K., Chinni, S., & Pasumarthi, K. B. (2015, Apr 1). Atrial natriuretic peptide inhibits cell cycle activity of embryonic cardiac progenitor cells via its NPRA receptor signaling axis. *Am J Physiol Cell Physiol, 308*(7), C557-569. https://doi.org/10.1152/ajpcell.00323.2014

Hotchkiss, A., Feridooni, T., Zhang, F., & Pasumarthi, K. B. S. (2014, 2014/05/01/). The effects of calcium channel blockade on proliferation and differentiation of cardiac progenitor cells. *Cell Calcium, 55*(5), 238-251. https://doi.org/https://doi.org/10.1016/j.ceca.2014.02.018

Hottinger, D. G., Beebe, D. S., Kozhimannil, T., Prielipp, R. C., & Belani, K. G. (2014). Sodium nitroprusside in 2014: A clinical concepts review. *Journal of anaesthesiology, clinical pharmacology, 30*(4), 462-471. https://doi.org/10.4103/0970-9185.142799

Ittaman, S. V., VanWormer, J. J., & Rezkalla, S. H. (2014). The role of aspirin in the prevention of cardiovascular disease. *Clinical medicine & research, 12*(3-4), 147-154. https://doi.org/10.3121/cmr.2013.1197

Jeziorowska, D., Korniat, A., Salem, J.-E., Fish, K., & Hulot, J.-S. (2015, 2015/10/03). Generating patient-specific induced pluripotent stem cells-derived cardiomyocytes for the treatment of cardiac diseases. *Expert Opinion on Biological Therapy, 15*(10), 1399-1409. https://doi.org/10.1517/14712598.2015.1064109

Johnson, R. D., & Camelliti, P. (2018). Role of Non-Myocyte Gap Junctions and Connexin Hemichannels in Cardiovascular Health and Disease: Novel Therapeutic Targets? *International journal of molecular sciences, 19*(3), 866. https://doi.org/10.3390/ijms19030866

Kaba, R. A., Coppen, S. R., Dupont, E., Skepper, J. N., Elneil, S., Haw, M. P., Pepper, J. R., Yacoub, M. H., Rothery, S., & Severs, N. J. (2001, 2001/01/01). Comparison of Connexin 43, 40 and 45 Expression Patterns in the Developing Human and Mouse Hearts. *Cell communication & adhesion, 8*(4-6), 339-343. https://doi.org/10.3109/15419060109080750

Karaki, H., Ozaki, H., Hori, M., Mitsui-Saito, M., Amano, K.-I., Harada, K.-I., Miyamoto, S., Nakazawa, H., Won, K.-J., & Sato, K. (1997). Calcium Movements, Distribution, and Functions in Smooth Muscle. *Pharmacological Reviews, 49*(2), 157-230.

Kezerashvili, A., Marzo, K., & De Leon, J. (2012). Beta blocker use after acute myocardial infarction in the patient with normal systolic function: when is it "ok" to discontinue? *Current cardiology reviews, 8*(1), 77-84. https://doi.org/10.2174/157340312801215764

Khalil, M. E., Basher, A. W., Brown, E. J., & Alhaddad, I. A. (2001, 2001/06/01/). A remarkable medical story: benefits of angiotensin-converting enzyme inhibitors in cardiac patients. *Journal of the American College of Cardiology, 37*(7), 1757-1764. https://doi.org/https://doi.org/10.1016/S0735-1097(01)01229-3

Kim, H. J., Tsoy, I., Park, M. K., Lee, Y. S., Lee, J. H., Seo, H. G., & Chang, K. C. (2006, May). Iron released by sodium nitroprusside contributes to heme oxygenase-1 induction via the cAMP-protein kinase A-mitogen-activated protein kinase pathway in RAW 264.7 cells. *Mol Pharmacol, 69*(5), 1633-1640. https://doi.org/10.1124/mol.105.020487

Lanner, J. T., Georgiou, D. K., Joshi, A. D., & Hamilton, S. L. (2010). Ryanodine receptors: structure, expression, molecular details, and function in calcium release. *Cold Spring Harbor perspectives in biology, 2*(11), a003996-a003996. https://doi.org/10.1101/cshperspect.a003996

Leite, C., Almeida, T., Lopes, C., & Silva, V. (2015, 05/08). Multipotent stem cells of the heart – Do they have therapeutic promise? *Frontiers in Physiology, Front. Physiol.* https://doi.org/10.3389/fphys.2015.00123

Li, Y., Kranias, E. G., Mignery, G. A., & Bers, D. M. (2002). Protein Kinase A Phosphorylation of the Ryanodine Receptor Does Not Affect Calcium Sparks in Mouse Ventricular Myocytes. *Circulation Research, 90*(3), 309-316. https://doi.org/doi:10.1161/hh0302.105660

Liang, X., Evans, S. M., & Sun, Y. (2015). Insights into cardiac conduction system formation provided by HCN4 expression. *Trends in cardiovascular medicine, 25*(1), 1-9. https://doi.org/10.1016/j.tcm.2014.08.009

Liu, Y. W., Chen, B., Yang, X., Fugate, J. A., Kalucki, F. A., Futakuchi-Tsuchida, A., Couture, L., Vogel, K. W., Astley, C. A., Baldessari, A., Ogle, J., Don, C. W., Steinberg, Z. L., Seslar, S. P., Tuck, S. A., Tsuchida, H., Naumova, A. V., Dupras, S. K., Lyu, M. S., Lee, J., Hailey, D. W., Reinecke, H., Pabon, L., Fryer, B. H., MacLellan, W. R., Thies, R. S., & Murry, C. E. (2018, Aug). Human embryonic stem cell-derived cardiomyocytes restore function in infarcted hearts of non-human primates. *Nat Biotechnol, 36*(7), 597-605. https://doi.org/10.1038/nbt.4162

Livak, K. J., & Schmittgen, T. D. (2001, Dec). Analysis of relative gene expression data using real-time quantitative PCR and the 2(-Delta Delta C(T)) Method. *Methods, 25*(4), 402-408. https://doi.org/10.1006/meth.2001.1262

López-Unzu, M. A., Durán, A. C., Soto-Navarrete, M. T., Sans-Coma, V., & Fernández, B. (2019). Differential expression of myosin heavy chain isoforms in cardiac segments of gnathostome vertebrates and its evolutionary implications. *Frontiers in zoology, 16*, 18-18. https://doi.org/10.1186/s12983-019-0318-9

Lucia, C. d., Eguchi, A., & Koch, W. J. (2018, 2018-August-10). New Insights in Cardiac β-Adrenergic Signaling During Heart Failure and Aging [Review]. *Frontiers in Pharmacology, 9*(904). https://doi.org/10.3389/fphar.2018.00904

Madamanchi, A. (2007). Beta-adrenergic receptor signaling in cardiac function and heart failure. *McGill journal of medicine : MJM : an international forum for the advancement of medical sciences by students, 10*(2), 99-104.

McMullen, N. M., Zhang, F., Hotchkiss, A., Bretzner, F., Wilson, J. M., Ma, H., Wafa, K., Brownstone, R. M., & Pasumarthi, K. B. (2009, Nov). Functional characterization of cardiac progenitor cells and

their derivatives in the embryonic heart post-chamber formation. *Dev Dyn, 238*(11), 2787-2799. https://doi.org/10.1002/dvdy.22112

Mezzano, V., Pellman, J., & Sheikh, F. (2014). Cell junctions in the specialized conduction system of the heart. *Cell communication & adhesion, 21*(3), 149-159. https://doi.org/10.3109/15419061.2014.905928

Mikawa, T., Gourdie, R. G., Takebayashi-Suzuki, K., Kanzawa, N., Hyer, J., Pennisi, D. J., Poma, C. P., Shulimovich, M., Diaz, K. G., Layliev, J., & Prasad, A. (2003). Induction and Patterning of the Purkinje Fibre Network. In *Development of the Cardiac Conduction System* (pp. 142-156). https://doi.org/https://doi.org/10.1002/0470868066.ch9

Miquerol, L., Beyer, S., & Kelly, R. G. (2011). Establishment of the mouse ventricular conduction system. *Cardiovascular Research, 91*(2), 232-242. https://doi.org/10.1093/cvr/cvr069

Monfredi, O., Dobrzynski, H., Mondal, T., Boyett, M. R., & Morris, G. M. (2010, 2010/11/01). The Anatomy and Physiology of the Sinoatrial Node—A Contemporary Review [https://doi.org/10.1111/j.1540-8159.2010.02838.x]. *Pacing and Clinical Electrophysiology, 33*(11), 1392-1406. https://doi.org/https://doi.org/10.1111/j.1540-8159.2010.02838.x

Morris, M. C., Todres, I. D., & Schleien, C. L. (2009). CHAPTER 40 - Cardiopulmonary Resuscitation. In C. J. Coté, J. Lerman, & I. D. Todres (Eds.), *A Practice of Anesthesia for Infants and Children (Fourth Edition)* (pp. 833-845). W.B. Saunders. https://doi.org/https://doi.org/10.1016/B978-141603134-5.50044-5

Moskowitz, A., Andersen, L. W., Huang, D. T., Berg, K. M., Grossestreuer, A. V., Marik, P. E., Sherwin, R. L., Hou, P. C., Becker, L. B., Cocchi, M. N., Doshi, P., Gong, J., Sen, A., & Donnino, M. W. (2018). Ascorbic acid, corticosteroids, and thiamine in sepsis: a review of the biologic rationale and the present state of clinical evaluation. *Critical care (London, England), 22*(1), 283-283. https://doi.org/10.1186/s13054-018-2217-4

Ng, S. Y., Wong, C. K., & Tsang, S. Y. (2010). Differential gene expressions in atrial and ventricular myocytes: insights into the road of applying embryonic stem cell-derived cardiomyocytes for future therapies. *American Journal of Physiology-Cell Physiology, 299*(6), C1234-C1249. https://doi.org/10.1152/ajpcell.00402.2009

Pallante, Giovannone, S., Fang-Yu, L., Zhang, J., Liu, N., Kang, G., Dun, W., Boyden, P. A., & Fishman, G. I. (2010). Contactin-2 expression in the cardiac Purkinje fiber network. *Circulation. Arrhythmia and electrophysiology, 3*(2), 186-194. https://doi.org/10.1161/CIRCEP.109.928820

Pallante, B., Giovannone, S., Fang-Yu, L., Zhang, J., Liu, N., Kang, G., Dun, W., Boyden, P., & Fishman, G. (2010, 04/01). Contactin-2 Expression in the Cardiac Purkinje Fiber Network. *Circ Arrhythm Electrophysiol, 3*, 186-194. https://doi.org/10.1161/CIRCEP.109.928820

Paravati, S., Rosani, A., & Warrington, S. J. (2021). Physiology, Catecholamines. In *StatPearls*. StatPearls Publishing.

Parish, R. C., & Miller, L. J. (1992, 1992/01/01). Adverse Effects of Angiotensin Converting Enzyme (ACE) Inhibitors. *Drug Safety, 7*(1), 14-31. https://doi.org/10.2165/00002018-199207010-00004

Parmacek, M. S. (2006). Cardiac stem cells and progenitors: developmental biology and therapeutic challenges. *Transactions of the American Clinical and Climatological Association, 117*, 239-256.

Patel, R., & Kos, L. (2005). Endothelin-1 and Neuregulin-1 convert embryonic cardiomyocytes into cells of the conduction system in the mouse. *Developmental Dynamics, 233*(1), 20-28. https://doi.org/https://doi.org/10.1002/dvdy.20284

Pearson, K. L., Hunter, T., & Janknecht, R. (1999, Dec 23). Activation of Smad1-mediated transcription by p300/CBP. *Biochim Biophys Acta, 1489*(2-3), 354-364. https://doi.org/10.1016/s0167-4781(99)00166-9

Perino, M. G., Yamanaka, S., Riordon, D. R., Tarasova, Y., & Boheler, K. R. (2017). Ascorbic acid promotes cardiomyogenesis through SMAD1 signaling in differentiating mouse embryonic stem cells. *PLOS ONE, 12*(12), e0188569. https://doi.org/10.1371/journal.pone.0188569

Pillai, P., Corrigan, C. J., & Ying, S. (2011). Airway epithelium in atopic and nonatopic asthma: similarities and differences. *ISRN allergy, 2011*, 195846-195846. https://doi.org/10.5402/2011/195846

Poelmann, R. E., & Gittenberger-de Groot, A. C. (1999, 1999/03/15/). A Subpopulation of Apoptosis-Prone Cardiac Neural Crest Cells Targets to the Venous Pole: Multiple Functions in Heart Development? *Developmental Biology, 207*(2), 271-286. https://doi.org/https://doi.org/10.1006/dbio.1998.9166

Prabhu, S. D., & Frangogiannis, N. G. (2016). The Biological Basis for Cardiac Repair After Myocardial Infarction: From Inflammation to Fibrosis. *Circulation Research, 119*(1), 91-112. https://doi.org/10.1161/CIRCRESAHA.116.303577

Procaccini, D. E., Sawyer, J. E., & Watt, K. M. (2019). 19 - Pharmacology of Cardiovascular Drugs. In R. M. Ungerleider, J. N. Meliones, K. Nelson McMillan, D. S. Cooper, & J. P. Jacobs (Eds.), *Critical Heart Disease in Infants and Children (Third Edition)* (pp. 192-212.e196). Elsevier. https://doi.org/https://doi.org/10.1016/B978-1-4557-0760-7.00019-X

Ramos, K., & Acosta, D. (1983, 1983/01/01/). Preventory by L(−) ascorbic acid of isoproterenol-induced cardiotoxicity in primary cultures of rat myocytes. *Toxicology, 26*(1), 81-90. https://doi.org/https://doi.org/10.1016/0300-483X(83)90059-8

Rehsia, N. S., & Dhalla, N. S. (2010, Winter). Mechanisms of the beneficial effects of beta-adrenoceptor antagonists in congestive heart failure. *Experimental and clinical cardiology, 15*(4), e86-e95.

Ribeiro da Silva, A., Neri, E. A., Turaça, L. T., Dariolli, R., Fonseca-Alaniz, M. H., Santos-Miranda, A., Roman-Campos, D., Venturini, G., & Krieger, J. E. (2020, 2020/09/30). NOTCH1 is critical for fibroblast-mediated induction of cardiomyocyte specialization into ventricular conduction system-like cells in vitro. *Scientific Reports, 10*(1), 16163. https://doi.org/10.1038/s41598-020-73159-0

Richardson, W. J., Clarke, S. A., Quinn, T. A., & Holmes, J. W. (2015). Physiological Implications of Myocardial Scar Structure. *Compr Physiol, 5*(4), 1877-1909. https://doi.org/10.1002/cphy.c140067

Ross, S. D., Allen, I. E., Connelly, J. E., Korenblat, B. M., Smith, M. E., Bishop, D., & Luo, D. (1999). Clinical Outcomes in Statin Treatment Trials: A Meta-analysis. *Archives of Internal Medicine, 159*(15), 1793-1802. https://doi.org/10.1001/archinte.159.15.1793

Saleh, M., & Ambrose, J. A. (2018). Understanding myocardial infarction. *F1000Research, 7*, F1000 Faculty Rev-1378. https://doi.org/10.12688/f1000research.15096.1

Schulte, J. S., Seidl, M. D., Nunes, F., Freese, C., Schneider, M., Schmitz, W., & Müller, F. U. (2012). CREB critically regulates action potential shape and duration in the adult mouse ventricle. *American Journal of Physiology-Heart and Circulatory Physiology, 302*(10), H1998-H2007. https://doi.org/10.1152/ajpheart.00057.2011

Sedmera, D., Pexieder, T., Vuillemin, M., Thompson, R. P., & Anderson, R. H. (2000, Apr 1). Developmental patterning of the myocardium. *Anat Rec, 258*(4), 319-337. https://doi.org/10.1002/(sici)1097-0185(20000401)258:4<319::Aid-ar1>3.0.Co;2-o

Shiba, Y., Gomibuchi, T., Seto, T., Wada, Y., Ichimura, H., Tanaka, Y., Ogasawara, T., Okada, K., Shiba, N., Sakamoto, K., Ido, D., Shiina, T., Ohkura, M., Nakai, J., Uno, N., Kazuki, Y., Oshimura, M., Minami, I., & Ikeda, U. (2016, Oct 20). Allogeneic transplantation of iPS cell-derived cardiomyocytes regenerates primate hearts. *Nature, 538*(7625), 388-391. https://doi.org/10.1038/nature19815

Singla, D. K. (2009, Aug). Embryonic stem cells in cardiac repair and regeneration. *Antioxid Redox Signal, 11*(8), 1857-1863. https://doi.org/10.1089/ars.2009.2491

Smith, T. K., & Bader, D. M. (2007). Signals from both sides: Control of cardiac development by the endocardium and epicardium. *Seminars in cell & developmental biology, 18*(1), 84-89. https://doi.org/10.1016/j.semcdb.2006.12.013

Srivastava, D., & Olson, E. N. (2000, 2000/09/01). A genetic blueprint for cardiac development. *Nature, 407*(6801), 221-226. https://doi.org/10.1038/35025190

Stevenson, W. G., Friedman, P. L., Kocovic, D., Sager, P. T., Saxon, L. A., & Pavri, B. (1998). Radiofrequency Catheter Ablation of Ventricular Tachycardia After Myocardial Infarction. *Circulation, 98*(4), 308-314. https://doi.org/doi:10.1161/01.CIR.98.4.308

Stöckigt, F., Brixius, K., Lickfett, L., Andrié, R., Linhart, M., Nickenig, G., & Schrickel, J. W. (2012). Total Beta-Adrenoceptor Knockout Slows Conduction and Reduces Inducible Arrhythmias in the Mouse Heart. *PLOS ONE, 7*(11), e49203. https://doi.org/10.1371/journal.pone.0049203

Sturgill, M. G., Kelly, M., & Notterman, D. A. (2011). Chapter 25 - Pharmacology of the Cardiovascular System. In B. P. Fuhrman & J. J. Zimmerman (Eds.), *Pediatric Critical Care (Fourth Edition)* (pp. 277-305). Mosby. https://doi.org/https://doi.org/10.1016/B978-0-323-07307-3.10025-4

Takebayashi-Suzuki, K., Pauliks, L. B., Eltsefon, Y., & Mikawa, T. (2001, 2001/06/15/). Purkinje Fibers of the Avian Heart Express a Myogenic Transcription Factor Program Distinct from Cardiac and Skeletal Muscle. *Developmental Biology, 234*(2), 390-401. https://doi.org/https://doi.org/10.1006/dbio.2001.0270

Talan, M. I., Ahmet, I., Xiao, R.-P., & Lakatta, E. G. (2011). β_2 AR agonists in treatment of chronic heart failure: long path to translation. *Journal of molecular and cellular cardiology, 51*(4), 529-533. https://doi.org/10.1016/j.yjmcc.2010.09.019

Tan, C. M. J., & Lewandowski, A. J. (2020). The Transitional Heart: From Early Embryonic and Fetal Development to Neonatal Life. *Fetal Diagnosis and Therapy, 47*(5), 373-386. https://doi.org/10.1159/000501906

Thygesen, K., Alpert Joseph, S., & White Harvey, D. (2007, 2007/11/27). Universal Definition of Myocardial Infarction. *Journal of the American College of Cardiology, 50*(22), 2173-2195. https://doi.org/10.1016/j.jacc.2007.09.011

Tsai, S. Y., Maass, K., Lu, J., Fishman, G. I., Chen, S., & Evans, T. (2015, Jun 9). Efficient Generation of Cardiac Purkinje Cells from ESCs by Activating cAMP Signaling. *Stem Cell Reports, 4*(6), 1089-1102. https://doi.org/10.1016/j.stemcr.2015.04.015

van den Borne, S. W., Diez, J., Blankesteijn, W. M., Verjans, J., Hofstra, L., & Narula, J. (2010, Jan). Myocardial remodeling after infarction: the role of myofibroblasts. *Nat Rev Cardiol, 7*(1), 30-37. https://doi.org/10.1038/nrcardio.2009.199

van den Bos, E. J., van der Giessen, W. J., & Duncker, D. J. (2008). Cell transplantation for cardiac regeneration: where do we stand? *Netherlands heart journal : monthly journal of the Netherlands Society of Cardiology and the Netherlands Heart Foundation, 16*(3), 88-95. https://doi.org/10.1007/BF03086124

Vavetsi, S., Nikolaou, N., Tsarouhas, K., Lymperopoulos, G., Kouzanidis, I., Kafantaris, I., Antonakopoulos, A., Tsitsimpikou, C., & Kandylas, J. (2008). Consecutive administration of atropine and isoproterenol for the evaluation of asymptomatic sinus bradycardia. *EP Europace, 10*(10), 1176-1181. https://doi.org/10.1093/europace/eun211

Verheule, S., & Kaese, S. (2013, 2013-June-27). Connexin diversity in the heart: insights from transgenic mouse models [Review]. *Frontiers in Pharmacology, 4*(81). https://doi.org/10.3389/fphar.2013.00081

Viragh, S., & Challice, C. E. (1977, Apr). The development of the conduction system in the mouse embryo heart. II. Histogenesis of the atrioventricular node and bundle. *Dev Biol, 56*(2), 397-411. https://doi.org/10.1016/0012-1606(77)90279-2

Wang, W. T., Hellkamp, A., Doll, J. A., Thomas, L., Navar, A. M., Fonarow, G. C., Julien, H. M., Peterson, E. D., & Wang, T. Y. (2018). Lipid Testing and Statin Dosing After Acute Myocardial Infarction. *Journal of the American Heart Association, 7*(3), e006460. https://doi.org/doi:10.1161/JAHA.117.006460

Weisse, A. B. (2011). Cardiac surgery: a century of progress. *Texas Heart Institute journal, 38*(5), 486-490.

Wen, A. Y., Sakamoto, K. M., & Miller, L. S. (2010). The role of the transcription factor CREB in immune function. *Journal of immunology (Baltimore, Md. : 1950), 185*(11), 6413-6419. https://doi.org/10.4049/jimmunol.1001829

Willecke, K., Eiberger, J., Degen, J., Eckardt, D., Romualdi, A., Güldenagel, M., Deutsch, U., & Söhl, G. (2002). Structural and Functional Diversity of Connexin Genes in the Mouse and Human Genome. *383*(5), 725-737. https://doi.org/doi:10.1515/BC.2002.076

Wong, A., Hwang, S. M., Cheng, H. Y., & Crooke, S. T. (1987, Apr). Structure-activity relationships of beta-adrenergic receptor-coupled adenylate cyclase: implications of a redox mechanism for the action of agonists at beta-adrenergic receptors. *Mol Pharmacol, 31*(4), 368-376.

Wu, S. M., Fujiwara, Y., Cibulsky, S. M., Clapham, D. E., Lien, C. L., Schultheiss, T. M., & Orkin, S. H. (2006, Dec 15). Developmental origin of a bipotential myocardial and smooth muscle cell precursor in the mammalian heart. *Cell, 127*(6), 1137-1150. https://doi.org/10.1016/j.cell.2006.10.028

Xiao, Y.-F. (2011). Cell and gene therapy for arrhythmias: Repair of cardiac conduction damage. *Journal of geriatric cardiology : JGC, 8*(3), 147-158. https://doi.org/10.3724/SP.J.1263.2011.00147

Yan, L., Jia, Z., Cui, J., Yang, H., Yang, H., Zhang, Y., & Zhou, C. (2011). Beta-adrenergic signals regulate cardiac differentiation of mouse embryonic stem cells via mitogen-activated protein kinase pathways. *Development, Growth & Differentiation, 53*(6), 772-779. https://doi.org/https://doi.org/10.1111/j.1440-169X.2011.01284.x

Yoshiyama, M., Nakamura, Y., Omura, T., Izumi, Y., Matsumoto, R., Oda, S., Takeuchi, K., Kim, S., Iwao, H., & Yoshikawa, J. (2005). Angiotensin converting enzyme inhibitor prevents left ventricular remodelling after myocardial infarction in angiotensin II type 1 receptor knockout mice. *Heart (British Cardiac Society), 91*(8), 1080-1085. https://doi.org/10.1136/hrt.2004.035618

Yuasa, S., & Fukuda, K. (2008, 2008/12/01/). Multiple roles for BMP signaling in cardiac development. *Drug Discovery Today: Therapeutic Strategies, 5*(4), 209-214. https://doi.org/https://doi.org/10.1016/j.ddstr.2008.12.001

Zhang, Zhao, J., Mandveno, A., & Potter, J. D. (1995, Jun). Cardiac troponin I phosphorylation increases the rate of cardiac muscle relaxation. *Circ Res, 76*(6), 1028-1035. https://doi.org/10.1161/01.res.76.6.1028

Zhang, F., & Pasumarthi, K. B. (2007, May-Jun). Ultrastructural and immunocharacterization of undifferentiated myocardial cells in the developing mouse heart. *J Cell Mol Med, 11*(3), 552-560. https://doi.org/10.1111/j.1582-4934.2007.00044.x